Book page numbers

680
690
700
710
720
730
740
750
760
770
780
790

7-130
8-10
8-20
8-30
8-40
8-50
8-60
8-70
8-80
8-90
8-100

Ch.8 pdf. page numbers

CHAPTER 8

SYMMETRY ANALYSIS
FOR SEMICLASSICAL AND QUANTUM
MECHANICS: DYNAMICS
WITH HIGH QUANTA

The classical world with all its detailed motion should in principle be described in terms of basic quantum states. In practice, however, the detailed correspondence between classical and quantum descriptions can be fairly subtle and complex. In Chapters 3, 4 and 7 we considered some elementary examples of classical spontaneous symmetry breaking. There, certain combinations of eigenstates were shown to be represented by localized wave packets that corresponded to systems being trapped into quasiclassical configurations with lower symmetry. In this chapter some theory involving wave packets and so-called coherent states will be developed in order to clarify the connection between quantum and classical phenomena. The main application of these theories will be to systems with high quantum numbers. The resulting methodology is loosely referred to as SEMICLASSICAL mechanics.

As we have already noted in Chapters 5–7, states with high quanta (particularly angular quanta with J greater than 5 or 10) can be very complicated, and computations involving them can be extremely laborious. Often this means that the problem is treated numerically and exact eigensolutions are found by computer diagonalization. However, large-scale numerical solutions may not expose interesting physical phenomena or lead one directly toward a better theoretical understanding. One should not be content to just have a computer experiment that parrots some laboratory spectra.

Furthermore, there should be much more to quantum mechanics than the study of individual eigenstates. An eigenfunction is stationary in the sense that only its overall phase ($\psi_m(t) = e^{-iE_m t/\hbar}\psi_m(0)$) is time dependent, while its probability distribution ($\psi_m^*\psi_m$) is forever frozen. By studying individual eigenstates you learn all the ways that a quantum system can play dead! Only

by combining two or more eigenstates with different energy phase factors can you get something to actually move. The rate of such motion is determined by the energy differences $(E_m - E_n)$, that is, transition or "beat" frequencies $(\omega_{mn} = (E_m - E_n)/\hbar)$, as explained in Chapter 2, Sections 2.3.A and 2.3.B. In fact, a single eigenstate is really unobservable. Only through combinations of eigenstates or transitions between them can a quantum system exhibit change or dynamics.

Classical mechanics, on the other hand, seems better equipped to describe dynamics or motion. This is because one is better able to visualize how classical objects move even if the equations of motion are difficult to solve analytically. An important part of semiclassical mechanics is to provide ways to visualize and understand quantum dynamics and to compare it to the classical dynamics which approximates it in the limit of high quantum numbers. We shall compare quantum and semiclassical theory for vibrational and rotational dynamics. This will include applications to atomic and molecular spectroscopy. Also, we shall introduce and compare quantum and semiclassical theories of radiation which are fundamental to the theory of spectroscopy in general.

8.1 CONTACT TRANSFORMATIONS, ACTIONS, AND SEMICLASSICAL WAVE FRONTS

The principles involving the action functions are introduced and it is shown how they enter the study of semiclassical dynamics. This treatment includes ways to visualize action transformations geometrically.

A. Contact Transformations

Consider a curve $y(x)$ in a two-dimensional coordinate space (x, y) as shown in Figure 8.1.1(a). This curve may be related to another curve $Y(X)$ in a (generally) different space (X, Y) by what is called a CONTACT TRANSFORMATION. To define a contact transformation one ultimately requires what is called a GENERATOR function $S(x, y : X, Y)$. Then for a fixed value of the generator [say $S(x, y : X, Y) = 10$] one generates a family of curves in the (X, Y) space as shown in Figure 8.1.1. There is one *curve* $S(x_j y_j : X, Y) = 10$ in the (X, Y) space for each *point* (x_j, y_j) on the curve $y(x)$. The envelope(s) or contacting curve(s) of this family comprise the desired contact transformation(s) $Y(X)$ for a particular value of the generator. (Here $S = 10$.) A schematic example of a family and its contact curve are shown in Figure 8.1.1(b).

As we have said, each point $(x, y(x))$ is associated with a curve in (X, Y) space. In addition we shall associate each point $(x_j, y(x_j))$ with the contact point $(X_j, Y(X_j))$ where that curve is tangent to the family envelope $Y(X)$. The points $(X_j, Y(X_j))$ are the ones for which the value of $S(x, y(x) : X, Y)$
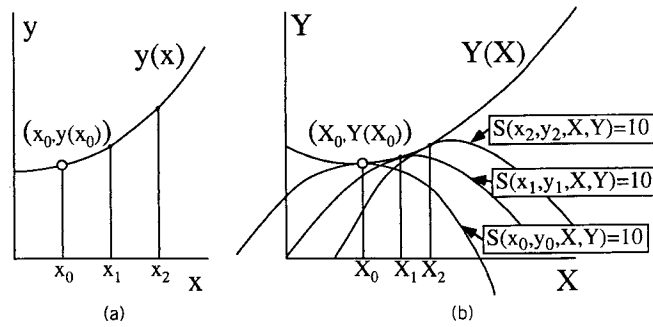
Figure 8.1.1   Geometry of a general contact transformation.

is least sensitive to a small change in x. From Figure 8.1.1(b) you can see that a change of x causes the $S = 10$ curve to slide along the envelope. As the new contact point slides a small distance away from the old contact point $(X, Y(X))$, the latter is still practically on top of the new $S = 10$ curve; that is, S does not change at first near the point $(X, Y(X))$. Therefore we find these points by solving

$$\left. \frac{\partial S(x, y(x) : X, Y)}{\partial x} \right|_{x = x_j} = 0 \qquad (8.1.1a)$$

and

$$S(x, y(x) : X, Y) = \text{constant}. \qquad (8.1.1b)$$

One should notice that a contact transformation goes either way; each point $(X_j, Y(X_j))$ generates a curve tangent to the $y(x)$ curve at $(x_j, y(x_j))$. Then the following equation would be applicable, too:

$$\left. \frac{\partial S(x, y : X, Y)}{\partial X} \right|_{X = X_j} = 0. \qquad (8.1.1c)$$

The LEGENDRE TRANSFORMATION is an example of a contact transformation in which the transformed curve contacts or envelopes a family of straight lines. In its simplest form each point $(x_j, y_j = y(x_j))$ generates a line $Y = x_j X - y_j$ in (X, Y) coordinates, i.e., a line of slope x_j and Y intercept $-y_j$ as shown in Figure 8.1.2. This is equivalent to having the generator relation

$$S(x, y : XY) = y + Y - xX = 0.$$
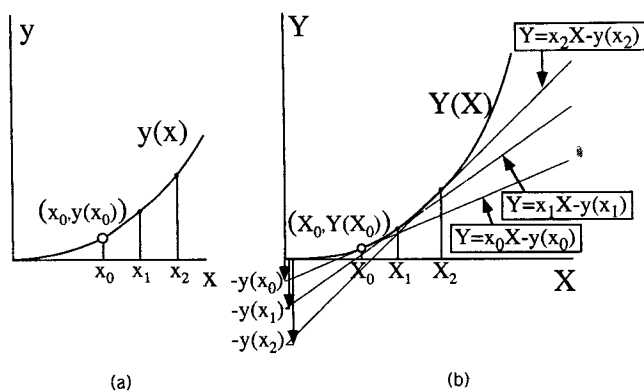
Figure 8.1.2   Geometry of a Legendre contact transformation.

From the derivative equations (8.1.1a) and (8.1.1c) we find

$$\frac{\partial S}{\partial x} = 0, \qquad X = \frac{\partial y}{\partial x}, \tag{8.1.2a}$$

$$\frac{\partial S}{\partial X} = 0, \qquad x = \frac{\partial Y}{\partial X}. \tag{8.1.2b}$$

This is combined with the generator relation $S = 0$ or

$$Y = xX - y \tag{8.1.2c}$$

to yield the desired Legendre transformation.

One of the best known examples of a Legendre transformation is the transformation between the Lagrangian function $y(x) \equiv L(\dot{q})$ and the Hamiltonian function $Y(X) \equiv H(p)$. Here the independent variables are velocity $(x \equiv \dot{q})$ and momentum $(X = p)$. The transformation equations (8.1.2a)–(8.1.2c) yield the relations

$$p = \frac{\partial L}{\partial \dot{q}}, \tag{8.1.3a}$$

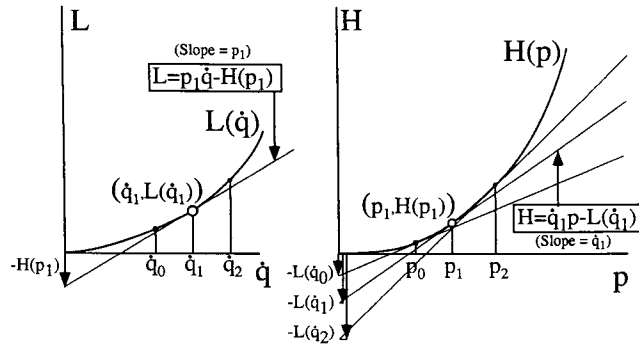$$\dot{q} = \frac{\partial H}{\partial p}, \tag{8.1.3b}$$

and

$$H(p) = p\dot{q} - L, \tag{8.1.3c}$$

respectively. The slope $\dot{q}$ of the contacting lines which are indicated in Figure

Figure 8.1.3 Geometry of Legendre transformation between Lagrangian and Hamiltonian functions.

8.1.3(b) will be shown to have an important interpretation in semiclassical wave mechanics. Slope p is inversely proportional to a wave phase velocity, and slope $\dot{q}$ corresponds to a wave group velocity. [Given the single-particle de Broglie relations $H \to \hbar\omega$ and $p \to \hbar k$ this geometrical interpretation of phase velocity (ω/k) and group velocity $(d\omega/dk)$ is an elementary consequence of dispersion theory.]

B. Action Functions

An important application of contact transformations involves the transformation of a classical particle or system from one point [say $(x = x_0, \, y = y_0, \dots)$] to another point [say $(x = X, \, y = Y, \dots)$] which lies along its natural trajectory of motion. The transformations which do this are called "active" (as opposed to "passive") transformations because they represent an actual change of position rather than just a relabeling of coordinates or state variables. The generators of these transformations are called ACTIONS. (This might suggest that the generators of passive transformations should be called "passions.")

The development of the idea of action generators requires one to ask what is so special about a particular classical trajectory or "natural path" followed by a classical system. Part of the answer, as we shall show, is that the action achieves an extreme value (in fact a locally minimum value) for a natural path. Nearby paths must have greater action, but, more importantly, paths which are very close to the natural one must have practically the *same* action. The concept of a stationary action value for a natural path is a key to the understanding of the action generators.

The first type of action function which we shall study is defined by the following time integral of a Lagrangian L which we take to have no explicit
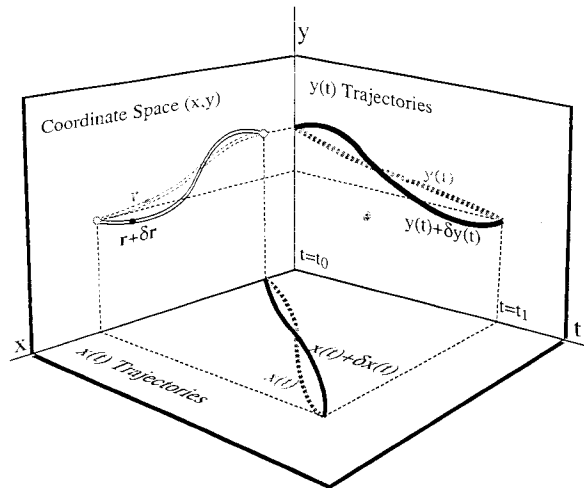
Figure 8.1.4 A comparison of paths appropriate for Hamilton's principle function S_p.

time dependence:

$$S_P(\mathbf{r}_0, t_0 : \mathbf{r}_1, t_1) = \int_{t_0}^{t_1} L(\mathbf{r}(t), \dot{\mathbf{r}}(t))\, dt. \qquad (8.1.4)$$

This is called HAMILTON'S PRINCIPLE FUNCTION since it is the subject of Hamilton's principle, which we shall discuss shortly. This discussion involves a comparison of the value of S_P for two nearby paths $\mathbf{r}(t)$ and $\mathbf{r}(t) + \delta\mathbf{r}(t)$. Two such paths are sketched in Figure 8.1.4 for a two-dimensional system with coordinates $\mathbf{r} = (x, y)$. The third dimension of the figure is time.

Here we compare the action for curves whose end points are fixed in space and time, i.e., $\delta\mathbf{r}(t_0) = 0 = \delta\mathbf{r}(t_1)$. A range of positions, velocities, accelerations, jerks, etc., will be considered, but total travel time is fixed. For a small difference function $\delta\mathbf{r}(t)$ one has

$$
\begin{aligned}
S_P(\mathbf{r}_0, t_0 : r_1, t_1)_{\mathrm{PATH}(r+\delta r)} &= \int_{t_0}^{t_1} L(\mathbf{r} + \delta\mathbf{r}, \dot{r} + \delta\dot{\mathbf{r}})\, dt \\
&= \int_{t_0}^{t_1} L(r, \dot{r})\, dt + \int_{t_0}^{t_1} \left(\frac{\partial L}{\delta\mathbf{r}}\, \delta\mathbf{r} + \frac{\partial L}{\partial \dot{\mathbf{r}}}\, \delta\dot{\mathbf{r}} \right) dt + 0(\delta^2) \\
&= S_P(\mathbf{r}_0, t_0 : \mathbf{r}_1, t_1)_{\mathrm{PATH}(r)} + \frac{\partial L}{\partial \dot{\mathbf{r}}}\, \delta r \Big|_{t_0}^{t_1} \\
&\quad + \int_{t_0}^{t_1} \left(\frac{\partial L}{\partial \mathbf{r}} - \frac{d}{dt}\frac{\partial L}{\partial \dot{\mathbf{r}}} \right) \delta\mathbf{r}\, dt, \\
&\quad + 0(\delta^2), \qquad\qquad\qquad\qquad (8.1.5)
\end{aligned}
$$

where an integration by parts was performed and $0(\delta^2)$ represents presumably negligible terms of second or higher order in δr. If (and only if) the path $\mathbf{r}(t)$ is adjusted so that the Lagrange equations $[\partial L/\partial \mathbf{r} - d/dt(\partial L/\partial \dot{\mathbf{r}}) = 0]$ are always satisfied, then Hamilton's principle

$$S_P(\mathbf{r}_0, t_0 : \mathbf{r}_1, t_1)_{\text{PATH}(r+\delta r)} = S_P(\mathbf{r}_0, t_0 : \mathbf{r}_1, t_1)_{\text{PATH}(r)} \qquad (8.1.6)$$

is satisfied to a precision of second order.

Another type of action which we shall consider here is defined by the spatial integral

$$S_H(\mathbf{r}_0 : \mathbf{r}_1) = \int_{\mathbf{r}_0}^{\mathbf{r}_1} \mathbf{p} \cdot d\mathbf{r}. \qquad (8.1.7)$$

This is known as HAMILTON'S CHARACTERISTIC FUNCTION or REDUCED ACTION for reasons that will be mentioned later. Using the Legendre transformation (8.1.3c) one can convert S_H to a time integral and relate it to the action S_P. Using (8.1.3c) we have (with $\mathbf{q} \equiv \mathbf{r}$)

$$S_H(\mathbf{r}_0 : \mathbf{r}_1) = \int_{t_0}^{t_1} \mathbf{p} \cdot \dot{\mathbf{r}} \, dt = \int_{t_0}^{t_1} [H(\mathbf{p}, \mathbf{r}) + L(\mathbf{r}\dot{\mathbf{r}})] \, dt. \qquad (8.1.8)$$

However, it is necessary to carefully define the time limits of integration.

It is convenient to let the time limits be determined by the natural motion for a fixed value of the Hamiltonian: $H = $ constant. (For Lagrangians with no explicit time dependence, the Hamiltonian is a constant of motion.) We shall use the notation $S_H(\mathbf{r}_0 : \mathbf{r}_1)$ to remind us that the travel times between $\mathbf{r}_0$ and $\mathbf{r}_1$ are not fixed but depend upon how much energy $\varepsilon = H$ is given. This means that a comparison of path integrals will have to allow for a variation of travel time $(t_1 - t_0)$. If we fix H and let $t_0 = 0$ then we must expect t_1 to have a different value $t_1 + \Delta t$ for a different path as indicated in Figure 8.1.5. The H-fixed action for a modified path $\mathbf{r}(t) + \Delta \mathbf{r}(t)$ will be

$$S_H(\mathbf{r}_0 : \mathbf{r}_1)_{\text{PATH}(r+\Delta r)}$$

$$= \int_0^{t_1 + \Delta t} [H + L(\mathbf{r} + \Delta \mathbf{r}, \dot{\mathbf{r}} + \Delta \dot{\mathbf{r}})] \, dt$$

$$= Ht_1 + \int_0^{t_1} L(\mathbf{r} + \Delta \mathbf{r}, \dot{\mathbf{r}} + \Delta \dot{\mathbf{r}}) \, dt + H\Delta t +$$

$$\int_{t_1}^{t_1 + \Delta t} L(\mathbf{r} + \Delta \mathbf{r}, \dot{\mathbf{r}} + \Delta \dot{\mathbf{r}}) \, dt$$

$$= S_H(\mathbf{r}_0 : \mathbf{r}_1)_{\text{PATH}(r)} + \int_0^{t_1} \left(\frac{\partial L}{\partial \dot{\mathbf{r}}} \Delta \dot{\mathbf{r}} \right) dt + H\Delta t + L(\mathbf{r}_1, \dot{\mathbf{r}}_1) \Delta t$$

$$= S_H(\mathbf{r}_0 : \mathbf{r}_1)_{\text{PATH}(r)} + \int_0^{t_1} \left(\frac{\partial L}{\partial \mathbf{r}} - \frac{d}{dt} \left(\frac{\partial L}{\partial \dot{\mathbf{r}}} \right) \right) \Delta \mathbf{r} \, dt + \frac{\partial L}{\partial \dot{\mathbf{r}}} \Delta \mathbf{r}(t_1)$$

$$+ H\Delta t + L\Delta t + 0(\Delta^2). \qquad (8.1.9)$$
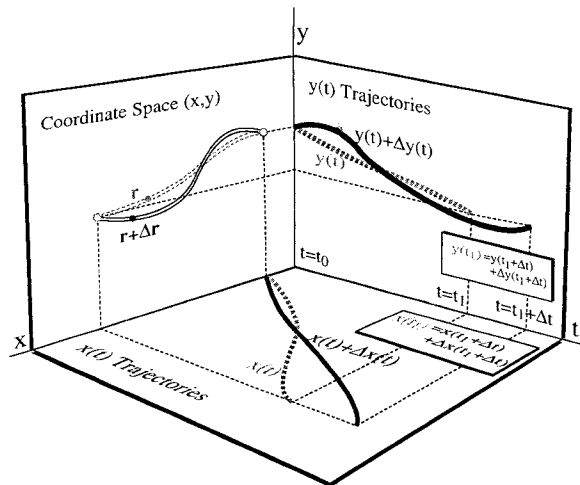
Figure 8.1.5 A comparison of paths appropriate for Hamilton's characteristic function S_H.

Here we have again integrated by parts and let $\Delta \mathbf{r}(t_0) = 0$. The value $\Delta \mathbf{r}(t_1)$ at the upper limit is obtained by solving the equation

$$\mathbf{r}(t_1) = \mathbf{r}(t_1 + \Delta t) + \Delta \mathbf{r}(t_1 + \Delta t)$$

$$= \mathbf{r}(t_1) + \left.\frac{\partial \mathbf{r}}{\partial t}\right|_{t_1} \Delta t + \Delta \mathbf{r}(t_1) + 0(\Delta^2) \qquad (8.1.10)$$

for small Δt. (See Figure 8.1.5, which shows components of this equation.) One then substitutes the result

$$\Delta \mathbf{r} = -\left.\frac{\partial \mathbf{r}}{\partial t}\right|_{t_1} \Delta t = -\dot{\mathbf{r}}(t_1)\,\Delta t \qquad (8.1.11)$$

into (8.1.9). For natural paths $\mathbf{r}(t)$ this yields

$$S_H(\mathbf{r}_0 : \mathbf{r}_1)_{\text{PATH}(r + \Delta r)} = S_H(\mathbf{r}_0 : \mathbf{r}_1)_{\text{PATH}(r)} + \left(L - \frac{\partial L}{\partial \dot{\mathbf{r}}}\dot{\mathbf{r}} + H\right)\Delta t + 0(\Delta^2)$$

$$= S_H(\mathbf{r}_0 : \mathbf{r}_1)_{\text{PATH}(r)} + 0(\Delta^2), \qquad (8.1.12)$$

where (8.1.3c) was used. This shows that the time-independent action S_H reaches an extreme value on natural paths.

Finally, let us consider the change in the action S_P if we vary time *and* position of the destination point by arbitrary amounts dt_1 and $d\mathbf{r}_1$, respectively, but we "aim" the initial momenta so as to follow a natural path $\mathbf{r}(t) + d\mathbf{r}(t)$ to this end point. (As usual let us keep the starting point $\mathbf{r}_0$ and

time t_0 the same for both paths.) By following the same procedures that were used in (8.1.9), we have

$$S_P(\mathbf{r}_0, t_0 : \mathbf{r}_1 + d\mathbf{r}_1, t_1 + dt)_{\text{PATH}(r+dr)}$$

$$= \int_{t_0}^{t_1 + dt_1} L(\mathbf{r} + dr, \dot{\mathbf{r}} + d\dot{\mathbf{r}}) \, dt$$

$$= S_P(\mathbf{r}_0, t_0 : \mathbf{r}_1, t_1)_{\text{PATH}(r)} + \frac{\partial L}{\partial \dot{\mathbf{r}}} \, d\mathbf{r}(t_1) + L(\mathbf{r}_1 \mathbf{r}_1) \, dt + 0(d^2).$$

$$(8.1.13)$$

Instead of (8.1.10) we need equations which include the arbitrarily chosen $d\mathbf{r}_1$

$$\mathbf{r}(t_1) + d\mathbf{r}_1 = \mathbf{r}(t_1 + dt_1) + d\mathbf{r}(t_1 + dt_1),$$
$$\mathbf{r}_1 + d\mathbf{r}_1 = \mathbf{r}_1 + \dot{\mathbf{r}}_1 \, dt_1 + d\mathbf{r}(t_1),$$
$$d\mathbf{r}(t_1) = d\mathbf{r}_1 - \dot{\mathbf{r}}_1 \, dt_1. \qquad (8.1.14)$$

Substituting this result into (8.1.13) yields

$$S_P(r_0, t_0 : \mathbf{r}_1 + d\mathbf{r}_1, t_1 + dt_1) - S_P(\mathbf{r}_0, t_0 : \mathbf{r}_1, t_1)$$

$$= \mathbf{p}(t_1) \cdot d\mathbf{r}_1 + \left(L(\mathbf{r}_1 \dot{\mathbf{r}}_1) - \mathbf{p}(t_1) \cdot \dot{\mathbf{r}}_1 \right) dt_1,$$

$$dS_P = \mathbf{p} \cdot d\mathbf{r}_1 - H \, dt_1, \qquad (8.1.15a)$$

where the Legendre equations

$$\mathbf{p} = \frac{\partial L}{\partial \dot{\mathbf{r}}} \quad \text{and} \quad H = \mathbf{p} \cdot \dot{\mathbf{r}} - L \qquad (8.1.15b)$$

from (8.1.3) are used. Note that the changes in S_P due to changes in H are of second order in $d\mathbf{r}_1$ and dt_1 and are therefore neglected.

The differential form (8.1.15a) is called the POINCARÉ-CARTAN IN-VARIANT. From it we derive two very important equations

$$\frac{\partial S_P(\mathbf{r}_0, t_0 : \mathbf{r}, t)}{\partial \mathbf{r}} = \mathbf{p}, \qquad (8.1.16a)$$

$$\frac{\partial S_P(\mathbf{r}_0, t_0 : \mathbf{r}, t)}{\partial t} = -H(\mathbf{p}, \mathbf{r}). \qquad (8.1.16b)$$

The combination of these two equations leads to the TIME-DEPEN-DENT HAMILTON-JACOBI equation for the principal action generator.

$$-\frac{\partial S_P}{\partial t} = H\left(\frac{\partial S_P}{\partial \mathbf{r}}, \mathbf{r} \right). \qquad (8.1.17)$$

A related set of equations exists for determining the time-independent action generator S_H. From (8.1.8) we have

$$S_H(\mathbf{r}_0:\mathbf{r}_1) = (t_1 - t_0)H + \int_{t_0}^{t_1} L\,dt = (t_1 - t_0)H + S_P(\mathbf{r}_0, t_0:\mathbf{r}_1, t_1),$$

$$(8.1.18)$$

where we are assuming natural paths in all integrations. Also, the travel time $t_1 - t_0$ depends on the chosen value of energy $\varepsilon = H$ as before. (The initial time t_0 may be chosen to be zero without loss of generality.) Now a variation of the destination point $\mathbf{r}_1$ to $\mathbf{r}_1 + d\mathbf{r}_1$ causes a change,

$$dS_H = dt_1 H + dS_P = \mathbf{p} \cdot d\mathbf{r}_1, \qquad (8.1.19)$$

in which time dependence is removed. (Hence, the name "reduced action" is used for S_H.) This leads to the TIME-DEPENDENT HAMILTON-JACOBI equations

$$\frac{\partial S_H(\mathbf{r}_0:\mathbf{r})}{\partial \mathbf{r}} = \mathbf{p}, \qquad (8.1.20a)$$

$$H\left(\frac{\partial S_H}{\partial \mathbf{r}}, \mathbf{r}\right) = \varepsilon = \text{constant}. \qquad (8.1.20b)$$

C. Generators for Classical Trajectories and Wave Fronts

Let us consider some elementary solutions to the Hamilton-Jacobi equations. Possibly the simplest case is the one treated at the beginning of sophomore mechanics involving a massive body falling in a uniform gravitational field ($f = mg$). Then the Hamiltonian is

$$\varepsilon = H(\mathbf{p},\mathbf{r}) = (1/2m)\mathbf{p} \cdot \mathbf{p} - fy = (1/2m)\left(p_x^2 + p_y^2\right) - fy, \quad (8.1.21)$$

where we neglect the third spatial dimension. The HJ equation (8.1.20) becomes

$$(1/2m)\left[\left(\frac{\partial S_H}{\partial x}\right)^2 + \left(\frac{\partial S_H}{\partial y}\right)^2\right] - fy = \varepsilon. \qquad (8.1.22)$$

This example allows a separation of variables $S_H(x, y) = s_x(x) + s_y(y)$ to yield two ordinary differential equations:

$$(1/2m)\left(\frac{ds_x}{dx}\right)^2 = \varepsilon_x, \qquad 1/2m\left(\frac{ds_y}{dy}\right)^2 - fy = \varepsilon_y, \quad (8.1.23a)$$

where the separated parts satisfy

$$S_H(x_0, y_0 : x_1, y_1) = s_x(x_1) + s_y(y_1), \qquad (8.1.23\text{b})$$

$$\varepsilon = \varepsilon_x + \varepsilon_y. \qquad (8.1.23\text{c})$$

The solutions to the separate HJ equations are

$$\begin{aligned} s_x &= [2m\varepsilon_x]^{1/2}(x_1 - x_0) \\ &= m\dot{x}_0(x_1 - x_0), \qquad (8.1.24\text{a}) \end{aligned}$$

$$\begin{aligned} s_y &= (1/3mf)\big[2m(\varepsilon_y + fy)\big]^{3/2}\Big|_{y_0}^{y_1} \\ &= (m^2/3f)\big[\dot{y}_1^3 - \dot{y}_0^3\big], \qquad (8.1.24\text{b}) \end{aligned}$$

where we use the definitions of momentum and velocity which apply to this problem:

$$p_x = m\dot{x} = [2m\varepsilon_x]^{1/2}, \qquad (8.1.24\text{c})$$

$$p_y = m\dot{y} = \big[2m(\varepsilon_y + fy)\big]^{1/2}. \qquad (8.1.24\text{d})$$

The time-dependent action is given by

$$S_P = S_H - \varepsilon T \qquad (8.1.25)$$

according to (8.1.18), where the travel time is $T = t_1 - t_0$, and $\varepsilon = H$ is the total energy. We now write the action S_P in various different forms in order to exhibit its physical and mathematical properties using examples. To do this we will use the falling-body time-trajectory solutions,

$$x_1 = x_0 + \dot{x}_0 T, \qquad \dot{x}_1 = \dot{x}_0, \qquad (8.1.26\text{a})$$

$$y_1 = y_0 + \dot{y}_0 T + (f/2m)T^2, \qquad \dot{y}_1 = \dot{y}_0 + (f/m)T, \qquad (8.1.26\text{b})$$

obtained by elementary means. (One should not get the impression that action theory is a convenient way to compute specific trajectories. Rather it is a way to analyze *families* of trajectories.)

By combining (8.1.23), (8.1.25) and the second lines of (8.1.26) we have

$$S_P = m\dot{x}_0(x_1 - x_0) + (m^2/3f)\big[(\dot{y}_0 + fT/m)^3 - \dot{y}_0^3\big] - \left(\frac{m}{2}\dot{x}_0 + \frac{m}{2}\dot{y}_0^2 - fy_0\right)T,$$

$$S_P = \frac{m\dot{x}_0}{2}(x_1 - x_0) + \frac{mT}{2}\dot{y}_0^2 + fTy_0 + fT^2\dot{y}_0 + \frac{f^2 T^3}{3m}. \qquad (8.1.27)$$

Solving for $(\dot{x}_0, \dot{y}_0)$ in the first line of (8.1.26) leads to the standard form for S_P:

$$S_P(\mathbf{r}_0, 0 : \mathbf{r}_1, T) = \frac{m(x_1 - x_0)^2}{2T} + \frac{m(y_1 - y_0)^2}{2T} + \frac{fT}{2}(y_1 + y_0) - \frac{f^2 T^3}{24m}.$$
(8.1.28)

On the other hand, we may write S_P as a function exclusively of time T and initial conditions:

$$S_P(\mathbf{r}_0, 0 : \mathbf{r}_1(T), T) = \frac{m\dot{x}_0^2 T}{2} + \frac{m\dot{y}_0^2 T}{2} + fTy_0 + fT^2 \dot{y}_0 + \frac{f^2 T^3}{3m}. \quad (8.1.29)$$

The latter could be obtained most easily by direct integration of the definition (8.1.4) of S_P. However, in so doing, one loses the crucial functional dependence in (8.1.28), which makes S_P a generator. It is instructive to compare the partial and total time derivatives of S_P:

$$\frac{\partial S_P(\mathbf{r}_0, 0 : \mathbf{r}_1, T)}{\partial T} = -H, \quad (8.1.30a)$$

$$\frac{dS_P(\mathbf{r}_0, 0 : \mathbf{r}_1(T), T)}{dT} = L, \quad (8.1.30b)$$

which are expressions of the HJ equation (8.1.17) and the principle function definitions, (8.1.4), respectively:

$$\frac{\partial S_P}{\partial T} = -\frac{m}{2T^2}\left[(x_1 - x_0)^2 + (y_1 - y_0)^2\right] + \frac{f(y_1 + y_0)}{2} - \frac{f^2 T^2}{8m} = -H,$$
(8.1.30a)$_\text{x}$

$$\frac{dS_P}{dT} = \frac{m\dot{x}_0^2}{2} + \frac{m\dot{y}_0^2}{2} + fy_0 + 2fy_0 T + \frac{f^2 T^2}{m} = L. \quad (8.1.30b)_\text{x}$$

The consistency of the examples may be verified using solutions (8.1.26). Finally, the following energy derivative formula is important:

$$\frac{\partial S_H}{\partial \varepsilon} = T. \quad (8.1.31)$$

This follows from (8.1.25) and the fact that S_P does not depend explicitly on energy ($\partial S_P / \partial \varepsilon = 0$).

Examples involving curves with $S_H =$ constant are shown in Figure 8.1.6. The first figure, 8.1.6(a), shows a family of projectile trajectories with $H =$

$\varepsilon = 128$ J(oule) and $F = -4$ N(ewton). The corresponding generator curves $S_H(0, 0 : x, y) = 50, 100, 150, \ldots, $ J $\cdot$ s) and so forth are shown superimposed onto the trajectories in the second figure, 8.1.6(b). The curves with $S_H = 50$ to $S_H = 300$, or so, are ovals with increasing radius. They are clearly orthogonal to outgoing projectile trajectories in accordance with the equation (8.1.19):

$$0 = dS_H = \mathbf{p} \cdot d\mathbf{r}.$$

(a)

(b)
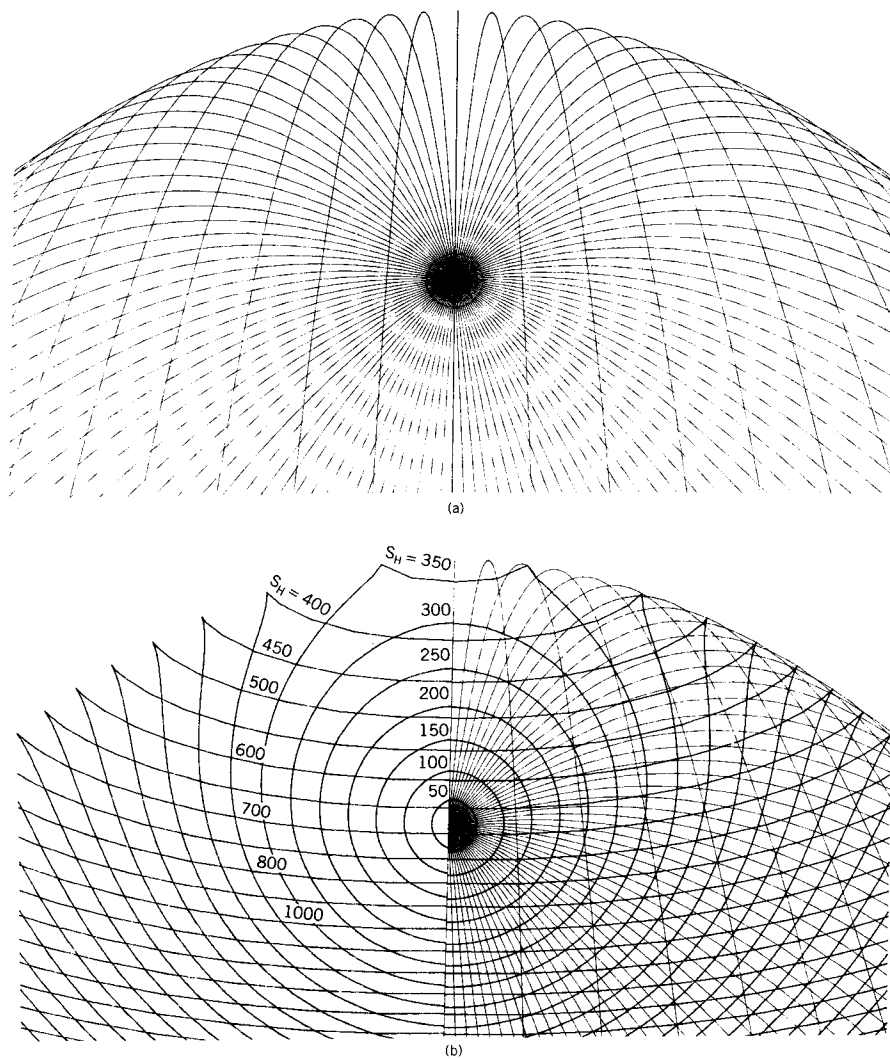
Figure 8.1.6 Classical trajectory families and constant characteristics action curves. (a) Isoenergetic family of trajectories. (b) Isoenergetic family of constant S_H curves.

For $S_H = 350$ or higher the curves vaguely resemble the outline of a bat's head with two ears pointing at the parabolic caustic that marks the classical turning points along the upper boundary of the trajectory region. The ears should be pointed cusps with zero angle at the points. The plot is not precise enough to show this for the first few bat's heads.

The S_H curves can be regarded as wave fronts emerging from the original point and propagating outward until they are reflected by the upper classical turning boundary. The reflected S waves are orthogonal to downward traveling trajectories. The time behavior of these S waves can be deduced by defining them in terms of Hamilton's principle action S_P for constant H:

$$S_P(\mathbf{0}, 0 : \mathbf{r}, T) = S_H(\mathbf{0} : \mathbf{r}) - HT = \text{constant}. \qquad (8.1.32)$$

Then a point $\mathbf{r} + d\mathbf{r}$ having the same S_P value at a later time would satisfy the equation

$$S_P(\mathbf{0}, 0 : \mathbf{r} + d\mathbf{r}, T + dT) - S_P(\mathbf{0}, 0 : \mathbf{r}, T) = 0 = dS_P. \qquad (8.1.33)$$

For constant $H = \varepsilon$ this becomes

$$dS_P = 0 = dS_H - \varepsilon \, dT,$$

$$0 = p \cdot d\mathbf{r} - \varepsilon \, dT. \qquad (8.1.34)$$

For $d\mathbf{r}$ chosen in the direction of the momentum vector $\dot{\mathbf{p}}$ this gives the S-wave phase velocity:

$$\frac{d|\mathbf{r}|}{dT} = \frac{\varepsilon}{|\mathbf{p}|}. \qquad (8.1.35)$$

In this simple example the $\mathbf{p}$ vector ($\mathbf{p} = m\mathbf{v} = m\dot{\mathbf{r}}$) points in the direction of the particle velocity $\dot{\mathbf{r}}$. This will not always be so. For a general Hamiltonian, the coordinate velocity

$$\dot{\mathbf{r}} = \frac{\partial H}{\partial \mathbf{p}}.$$

has a different direction and magnitude than $\mathbf{p}$. Note that the phase velocity (8.1.35) varies inversely with the momentum and (in this case) particle velocity. One can see in Figure 8.1.6(b) that the spacing between S-wave fronts decreases as the corresponding particles pick up speed. Particle velocity corresponds to group velocity in the wave picture, but one needs more than a single energy ε (or frequency $\nu = \varepsilon/h$) to observe it. The connection between action "wave fronts" and quantum waves will be discussed shortly.

It should be noted that the S-wave fronts do not generally have simple analytic expressions, particularly when one requires constant energy. The "bat's head" wave fronts in Figure 8.1.6(b) may be obtained by solving cubic equations derived from (8.1.24) and (8.1.25) at each point along a trajectory. The S_P equations (8.1.28) are deceptively simple equations for displaced circles; however, that is not for constant energy. Correct $T(\varepsilon)$ dependence leads again to cubic equations. So, even for this simple sophomore mechanics problem the analytic treatment of action is difficult!

Since exact analytic action expressions are going to be difficult or impossible in most problems, one needs to try other approaches. A general numerical approach which turns out to be quite simple involves numerical integration of the first-order Hamilton's equations:

$$\dot{\mathbf{q}} = \frac{\partial H}{\partial \mathbf{p}}, \tag{8.1.36a}$$

$$\dot{\mathbf{p}} = -\frac{\partial H}{\partial \mathbf{q}}, \tag{8.1.36b}$$

$$\dot{S}_P = L = \mathbf{p}\dot{\mathbf{q}} - H. \tag{8.1.36c}$$

In this way an arbitrary Hamiltonian (even a time-dependent one) can be converted into a family of trajectories and action surfaces. The desired constant-S_H surfaces are contours of constant $= (S_P + Ht)$. In fact, this technique for solving the HJ partial differential equation is known as "integration along characteristics." For this reason S_H is also known as a characteristic function or integral.

We will consider how the classical equations of motion may be used to find multidimensional quantum eigenfunctions using coherent wave and wave-packet propagation properties. Now we consider the elementary connection between the S waves of the HJ equation and the ψ waves of the Schrödinger equation.

D. Semiclassical Approximation for Schrödinger Equation

We have seen that the action function S_P behaves very much like a wave phase function. It is instructive to study the substitution

$$\psi(r, t) = \psi_0 e^{iS_P/\hbar} \tag{8.1.37}$$

in Schrödinger's equation:

$$i\hbar \frac{\partial \psi}{\partial t} = H\psi = \left[(1/2m)p^2 + V(\mathbf{r}) \right]\psi$$

$$= -(\hbar^2/2m)\nabla^2\psi + V(\mathbf{r})\psi.$$

The result is (we drop the subscript p from the action)

$$-\psi\frac{\partial S}{\partial t} = -\psi(\hbar i/2m)\,\nabla^2 S + \psi\left[(1/2m)\left(\frac{\partial S}{\partial \mathbf{r}}\right)^2 + V\right]$$

$$(\hbar i/2m)\,\nabla^2 S = \frac{\partial S}{\partial t} + H\left(\frac{\partial S}{\partial r},\mathbf{r}\right) \qquad (8.1.38)$$

In a limit in which the left-hand term vanishes, the Schrödinger equation reduces to the HJ equation (8.1.17). This is the semiclassical limit in which $\hbar\nabla^2 S \ll (\nabla S)^2 = p^2$, or

$$\hbar\frac{d^2 S}{dx^2} = \hbar\frac{dp}{dx} \ll p^2.$$

By using the de Broglie relation $p = \hbar k = h/\lambda$ this becomes

$$\frac{dk}{dx}\bigg/k \ll k = 2\pi/\lambda. \qquad (8.1.39)$$

This states that the wavelength should be small enough so that the percentage change of momentum over a wavelength is a negligible fraction.

E. Huygen's Principle and Semiclassical Mechanics

The properties of envelope curves generated by contact transformations in semiclassical mechanics are closely connected with Huygen's principle of enveloping wave crests in the study of optics. In both studies there are wave fronts generated by functions $S(\mathbf{r}_0 : \mathbf{r})$ which depend upon extrema or stationary values of path integrals.

Consider a hypothetical action function $S_H(\mathbf{r}_0 : \mathbf{r})$ which would generate the curves (or surfaces) indicated in Figure 8.1.7; i.e., $S_H(\mathbf{r}_0 : \mathbf{r}) = 10$, 20, and 30 for fixed $\mathbf{r}_0$. Consider two points $\mathbf{r}_{10}$ and $\mathbf{r}'_{10}$ on the $S_H(\mathbf{r}_0 : \mathbf{r}) = 10$ wave front. They both required an accumulation of (at least) 10 units of action S_H for a trajectory that started at their common point of origin $\mathbf{r}_0$ with energy H held fixed. From each of these points one might generate a new set of constant action surfaces: $S_H(\mathbf{r}_{10}, \mathbf{r}) = 10$ around $\mathbf{r}_{10}$ and $S_H(\mathbf{r}'_{10}, \mathbf{r}) = 10$ around $\mathbf{r}'_{10}$. Points on these new curves represent a total expenditure of 20 units of action since departure from $\mathbf{r}_0$. But, on each of these intermediate curves there is only one point ($\mathbf{r}_{20}$ and $\mathbf{r}'_{20}$, respectively) for which *at least* 20 units of action is required to arrive there from $\mathbf{r}_0$. These are the contact points of the intermediate curves with the larger $S_H(\mathbf{r}_0 : \mathbf{r}) = 20$ curve. The contact points lie on the natural trajectory through the intermediate points
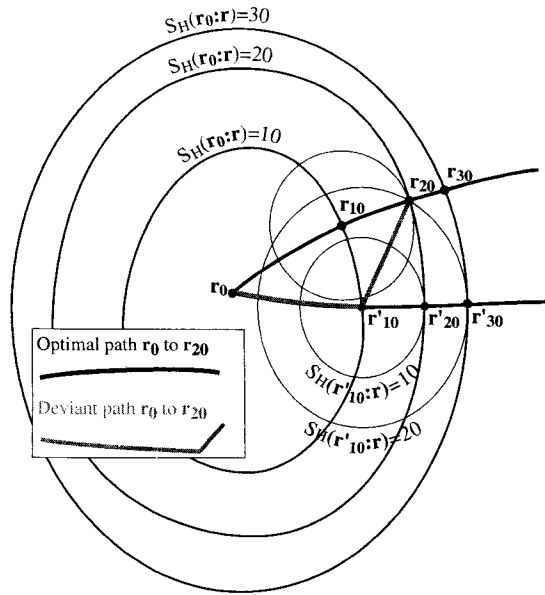
Figure 8.1.7 Comparison of paths and wave fronts for discussion of Huygen's principle. Paths which have locally extreme (i.e., minimal) values of S_H will lead to constructive interference and the formation of wave fronts which are envelopes of the wavelets belonging to nonextreme paths.

r_{10} and r'_{10}, respectively, since they correspond to extreme values of S_H according to the least-action principle.

To arrive at r_{20} by way of r'_{10}, for example, would require more than 20 action units. Figure 8.1.7 indicates the value would be 30; i.e., $S_H(r_0 : r'_{10}) + S_H(r'_{10} : r_{20}) = 30$. Only for trajectories which pass over or very near to $r = r_{10}$ will the action $S_H(r_0 : r_{20})$ achieve this minimum stationary value of 20 units.

In wave optics the same sort of reasoning is applied, only the S_H function is replaced by the optical travel-time function $T(r_0 : r)$

$$T(r_0 : r) = \int_{r_0}^{r} n \, ds,$$

(along optical path)

where $n = n(r)$ is the local index of refraction. The function T is called the INDICATRIX or "slowness" function, since the index n is inversely proportional to optical phase velocity. According to Fermat's principle, travel time $T(r_0 : r)$ is minimum for an optical path. The reason for this is that only the light near a stationary path will undergo constructive interference with other waves following nearby paths. Light waves which take the "wrong paths" interfere destructively; i.e., they "beat" each other to death!

Similarly, there are "wrong paths" in classical mechanics, such as path $(\mathbf{r}_0 \mathbf{r}'_{10} \mathbf{r}_{20})$ in Figure 8.1.7. The right paths, such as path $(\mathbf{r}_0 \mathbf{r}_{10} \mathbf{r}_{20})$, satisfy Newton's, Lagrange's, or Hamilton's equations along their entire lengths and thereby achieve locally minimum (and *stationary*) accumulations of the action S_H. This leads to an accumulation of the wave function due to constructive interference. The resulting waves have crests which parallel the enveloping constant action surfaces. (S_H = constant.)

The wavelike properties of action are one of the ingredients of the theory for Feynman's path integrals. The action functions are the phases of propagators which can be time dependent as in the following:

$$\langle \mathbf{r}_1, t_1 | \mathbf{r}_0, t_0 \rangle \simeq e^{iS_P(\mathbf{r}_0, t_0 : \mathbf{r}_1, t_1)}$$

or time independent with energy fixed as in the following:

$$\langle \mathbf{r}_1 | \mathbf{r}_0 \rangle \simeq e^{iS_H(\mathbf{r}_0 : \mathbf{r}_1)}.$$

Here $\langle A | B \rangle$ is the quantum probability amplitude for going from B to A as introduced in Section 1.1. Note that the completeness relation for amplitudes would require the following:

$$\langle \mathbf{r}_1 | \mathbf{r}_0 \rangle = \sum_{r'} \langle \mathbf{r}_1 | \mathbf{r}' \rangle \langle \mathbf{r}' | \mathbf{r}_0 \rangle \cong \sum_{r'} e^{iS_H(\mathbf{r}_0 : \mathbf{r}') + S_H(\mathbf{r}' : \mathbf{r}_1)}$$

$$\cong e^{iS_H(\mathbf{r}_0 : \mathbf{r}_1)}.$$

This is an algebraic statement of Huygen's principle as it applies to semiclassical paths. It also represents the starting point for the Feynman path-integral approach to quantum mechanics. This approach generally requires sums over *all* paths between end points.

The technology required to perform sums over *all* possible paths has not been developed to the point where it is generally applicable. For this reason the Feynman-Huygen path-integral approach to quantum mechanics is not used as much as it might be. However, for oscillating and rotating molecules there appears to be some simple ways to circumvent some of the difficulties associated with evaluating path sums. These new approaches involve the use of wave-packet or coherent-wave states, and this is discussed in the following sections.

8.2 COHERENT HARMONIC OSCILLATOR STATES

The eigenstates and ladder operators for a harmonic oscillator Hamiltonian of the form

$$H = (1/2\mu)p^2 + (\mu\omega^2/2)x^2 = \hbar\left(a^\dagger a + \tfrac{1}{2}\right) \qquad (8.2.1)$$

were derived in Section 4.4 for the case ($\omega = 1$). Excited eigenstates $|n\rangle$ may be defined by

$$|n\rangle = (a^\dagger)^n|0\rangle/\sqrt{n}\,! \qquad\qquad (8.2.2)$$

in terms of action on a ground state $|0\rangle$ by the creation operator

$$a^\dagger = (\mu\omega/2\hbar)^{1/2}(x - ip/\mu\omega). \qquad\qquad (8.2.3)$$

The destruction operators $a = (a^\dagger)$ and $a^\dagger$ generate an algebra whose representation in the $|n\rangle$ basis is defined by

$$a^\dagger|n\rangle = \sqrt{n+1}\,|n+1\rangle, \qquad\qquad (8.2.4\text{a})$$

$$a|n\rangle = \sqrt{n}\,|n-1\rangle, \qquad\qquad (8.2.4\text{b})$$

and

$$H|n\rangle = \hbar\omega\left(n + \tfrac{1}{2}\right)|n\rangle. \qquad\qquad (8.2.5)$$

The ground-state wave function

$$\langle x|0\rangle = \psi_0(x) = (\mu\omega/\pi\hbar)^{1/4}e^{-(\mu\omega/2\hbar)x^2}$$
$$= N_0 e^{-y^2/2} \qquad\qquad (8.2.6)$$

has the indicated Gaussian form. Using operations (8.2.2) and (8.2.3) one can generate from ψ_0 the other eigenfunctions

$$\psi_n(x) = N_0\left(\tfrac{1}{2}\right)^{n/2}H_n(y)e^{-y^2/2}/\sqrt{n}\,! \qquad\qquad (8.2.7)$$

in terms of the well-known Hermite polynomials $H_n(y)$ where the rescaled variable $y = (\mu\omega/\hbar)^{1/2}x$ is used. [Recall Eqs. (4.4.68)–(4.4.70).]

Now we consider other types of states or wave functions which can be generated from $|0\rangle$ or $\psi_0(x)$. Throughout the preceding chapters we have emphasized the use of states of the form $g|0\rangle$ or $P^\mu|0\rangle$ generated by action of group translation or projection operators on a localized state. Here this will lead to the idea of the coherent state and theories of wave-packet propagation.

The idea of translating the ground state is actually a quite natural one. Upon encountering a pendulum, spring-mass system, or other harmonic oscillator sitting quietly somewhere, most people would have the urge to disturb it. Some might simply pull it off its equilibrium position and let it go, while others more prone to violence might deliver an additional hefty impulse of momentum. We now do the same using various operators on the ground state $|0\rangle$.

The operator which moves a wave function by x_0 units in the translation or displacement operator defined by

$$D(x_0) = e^{-x_0(\partial/\partial x)} = e^{-ix_0 p/\hbar}.\qquad (8.2.8)$$

It performs the following functional translation:

$$D(x_0)\chi(x) = e^{-x_0(\partial/\partial x)}\chi(x)$$

$$= \chi(x_0) - x_0\frac{\partial\chi}{\partial x}\bigg|_0 + (x_0^2/2!)\frac{\partial\chi^2}{\partial x^2}\bigg|_0 - (x_0^3/3!)\frac{\partial^3\chi}{\partial x^3}\bigg|_0 + \cdots$$

$$= \chi(x - x_0).\qquad (8.2.9)$$

Similarly, the operator which boosts momentum by p_0 units is defined by

$$B(p_0) = e^{ip_0 x/\hbar} \qquad (= e^{-p_0(\partial/\partial p)}),\qquad (8.2.10)$$

where the parenthetical expression is the momentum space representation.

When combining these operations one observes that they do not commute and so the question arises: Should displacement or boost go first? A fair settlement involves defining a symmetric combination as follows:

$$Q(x_0, p_0) = e^{(i/\hbar)(p_0 x - x_0 p)}.\qquad (8.2.11)$$

Then we use a special case of the Baker-Campbell-Hausdorf theorem

$$e^{A+B} = e^A e^B e^{-[A,B]/2} = e^B e^A e^{[A,B]/2},\qquad (8.2.12)$$

which holds if

$$[A[A,B]] = 0 = [B,[A,B]].\qquad (8.2.13)$$

This shows that the Q operator can be factored either way:

$$Q(x_0, p_0) = e^{(i/\hbar)p_0 x}e^{(-i/\hbar)x_0 p}e^{-(x_0 p_0/2\hbar^2)[x,p]}$$

$$= e^{-ix_0 p_0/2\hbar}B(p_0)D(x_0) = e^{ix_0 p_0/2\hbar}D(x_0)B(p_0).\qquad (8.2.14)$$

We can also factor this operator when x and p are expressed in terms of $(a, a^\dagger)$ operators by solving (8.2.3) and its conjugate. We have

$$Q(x_0, p_0) = e^{ip_0(a+a^\dagger)/(2\hbar\mu\omega)^{1/2} - x_0(a-a^\dagger)(\mu\omega/2\hbar)^{1/2}}$$

$$= e^{\alpha_0 a^\dagger + \alpha_0^* a} = e^{-\alpha_0^*\alpha_0/2}e^{\alpha_0 a^\dagger}e^{\alpha_0^* a},\qquad (8.2.15a)$$

where we define a phase space position number

$$\alpha_0 \equiv [x_0 + ip_0/(\mu\omega)](\mu\omega/2\hbar)^{1/2}. \qquad (8.2.15b)$$

Also, the commutation relation $[a, a^\dagger] = 1$ was used.

Let us define by $|\alpha_0\rangle$ the state obtained by operating with $Q(x_0, p_0)$ on the ground state $|0\rangle$:

$$|\alpha_0\rangle = Q(x_0, p_0)|0\rangle = e^{-|\alpha_0|^2/2}e^{\alpha_0 a^\dagger}|0\rangle$$

$$= e^{-|\alpha_0|^2/2} \sum_n (\alpha_0 a^\dagger)^n |0\rangle/n!. \qquad (8.2.16)$$

Here only the creation operator exponential contributes since $(a|0\rangle = 0)$. Using (8.2.2) one finds the expression

$$|\alpha_0\rangle = e^{-|\alpha_0|^2/2} \sum_n (\alpha_0)^n |n\rangle/\sqrt{n}\,!, \qquad (8.2.17)$$

which is the COHERENT or MINIMUM UNCERTAINTY wave-packet state. This type of state was first considered by Schrödinger and later applied and generalized by Schwinger, Glauber, and others. We consider its dynamical properties as time evolves.

The time evolution operator

$$T(t, 0) = e^{-itH/\hbar} \qquad (8.2.18)$$

produces solutions $(|\chi(t)\rangle = T(t, 0)|\chi(0)\rangle)$ to the time-dependent Schrödinger equation $(i\hbar|\chi\rangle = H|\chi\rangle)$. The evolution of eigenstates is simple:

$$|n(t)\rangle = T(t)|n(0)\rangle = e^{-i\omega(n+1/2)t}|n(0)\rangle, \qquad (8.2.19)$$

that is, no change except for an overall phase factor whose angular frequency is determined by the energy eigenvalue (8.2.5) and Planck's law $(\omega = E/\hbar)$. However, the evolution of a combination of eigenstates such as (8.2.17) may be much more complicated because different frequencies interfere.

Applying the evolution operator to coherent state $|\alpha_0\rangle$ yields

$$T(t)|\alpha_0\rangle = e^{-|\alpha_0|^2/2} \sum_n (\alpha_0)^n e^{-i\omega t(n+1/2)}|n\rangle/\sqrt{n}\,!$$

$$= e^{-i\omega t/2} e^{-|\alpha_0|^2/2} \sum_n (\alpha_0 e^{-i\omega t})^n |n\rangle/\sqrt{n}\,!. \qquad (8.2.20a)$$

This can be expressed in a simpler form:

$$T(t)|\alpha_0\rangle = e^{-i\omega t/2}|\alpha_t\rangle, \qquad (8.2.20b)$$

where the position number simply rotates with frequency ω in the complex plane:

$$\alpha_t = \alpha_0 e^{-i\omega t}. \tag{8.2.20c}$$

It is instructive to regard the complex quantity α_t as the POSITION PHASOR. A phasor is a common visualization aid which was introduced in Section 2.6 for discussing classical oscillation. Phasor space is the same as phase space except that the momentum or p axis is scaled down, by a factor $(\mu\omega)$ so that all orbits are circular. It is pedagogically useful to regard the complex α_t-phasor vector as a clock's sweep second hand which, according to (8.2.20c), moves clockwise at the rate of ω rad $\cdot$ Hz.

Therefore, the picture of an evolving coherent state is fairly simple: Imagine a phase space wave packet centered on the tip of the phasor α_t and orbiting around the phase clock as in Figure 8.2.1. The uncertainty $(\Delta p)(\Delta x)$ is the same for this state at all times as it is for the ground eigenstate, i.e., the absolute minimum value allowed by Heigenberg's relation:

$$(\Delta p)(\Delta x) = \hbar/2.$$

The coherent or minimum uncertainty state is just the ground state pulled off center in phase space.
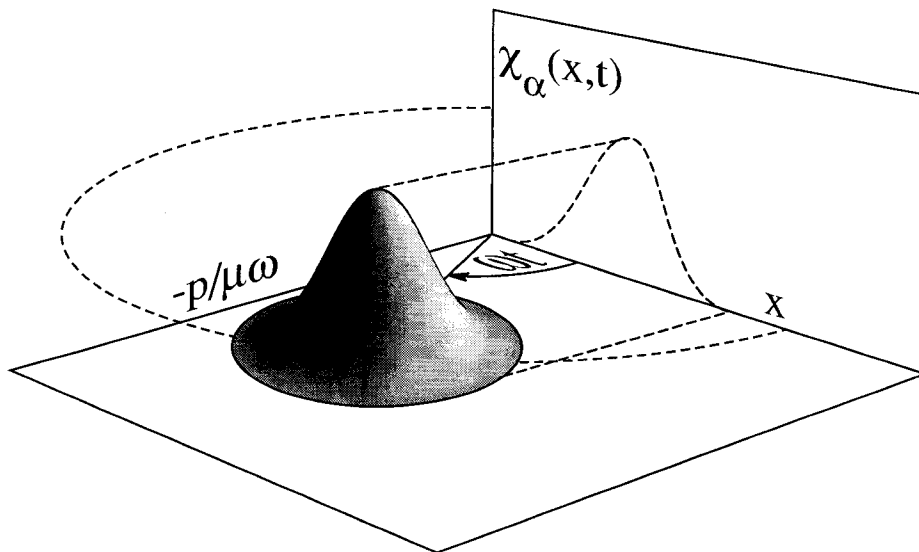
Figure 8.2.1   Sketch of wave packet rotating in phase plane. Corresponding classical phasor is indicated by vector α at the center of the phase plane distribution.

In order to plot the coherent wave packet in coordinate x space one needs the time-dependent translation operator in spatial form. Using the notation $Q(\alpha) = Q(x, p)$ the time transformation of Q is

$$TQ(\alpha_0)T^\dagger = e^{\alpha_0 T^\dagger aT + \alpha_0^* TaT^\dagger} = \exp\left(\alpha_0 e^{-i\omega t}a^\dagger + \alpha_0^* e^{i\omega t}a\right)$$
$$= Q(\alpha_t), \tag{8.2.21}$$

where the creation evolution is $Ta^\dagger T^\dagger = e^{-i\omega t}a^\dagger$. The classical phase components

$$x_t = x_0 \cos \omega t + (p_0/\mu\omega)\sin \omega t, \tag{8.2.22a}$$

$$p_t = p_0 \cos \omega t - x_0\mu\omega \sin wt \tag{8.2.22b}$$

of phasor

$$\alpha_t = \left[x_t + i(p_t/\mu\omega)\right](\mu\omega/2\hbar)^{1/2} \tag{8.2.22c}$$

are determined through (8.2.15b) and (8.2.20c). These components are the $|\alpha_t\rangle$ expectation values of position and momentum. This follows from the action of (a) and $(a^\dagger)$ on $|\alpha_t\rangle$ using (8.2.4):

$$a|\alpha_t\rangle = \alpha_t|\alpha_t\rangle, \tag{8.2.23a}$$

$$\langle\alpha_t|a^\dagger = \alpha_t^*\langle\alpha_t|. \tag{8.2.23b}$$

Then one has

$$\langle\alpha_t|x|\alpha_t\rangle = (2\hbar/\mu\omega)^{1/2}(\alpha_t + \alpha_t^*)/2$$
$$= x_t, \tag{8.2.24a}$$

$$\langle\alpha_t|p|\alpha_t\rangle = (2\mu\omega\hbar)^{1/2}(\alpha_t - \alpha_t^*)/2i$$
$$= p_t. \tag{8.2.24b}$$

The expectation value for the energy is constant, but the classical and quantum values differ slightly. The classical value is

$$E_c = \left(p_t^2/2\mu\right) + \tfrac{1}{2}\mu\omega^2 x_t^2 = |\alpha_t|^2\hbar\omega = |\alpha_0|^2\hbar\omega$$
$$= \langle\alpha_t|a^\dagger a|\alpha_t\rangle\hbar\omega = \langle n\rangle\hbar\omega, \tag{8.2.25}$$

where we note that average n is equal to $|\alpha|^2$. The quantum expectation value

$$E_q = \langle\alpha_t|H|\alpha_t\rangle = \langle\alpha_t|a^\dagger a + \tfrac{1}{2}|\alpha_t\rangle\hbar\omega$$
$$= E_0 + \hbar\omega/2 \tag{8.2.26}$$

is greater than E_c by the zero-point energy. The zero-point energy is the energy of state $|0\rangle$, which is the only state which is both a coherent state ($\alpha = 0$) and an eigenstate ($n = 0$) for the harmonic oscillator.

We can now derive the coherent wave function as a function of time. Combining (8.2.20) and (8.2.21), we have

$$\chi_{\alpha_0}(x,t) \equiv \langle x|T(t,0)|\alpha_0\rangle = \langle x|Q(\alpha_t)|0\rangle e^{-i\omega t/2}.$$

Now rewriting Q using (8.2.14), we obtain

$$\chi_{\alpha_0}(x,t) = e^{-ix_t p_t/2\hbar}\langle x|B(p_t)D(x_t)|0\rangle e^{-i\omega t/2}$$

$$= e^{-ix_t p_t/2\hbar+ip_t x/\hbar}D(x_t)\chi_0(x)e^{-i\omega t/2}, \qquad (8.2.27)$$

where (8.2.10) was used. Finally using (8.2.6) and (8.2.9), we get the coherent wave-packet formula:

$$\chi_{\alpha_0}(x,t) = e^{ix_t p_t/2\hbar-i\omega t/2}\left\{N_0 e^{-(\mu\omega/2\hbar)(x-x_t)^2+ip_t(x-x_t)/\hbar}\right\}. \qquad (8.2.28)$$

The real part (Re χ_α) and modulus ($|\chi_\alpha|$) of the coherent wave functions are plotted in Figures 8.2.2(a) and 8.2.2(b). Ten snapshots are shown for equal time intervals following the setting of classical initial conditions ($x = x_0$, $p = 0$). The x_0 value is chosen so that the classical energy $E_c = |\alpha_0|^2\hbar\omega$ is exactly five quanta ($5\hbar\omega$) in Figure 8.2.2(b) and 20 quanta in Figure 8.2.2(a). Note how the wave packet develops phase wrinkles inside a Gaussian modulus envelope as time increases. The envelope follows a classical oscillator trajectory but does not change its shape. The wrinkles inside are simply a measure of the momentum that packet has at each instant. It is interesting to note that the packet develops a wrinkle long before it has moved even a fraction of its length. This is because momentum and position grow linearly and quadratically, respectively, with time.

Because of this "early wrinkling" the quantum overlap of the $\chi_\alpha(t)$ packet with the initial $\chi_\alpha(0)$ function will vanish long before the packet has moved out of its initial neighborhood. One might view the wave packet as moving uniformly around the phasor clock in Figure 8.2.1, so that initially all its motion is along the imaginary p axis of momentum.

The bracketed factor in the wave function (8.2.28) represents the Gaussian packet with average momentum p_t, and it is centered around position x_t. The phase factor outside the bracket can be shown to be consistent with some fundamental views of quantum theory which are loosely referred to as action integral formalism or Feynman path integrals, which is mentioned in Section 8.3.
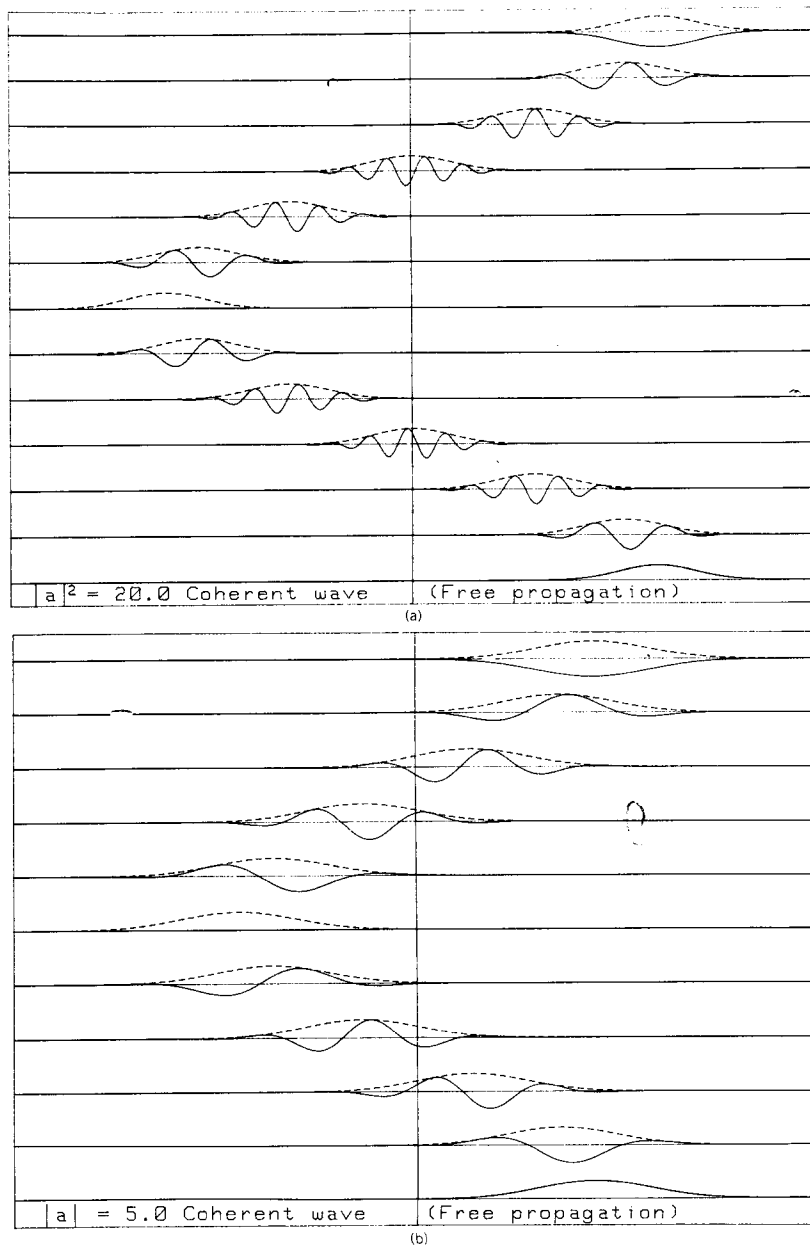
Figure 8.2.2 Coherent state wave packets at various times during oscillation.

According to these views one can associate each classical path with a so-called propagator θ of the form

$$\theta = e^{iS/\hbar}, \tag{8.2.29a}$$

where S_P is the principal action function given by (8.1.4); that is,

$$S_P = \int_0^t L\, dt, \tag{8.2.29b}$$

and L is the Lagrangian function which is related to the Hamiltonian H for the harmonic oscillator as follows:

$$L = p^2/2\mu - (\mu\omega^2/2)x^2 = p\frac{dx}{dt} - H. \tag{8.2.30}$$

If in the integral involving just $p\dot{x}$ [the integral of L without the H term is the "reduced action" S_H given by (8.1.7)] one takes coherent state expectation values of x and p, then one has

$$S_H = \int_0^t p_t\, dx_t = \int \left[2\mu\left(E_c - (\mu\omega^2/2)x_t^2\right)\right]^{1/2} dx_t$$

$$= x_t p_t/2 \big|_0^t + (E_c/\omega)\sin^{-1}\left(\frac{\mu\omega}{\sqrt{2\mu E_c}}x_t\right)\bigg|_0^t$$

$$= (x_t p_t - x_0 p_0)/2 + E_c t. \tag{8.2.31}$$

Now by including the expected value of the H term (i.e., $E_q = E_c + \hbar\omega/2$) the propagator becomes

$$\theta = e^{iS_P/\hbar} = e^{i(x_t p_t - x_0 p_0)/2\hbar - i\omega t/2}, \tag{8.2.32}$$

which agrees with the phase factor outside of (8.2.28) except for the initial phase $x_0 p_0$, which was set to zero.

8.3 COHERENT WAVE GENERATION OF EIGENFUNCTIONS

The coherent wave $\chi_\alpha(x, t)$ is a combination of oscillator eigenfunctions $\langle x|n\rangle = \chi_n(x)$:

$$\chi_\alpha(x, t) = \sum_{n=0}^{\infty} c_n \langle x|n\rangle e^{-i(n+1/2)\omega t}, \tag{8.3.1a}$$

where the coefficients

$$c_n = e^{-|\alpha|^2/2}(\alpha)^n/\sqrt{n}\,! \tag{8.3.1b}$$

follow from (8.2.17) and are amplitudes of a Poisson distribution. Examples of this distribution are shown in Figure 8.3.1 for a variety of α values. These are simple cases of what are called Frank-Condon overlap distributions in vibrational spectroscopy. Each distribution peaks for the coefficient c_n for which n is nearest to $|\alpha|^2$. The width of each distribution is roughly determined by

$$\Delta n = \left(\langle n^2 \rangle - \langle n \rangle^2\right)^{1/2} = \left(\langle \alpha|a^\dagger a a^\dagger a|\alpha \rangle - \langle \alpha|a^\dagger a|\alpha \rangle^2\right)^{1/2} \tag{8.3.2}$$
$$= |\alpha| = \langle n \rangle^{1/2},$$

i.e., the square root of n. For values of n outside of this width the coefficients c_n decrease rapidly. Hence, it is well known that χ_α can be well approximated by a relatively small number ($\sim 2\sqrt{n} = 2|\alpha|$) of terms in its infinite sum representation (8.3.1).

Until recently, it was not known that the "inverse" was true; that is, the same small number of time snapshots of a propagating $\chi_\alpha(x,t)$ wave could be combined to produce eigenfunctions χ_n. Since 1975 Heller, Davis, Tannor, DeLeon, and others have shown how to produce eigenfunctions in a variety of multidimensional potentials using this "inverse" idea. We consider the derivation of these ideas in connection with the one-dimensional harmonic oscillator.

The ideas are based upon an approximate but discrete Fourier inversion of expansion (8.3.1a) in the following form:

$$c_m \langle x|m \rangle \simeq \sum_{t_p=0}^{t_{n-1}} \chi_\alpha(x, t_p) e^{i(m+1/2)\omega t_p} \tag{8.3.3}$$

$$\simeq \sum e^{ix_t p_t(2\hbar)} e^{im\omega t_p} N_0 e^{-(\mu\omega/2\hbar)(x-x_t)^2 - ip_t(x-x_t)/\hbar}.$$

This approximate expression (8.3.3) would be exact if the sum was replaced by an integral $((1/\tau)\int_0^\tau dt)$, but here we are interested in showing that it is still very accurate for just a small number N of order $N \sim 4\sqrt{m}$ if we choose $|\alpha| \simeq \sqrt{m}$. For example, 10 terms ($N = 10$) or "snapshots" of $\chi_\alpha e^{i\phi(t)}$ with $|\alpha|^2 = 5$ and a phase $\phi(t) = (m + 1/2)\omega t_p$ for $p = 0, 1, \ldots, 9$ with $m = 5$ are drawn one above the other in Figure 8.3.2(a). Their sum is shown below in Figure 8.3.2(b) and it is seen to accurately reproduce the fifth excited eigenfunction $\langle x|5 \rangle$.

This inverse generation process might be described as an accumulation or "painting" of an eigenfunction by an oscillating phased packet. The accumu-
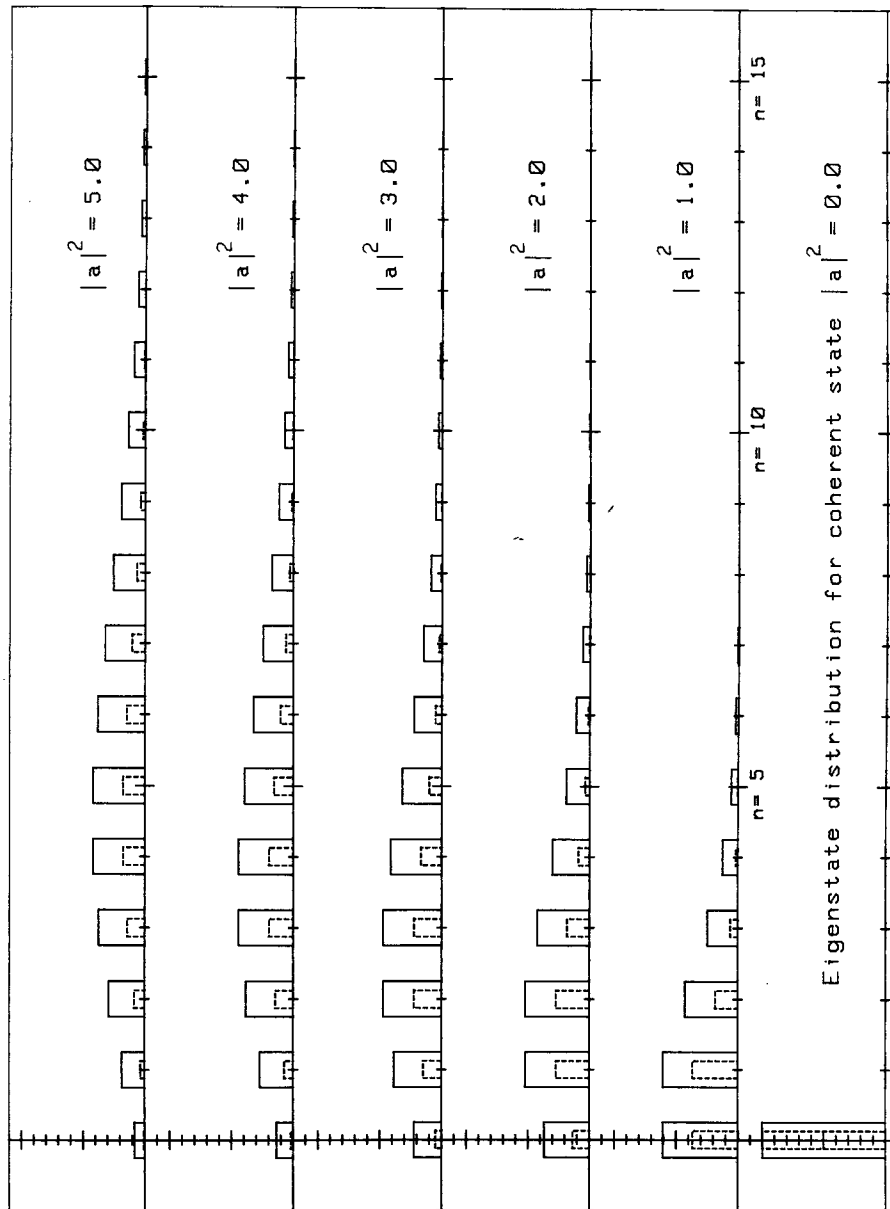
Figure 8.3.1 Poisson eigenstate distribution of amplitudes and probabilities in coherent state.

713
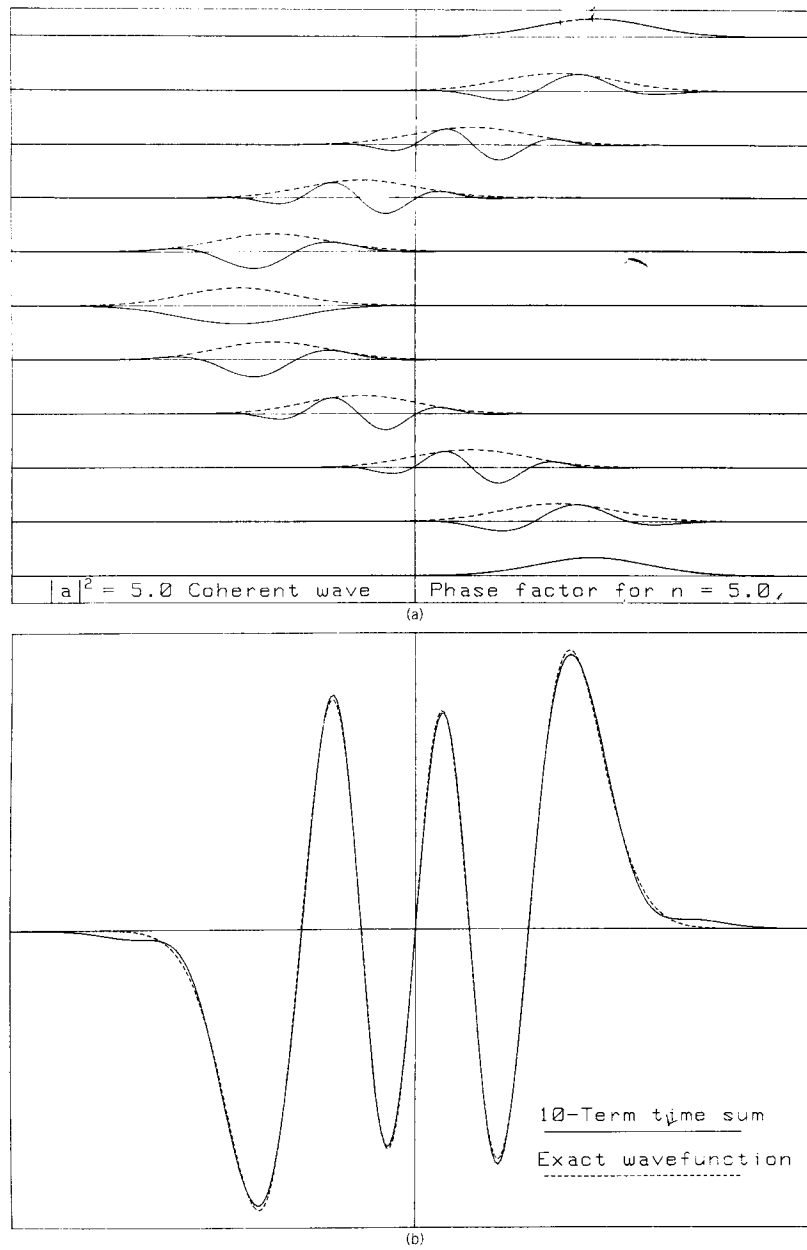
Figure 8.3.2   (a) Phased snapshots of coherent state. (b) Sum of snapshots in part (a) yields approximate eigenfunction.

lation of the same packet (i.e., $|\alpha|^2 = 5$) with a different phase (say one corresponding to $m = 4$) approximates a different eigenfunction (say $\langle x|4 \rangle$). In fact, one can try fractional m (say 4.75) in the phase, but such phases will cause the wave to destructively interfere or beat itself to death as time goes on. Only the integer values of m will continue to add constructively and to accumulate more and more of a particular eigenfunction $\langle x|m \rangle$ period after period. For integral m the phased packet is exactly periodic so only one period is needed. Any detuning of m from an integer leads to beating instead of accumulation; that is, the amplitude behaves like an undamped oscillator responding to a detuned force. We will come back to this idea of "tuning" later on.

Let us consider what the error will be in the approximation (8.3.3) for varying $|\alpha|^2$ and m. Consider a sum over N equally spaced time intervals within one oscillator period ($\tau = 2\pi/\omega$) of the form

$$(1/N) \sum_{t_p=0}^{t_{N-1}} \chi_\alpha(x, t_p) e^{i(m+1/2)t_p} = \sum_{n=0}^{\infty} c_n \langle n|x \rangle (1/N) \sum_{t_p=0}^{N-1} e^{i(m-n)2\pi p/N},$$

(8.3.4a)

where

$$t_p = 2\pi p/N \qquad (p = 0, 1, 2, \ldots, N-1) \tag{8.3.4b}$$

and (8.3.1a) was used. The sum on the extreme right-hand side of (8.3.4a) is a geometrical series which appears repeatedly in theoretical optics and spectroscopy. Setting $\delta = 2\pi(m-n)/N$ one has for this series the following:

$$\Sigma = \sum_{p=0}^{N-1} e^{ip\delta} = (1 + e^{i\delta} + e^{i2\delta} + \cdots + e^{i(N-1)\delta}), \tag{8.3.5}$$

or

$$e^{i\delta}\Sigma = e^{i\delta} + e^{i2\delta} + \cdots + e^{i(N-1)\delta} + e^{iN\delta}.$$

Subtracting the two foregoing series and solving gives

$$\Sigma = (1 - e^{iN\delta})/(1 - e^{i\delta}) = e^{i(N-1)\delta/2}[\sin(N\delta/2)]/\sin(\delta/2)$$

$$= e^{i(N-1)\pi(m-n)/N}[\sin \pi(m-n)]/\sin(\pi(m-n)/N). \tag{8.3.6}$$

The Σ function is called the spectral function in Section 8.4B(b). Here it determines the relative amounts of various eigenfunctions $\langle n|x \rangle$ which would show up in the wave-packet accumulation (8.3.4). If m is an integer then the

following expression results:

$$\Sigma = N\Big[\delta_{mn} + e^{i(N-1)\pi}\big(\delta_{m,n+N} \pm \delta_{m,n-N}\big)$$
$$+ e^{i2(N-1)\pi}\big(\delta_{m,n+2N} \pm \delta_{m,n-2N}\big) + \cdots\Big]. \qquad (8.3.7)$$

Substituting this into (8.3.4a) yields

$$(1/N)\sum_{t_p=0}^{t_{N-1}} \chi_\alpha(x,t_p)e^{(m+1/2)\omega t_p}$$
$$= c_m\langle m|x\rangle + e^{i(N-1)\pi}\big(c_{m+N}\langle m+N|x\rangle \pm c_{m-N}\langle m-N|x\rangle\big) + \cdots.$$
$$(8.3.8)$$

If N is large enough that $c_{m\pm N}, c_{m\pm 2N}, \ldots$, etc. are small compared to c_m, then (8.3.3) is a good approximation of the mth eigenfunction. Figure 8.3.1 shows the magnitude of the first correction coefficient c_{5+10} on the right-hand side of (8.3.8) for $(N = 10)$ and $(m = |\alpha|^2 = 5)$. The correction is a fraction

$$c_{15}/c_5 = \big[(5^{15}/15!)/(5^5/5!)\big]^{1/2} = 0.0299 \qquad (8.3.9)$$

of the desired result, that is, about 3%. This is about the error that is observed in Figure 8.3.2(b), and it shows up mostly at the turning points. Adding two more terms $(N = 12)$ would reduce the error to below 1%, and this shows how rapidly the accumulation procedure converges.

The accumulation procedure may be generalized to generate eigenfunctions for anharmonic potentials. In place of the wave packet in (8.3.3) or (8.2.28), one may accumulate the following wave function:

$$\chi(x,t) = e^{iS_P/\hbar}\big\{Ne^{-(\mu\omega/2\hbar)(x-x_t)^2+ip_t(x-x_t)/\hbar}\big\}, \qquad (8.3.10a)$$

where x_t and p_t are determined by *classical* Newton's or Hamilton's equations for the potential. The classical values are used to compute the action function

$$S_P = \int_0^t L\,dt = \int_0^t p_t\,dx_t - \int_0^t \langle\chi|H|\chi\rangle\,dt. \qquad (8.3.10b)$$

The Hamiltonian energy $\langle\chi|H|\chi\rangle$ is just the expectation value of H for wave function (8.3.10a) at time t. Eigenfunctions will be obtained in an accumulation of $(\chi e^{i\omega t})$ for those energies $E_q = \hbar\omega$ for which this quantity returns to its original value after one period. This is equivalent to demanding that

$$S = \int p_t\,dx_t - \int\langle H\rangle\,dt = 2\pi n\hbar,$$

which corresponds to the Bohr-Sommerfeld quantization rule.

A. Wave-Packet Propagation and Spectral Quantization

We describe here a semiclassical approximation which yields approximate eigenfunctions as well as eigenvalues. The original spectral quantization method was developed by De Leon and Heller for treating multidimensional anharmonic vibrational potentials. After describing the basic method we shall demonstrate an adaptation of it to rotational wave functions. The wave-packet quantization methods often use a minimum uncertainty state $|MU(q, p)\rangle$ or wave function $\langle|MU(q, p)\rangle$ which is localized around a certain point (q, p) in classical phase space. In the original formulation of this problem for vibrational mechanics, this state was chosen to be a (q, p) translation of an oscillator ground state. In this case the corresponding wave function $\langle|MU(q, p)\rangle$ is a translated complex Gaussian packet such as (8.2.28) but in several dimensions.

The method uses classical equations of motion to derive the time evolution of the phase variables $(p(t), q(t))$. It starts with a judicious choice of initial values $(p(0), q(0))$ which have a classical energy reasonably close to the eigenvalues that are desired. Then a path propagation state

$$|\Psi(t)\rangle = |MU(q(t), p(t))\rangle e^{(i/\hbar)S_p(t)} \qquad (8.3.11)$$

is obtained by numerically integrating the classical equations to obtain the phase variables $(q(t), p(t))$ and the classical action or Hamilton's principle function S_p:

$$S_p(t) = \int_0^t L\, dt = \int_0^t \left(\sum_i p_i \dot{q}_i - E_{cl} \right) dt. \qquad (8.3.12)$$

Generally, one defines a classical translation operator **CT** which has the effect of changing the (q, p) parameters of the wave packet to the correct classical values for each time t:

$$|MU(q(t), p(t))\rangle = \mathbf{CT}(q(t), p(t) : q(0), p(0))|MU(q(0), p(0))\rangle. \qquad (8.3.13)$$

The same **CT** operator can be used to set the initial wave packet, as well. The initial wave-packet expectation value of this operator, including the action phase, is called the time autocorrelation function:

$$\begin{aligned} AC(t) &\equiv \langle MU(q(0), p(0))|MU(q(t), p(t))\rangle e^{(i/\hbar)S_p(t)} \\ &= \langle \Psi(0)|\Psi(t)\rangle. \end{aligned} \qquad (8.3.14)$$

This function oscillates or "beats" each time the evolving wave packet returns on a classical path that is close enough to overlap with the initial

packet. The energy Fourier transform of the autocorrelation FTAC(E) provides information which can be used to generate eigenfunctions. The values $E = E_{FT}$ which are peaks of the following transform function,

$$\text{FTAC}(E) = \frac{1}{2T} \int_{-T}^{T} dt\, e^{(i/\hbar)Et} \text{AC}(t), \qquad (8.3.15)$$

can be used to obtain an approximate semiclassical eigenfunction by a Fourier integral of the propagation state:

$$|E_{FT}\rangle = \frac{1}{2T} \int_{-T}^{T} dt\, e^{(i/\hbar)E_{FT}t} |\Psi(t)\rangle. \qquad (8.3.16)$$

Finally, the desired semiclassical energy is computed by an expectation value of the quantum Hamiltonian:

$$E_{SC} = \langle E_{FT}|\mathbf{H}|E_{FT}\rangle / \langle E_{FT}|E_{FT}\rangle. \qquad (8.3.17)$$

This last step is necessary since, as we will see, the FTAC peaks $\{E_{FT}, E'_{FT}, \ldots\}$ may differ slightly from the desired quantum energy values $\{E_{SC}, E'_{SC}, \ldots\}$.

One way to understand the wave-packet method is to study the conditions which would cause (8.3.15) to have a peak or to make (8.3.16) keep accumulating a stationary state over longer and longer integration times. Such a peak or accumulation implies that E has been chosen so as to obtain a phase coherence or constructive interference each time the evolving wave packet returns to the neighborhood of the initial packet. This occurs when the action for a closed path satisfies certain quantization conditions. In general, these are the Einstein-Brillouin-Keller (EBK) quantization conditions applied to Hamilton's characteristic function S_H or "reduced action" given according to (8.1.7) by

$$S_H = S_p + Et = \int \mathbf{p} \cdot d\mathbf{q}. \qquad (8.3.18)$$

For a closed path the EBK quantization conditions are

$$\oint \mathbf{p} \cdot d\mathbf{q} = (n + \alpha)2\pi\hbar, \qquad (8.3.19)$$

where α is called the Maslov constant. In terms of the principle classical action (8.1.8) this gives

$$E_{SC}\tau + S_p = (n)2\pi\hbar, \qquad (8.3.20)$$

where τ is a classical period (or quasiperiod) for a closed (or nearly closed)

path and E_{SC} is the desired semiclassical approximation to the energy. This may be rewritten

$$E_{FT}\tau + S_p = (n)2\pi\hbar, \qquad (8.3.21)$$

where E_{FT} is a peak value in the FTAC (8.1.15). Let us write this as follows:

$$E_{FT} = E_{SC} + 2\pi\alpha\hbar/\tau. \qquad (8.3.22)$$

If the Maslov constant is not zero, then the value of E_{SC} is shifted from that of E_{FT}. From (8.3.14) one sees that condition (8.3.21) makes the phase in (8.3.15) or (8.3.16) come out to a multiple of 2π after classical period τ.

Hence the wave-packet method amounts to a numerical resonance or spectroscopy experiment in which one finds stationary states by "tuning" E to get a peak in (.3.15) and then "painting" the eigenfunction using (8.3.16). The resulting eigenfunction consists of a sum of a series of MU packets set out on a classical trajectory. The last step can be accomplished with a relatively small number of time steps. It is also helpful to "tune" the initial conditions $(q(0), p(0))$ in (8.3.13) to get the strongest peaks.

The rotational adaptation of wave-packet propagation involves a different type of minimum uncertainty state, phase variables, and classical translation operator. The latter is a rotation operator which affects the Euler angles $\{\alpha\beta\gamma\}$, and these angles are the rotational equivalent of phase variables. Recall from Section 7.4 that the angles $-\beta$, and $-\gamma$ are the RE surface coordinates. The wave-packet propagation can be viewed as taking place on the RE surface shown in Figure 7.4.1(b).

A form for the rotational wave packet is suggested by the discussion of angular-momentum cones in Section 7.4. A choice for a rotational minimum uncertainty wave packet is the wave function associated with the narrowest angular-momentum cone; that is,

$$|\mathrm{MU}(0,0,0)\rangle = \left|{J \atop J}\right\rangle. \qquad (8.3.23)$$

A good choice for an initial wave packet is one centered on some part of a quantizing RE surface path. Assuming that the point $(\beta = 0, \gamma = 0)$ is the center of an RE surface hill or valley, then the Kth quantizing path would be near to the point $(\beta_0 = -\Theta_K^J, \gamma_0 = 0)$. A suitable initial wave packet is therefore obtained by the following y rotation of initial state (23):

$$\left|\mathrm{MU}\left(0, -\Theta_K^J, 0\right)\right\rangle = \mathbf{R}\left(0, -\Theta_K^J, 0\right)|_J^J\rangle. \qquad (8.3.24)$$

(Negative Euler angles are used since the rotation is defined with respect to the body fixed frame.) The choice of initial angles is usually not so critical, but a good initial guess can reduce computational time somewhat.

The classically propagating wave-packet state (8.3.11) has the following form for the rotational problem:

$$|\Psi(t)\rangle = \mathbf{R}(\alpha(t),\beta(t),\gamma(t))|_J^J\rangle \exp[(i/h)S_p(t)]. \qquad (8.3.25)$$

The Euler angles and the action are obtained by numerical solutions of Hamilton's equations:

$$\dot{\delta} = \frac{\partial H}{\partial J_\delta}, \qquad \dot{J}_\delta = -\frac{\partial H}{\partial \delta}, \qquad \delta = \alpha, \beta, \gamma, \qquad (8.3.26a)$$

and

$$\dot{S}_p = L = J_\alpha \dot{\alpha} + J_\beta \dot{\beta} + J_\gamma \dot{\gamma} - E. \qquad (8.3.26b)$$

The initial conditions $(\alpha(0), \beta(0), \gamma(0))$ given by Eq. (8.3.24) may be used along with $S_p(0) = 0$ for the action.

The autocorrelation function is given in terms of the initial and final Euler angles:

$$AC(t) = \langle \Psi(0)|\Psi(t)\rangle = \left\langle \begin{matrix} J \\ J \end{matrix} \middle| \mathbf{R}^\dagger(\alpha(0),\beta(0),\gamma(0))\mathbf{R}(\alpha(t),\beta(t),\gamma(t)) \middle| \begin{matrix} J \\ J \end{matrix} \right\rangle$$

$$\times \exp[(i/h)S_p(t)]. \qquad (8.3.27)$$

The rotation product is reduced and represented by a Wigner D function:

$$AC(t) = \left\langle \begin{matrix} J \\ J \end{matrix} \middle| \mathbf{R}(\alpha_p, \beta_p, \gamma_p) \middle| \begin{matrix} J \\ J \end{matrix} \right\rangle \exp[(i/h)S_p(t)]$$

$$= D_{JJ}^J(\alpha_p, \beta_p, \gamma_p)\exp[(i/h)S_p(t)]. \qquad (8.3.28)$$

The group product rule and the D-function formula are given in Chapter 5. An example of a rotor autocorrelation function and its Fourier transform (8.3.15) are plotted in Figures 8.3.3(a) and 8.3.3(b), respectively. The beats due to the returning wave packet are shown in Figure 8.3.3(a). A peak in the transform at energy $E_{FT}(K = 8)$ has been singled out in Figure 8.3.3(b).

Each of the larger peaks $E_{FT}(K)$ indicates a possible eigensolution. According to Eqs. (8.3.16) and (8.3.24) the following state is an approximate eigenstate associated with that peak:

$$|E_{FT}(K)\rangle = \lim_{T \to \infty} \frac{1}{T} \int_{-T}^{T} dt \, \exp[(i/h)(E_{FT}(K) + S_p(t))]$$

$$\times \mathbf{R}(\alpha(t),\beta(t),\gamma(t)) \middle| \begin{matrix} J \\ J \end{matrix} \right\rangle. \qquad (8.3.29)$$
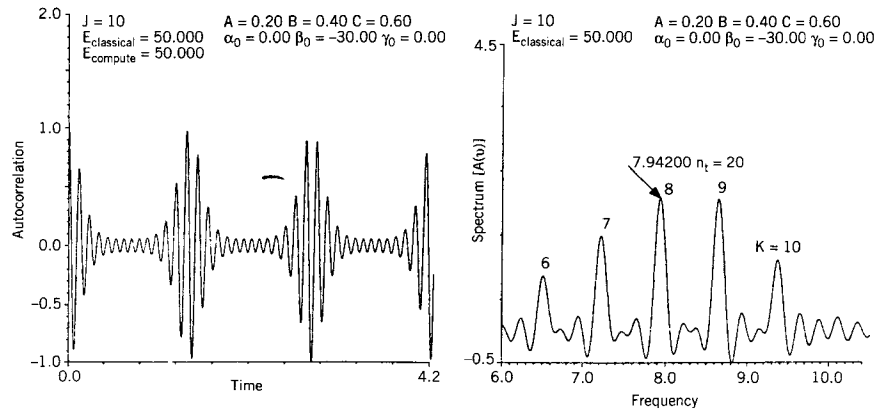
Figure 8.3.3   Wave-packet autocorrelation function and Fourier transform for asymmetric top. (a) Function AC(t) shows beats, (b) function FAC(ω) has peaks which correspond to possible eigenfunctions.

The representation of this state in the angular-momentum basis reduces to a Fourier transform of D functions:

$$\left\langle \frac{J}{K'} \,\middle|\, E_{\mathrm{FT}}(K) \right\rangle = \lim_{T \to \infty} \frac{1}{T} \int_{-T}^{T} dt \, \exp\!\left[(i/h)\left(E_{\mathrm{FT}}(K) + S_p(t) \right) \right]$$

$$\times D_{K'J}^{J*}\left(\alpha(t), \beta(t), \gamma(t) \right). \tag{8.3.30}$$

It can be shown that the coefficients (8.3.30) are always real. The coefficients for the example chosen in Figure 8.3.3(b) are the following:

$K' =$	10,	8,	6,	4,	2,	0,...
$\langle K' \vert E_{\mathrm{FT}}(8) \rangle =$	0.118,	0.929,	-0.339,	0.075,	-0.012,	0.001,...

(8.3.31)

These are to be compared with the exact values for a localized state, which are the following:

$$\alpha_{K'} = 0.129, 0.922, -0.347, 0.106, -0.062, 0.018, \ldots . \tag{8.3.32}$$

Finally, the semiclassical energy value for the wave-packet generated state (8.3.31) is given according to (8.3.17):

$$E_{\mathrm{SC}}(K = 8) = \left\langle E_{\mathrm{FT}}(8) \vert \mathbf{H} \vert E_{\mathrm{FT}}(8) \right\rangle / \left\langle E_{\mathrm{FT}}(8) \vert E_{\mathrm{FT}}(8) \right\rangle = 53.134. \tag{8.3.33}$$

This is to be compared with the quantum-mechanical values of 53.149 and 53.146 for the ($K = 8$) cluster. This completes an example of the most

elementary "bare bones" wave-packet propagation technique. More sophisticated treatments give more accurate wave functions and energy values by taking tunneling into account.

8.4 SEMICLASSICAL RADIATION THEORY FOR SPECTROSCOPY

The quantum theory of radiation and matter is absolutely necessary for an accurate analysis of the most detailed spectroscopic effects. However, such an analysis may be impractical for laser experiments which involve a large number of radiation quanta. In that case semiclassical theory of radiation is used to treat the radiation effects as classical perturbations of the quantum states of matter.

This section contains a description of quantum excitations in atoms or molecules due to classical radiation fields. This semiclassical approach will be compared with the purely classical oscillator resonance approach, which was discussed in Section 6.5. The concept of the oscillator strength of a quantum transition may be clearly stated through such a comparison.

Semiclassical theory of radiation and matter is usually treated using perturbation expansions. When the perturbations are only weakly resonant, one or two terms of such expansions contain most of the relevant information. Perturbation techniques are discussed at the end of this section. When the laser is resonant with a particular transition between two levels the perturbation approach is less convenient. Then one may use the two-level atom semiclassical approach which is discussed in the following Section 8.5. We will set the stage for a comparison of these approaches.

The first part of this section will be devoted to developing the classical formulation of electromagnetic interactions with matter. This includes a rather ticklish and still somewhat controversial question of $\mathbf{A} \cdot \mathbf{p}$ versus $\mathbf{E} \cdot \mathbf{r}$ interaction Hamiltonians.

A. Lagrangians and Hamiltonians for Electromagnetic Interactions

The derivation of the Lagrangian and Hamiltonian equations for the interaction of a particle or mass μ with electric and magnetic fields $\mathbf{E}$ and $\mathbf{B}$ begins with Newton's equation and the electromagnetic force relations:

$$\mu \frac{d\mathbf{v}}{dt} = \mathbf{F} = q[\mathbf{E} + \mathbf{v} \times \mathbf{B}] = q\left[-\nabla\Phi - \frac{\partial\mathbf{A}}{\partial t} + \mathbf{v} \times (\nabla \times \mathbf{A}) \right].$$

This expands to the following:

$$\mu \frac{d\mathbf{v}}{dt} = q\left[-\nabla\Phi - \frac{\partial\mathbf{A}}{\partial t} + \nabla(\mathbf{v} \cdot \mathbf{A}) - (\mathbf{v} \cdot \nabla)\mathbf{A} \right]. \qquad (8.4.1a)$$

Here the electric and magnetic fields are expressed in terms of scalar and vector potential fields Φ and $\mathbf{A}$, respectively:

$$\mathbf{E} = -\nabla\phi - \frac{\partial A}{\partial t}, \qquad \mathbf{B} = \nabla \times \mathbf{A}. \qquad (8.4.1b)$$

The total derivative of $\mathbf{A}$ experienced by the moving particle is

$$\frac{d\mathbf{A}}{dt} = \frac{\partial \mathbf{A}}{\partial t} + (\mathbf{v} \cdot \nabla)\mathbf{A}. \qquad (8.4.2)$$

Then the Lagrangian form of the force can be written as follows;

$$\mathbf{F} = \mu\frac{d\mathbf{v}}{dt} = q\left[-\frac{d\mathbf{A}}{dt} - \nabla(\Phi - \mathbf{v} \cdot \mathbf{A}) \right],$$

$$F = \mu\frac{d\mathbf{v}}{dt} = \frac{d}{dt}\frac{\partial}{\partial \mathbf{v}}(q\Phi - q\mathbf{v} \cdot \mathbf{A}) - \nabla(q\Phi - q\mathbf{v} \cdot \mathbf{A}). \qquad (8.4.3)$$

The Lagrangian function defined by

$$L = \mu(\mathbf{v} \cdot \mathbf{v})/2 - (q\Phi - q\mathbf{v} \cdot \mathbf{A}) \qquad (8.4.4a)$$

then satisfies the Lagrangian form of Newton's equations; that is,

$$\frac{d}{dt}\frac{\partial L}{\partial \mathbf{v}} - \frac{\partial L}{\partial \mathbf{r}} = 0. \qquad (8.4.4b)$$

The canonical form for the Hamiltonian function is found by Legendre transformation of L:

$$H = \Sigma\dot{q}_j p_j - L = \mathbf{v} \cdot \frac{\partial l}{\partial \mathbf{v}} - L \qquad \left(H = \frac{\mu}{2}(\mathbf{v} \cdot \mathbf{v}) + q\Phi \right), \qquad (8.4.5a)$$

$$H = (1/2\mu)(\mathbf{p} - q\mathbf{A}) \cdot (\mathbf{p} - q\mathbf{A}) + q\Phi, \qquad (8.4.5b)$$

$$H = p^2/2\mu - (q/2\mu)(\mathbf{p} \cdot \mathbf{A} + \mathbf{A} \cdot \mathbf{p}) + (q^2/2\mu)\mathbf{A} \cdot \mathbf{A} + q\Phi. \qquad (8.4.5c)$$

Here the canonical momentum is defined by

$$\mathbf{p} = \frac{\partial L}{\partial \mathbf{v}} = \mu\mathbf{v} + q\mathbf{A}. \qquad (8.4.5d)$$

The Hamiltonian expression in parentheses [Eq. (8.4.5a)] is quantitatively correct but incorrect in form, since Hamiltonians are supposed to be functions of coordinates $\mathbf{q} = \mathbf{r}$ and *momentum* $\mathbf{p}$, while Lagrangians are functions of $\mathbf{q}$ and *velocity* $d\mathbf{q}/dt = \mathbf{v}$.

In classical or semiclassical spectroscopic theory the radiation part of the electromagnetic fields is described in terms of plane waves:

$$\mathbf{A} = \hat{\mathbf{e}}(2|a|)\sin(\mathbf{k} \cdot \mathbf{r} - \omega t + \phi), \tag{8.4.6a}$$

$$-\frac{\partial \mathbf{A}}{\partial t} = E^{\text{rad}} = \hat{\mathbf{e}} E_0 \cos(\mathbf{k} \cdot \mathbf{r} - \omega t + \phi) \qquad (\text{where } E_0 = 2|a|\omega), \tag{8.4.6b}$$

$$\nabla \times \mathbf{A} = \mathbf{B}^{\text{rad}} = \hat{\mathbf{k}} \times \hat{\mathbf{e}} B_0 \cos(\mathbf{k} \cdot \mathbf{r} - \omega t + \phi) \qquad (\text{where } B_0 = 2|a|k). \tag{8.4.6c}$$

The wave vector $\mathbf{k}$ is transverse to the unit polarization vector $\hat{\mathbf{e}}$. This leads to the well-known transverse gauge conditions:

$$\nabla \cdot \mathbf{E}^{\text{rad}} = 0 = \nabla \cdot \mathbf{A}. \tag{8.4.7}$$

Since the standard quantum representation of the canonical momentum operator is a gradient $\mathbf{p} = (\hbar/i)\nabla$, $\mathbf{p} \cdot \mathbf{A}$ and $\mathbf{A} \cdot \mathbf{p}$ operators then have the same effect:

$$\mathbf{p} \cdot \mathbf{A}\psi(\mathbf{r}) = \mathbf{A} \cdot \mathbf{p}\psi(\mathbf{r}). \tag{8.4.8}$$

The time-dependent Schrödinger equation for a wave function $\psi(\mathbf{r}) = \langle \mathbf{r}|\psi \rangle$ using Hamiltonian (8.45c) is

$$i\hbar\frac{\partial \psi}{\partial t} = H\psi = \left[\frac{((\hbar/i)\nabla - q\mathbf{A})^2}{2\mu} + V(r)\right]\psi. \tag{8.4.9}$$

The potential $V(r)$ includes the electrostatic potential $q\Phi(r)$ and any additional atomic or molecular effective potentials due to forces which are not a direct result of electromagnetic fields. The Schrödinger equation expands to the following form using (8.4.8):

$$i\hbar\frac{\partial \psi}{\partial t} = \left[-\hbar^2\nabla^2/2\mu + V(r) - (q/\mu)\mathbf{A} \cdot (-\hbar i\nabla) + (q^2/2\mu)\mathbf{A} \cdot \mathbf{A}\right]\psi. \tag{8.4.10}$$

It is necessary to distinguish canonical momentum $\mathbf{p}(\alpha)$ [here represented by $(\hbar/i)\nabla$] from particle momentum $\mathbf{p}(\beta)$, where

$$\mathbf{p}(\beta) = \mathbf{p}(\alpha) - q\mathbf{A} \tag{8.4.11}$$

follows from (8.4.5d). Under certain conditions an alternative basis or picture can be obtained in which the particle momentum is also the canonical

momentum. One may use a boost transformation B of the form (8.2.10) to subtract $q\mathbf{A}$ from $\mathbf{p}(\alpha)$ as follows:

$$\mathbf{p}(\beta) = B\mathbf{p}(\alpha)B^\dagger = \mathbf{p}(\alpha) - q\mathbf{A}, \qquad (8.4.12a)$$

where

$$B = e^{iq\mathbf{A}\cdot\mathbf{r}/\hbar}, \qquad (8.4.12b)$$

This is possible only if $\mathbf{A}$ satisfies the conditions of the dipole approximation. These conditions require that the radiation wavelength $2\pi/k$ is long compared to atomic dimensions so that one may assume a zero gradient of $\mathbf{A}$ ($\nabla\mathbf{A} \cong 0$). Using the gradient representation of $\mathbf{p}(\alpha)$ it is easy to verify the boost transformation relations (8.4.12a) in the dipole approximation.

(a) *Transformation between Pictures*   The boost transformation B may be used to set up a new set of base states or a new "picture." The old α-picture basis $\{ \cdots |r\rangle_\alpha \cdots \}$ of position states is boosted into the new β-picture basis $\{ \cdots |r\rangle_\beta \cdots \}$, where the following relations hold:

$$|r\rangle_\beta = B|r\rangle_\alpha, \qquad |r\rangle_\alpha = B^\dagger|r\rangle_\beta,$$

$$_\beta\langle r| = {}_\alpha\langle r|B^\dagger, \qquad {}_\alpha\langle r| = {}_\beta\langle r|B. \qquad (8.4.13)$$

Now a given state $|\psi\rangle$ can be represented by an old α-picture wave function $\psi^\alpha(r) = {}_\alpha\langle r|\psi\rangle$ or a new β-picture wave function defined as follows (the conventional script $\mathscr{B}$ denotes a representation of the abstract B operator):

$$\psi^\beta(r) = {}_\beta\langle r|\psi\rangle = {}_\alpha\langle r|B^\dagger|\Psi\rangle$$

$$= \mathscr{B}^\dagger\psi^\alpha(r) = e^{-i\mathbf{A}\cdot\mathbf{r}/\hbar}\psi^\alpha(r), \qquad (8.4.14a)$$

$$\psi^\alpha(r) = \mathscr{B}\psi^\beta(r) = e^{i\mathbf{A}\cdot\mathbf{r}/\hbar}\psi^\beta(r). \qquad (8.4.14b)$$

This transformation is often treated as a *gauge transformation*; however, it may help to picture it physically as a boost. Neither interpretation is emphasized in the original literature. Synder and Richards discuss the general quantum transformation (8.4.14), while Goeppert-Mayer gave an equivalent classical canonical transformation. These papers are mentioned at the end of this chapter.

The first job of the boost operator $\mathscr{B}$ is to reduce the momentum factors $(\mathbf{p}(\alpha) - q\mathbf{A}) = -(\hbar i\nabla + q\mathbf{A})$ in the kinetic term of the α-picture Schrödinger equation (8.4.9) to simple gradients:

$$(\mathbf{p}(\alpha) - q\mathbf{A})\psi^\alpha = \mathscr{B}\mathbf{p}(\alpha)\mathscr{B}^\dagger\mathscr{B}\psi^\beta = \mathscr{B}\mathbf{p}(\alpha)\psi^\beta,$$

$$(\mathbf{p}(\alpha) - q\mathbf{A})^2\psi^\alpha = \mathscr{B}\mathbf{p}(\alpha)^2\psi^\beta.$$

Here (8.4.11) and (8.4.14) were used. The potential term in (8.4.9) is unchanged since $\mathscr{B}$ commutes with all coordinate operators ($\mathscr{B}$ is a function of coordinates only):

$$V(r)\psi^{\alpha} = V(r)\mathscr{B}\psi^{\beta} = \mathscr{B}V(r)\psi^{\beta}.$$

However, the time derivative does not commute with $\mathscr{B}$ if $d\mathbf{A}/dt \neq 0$:

$$i\hbar \frac{\partial \psi^{\alpha}}{\partial t} = i\hbar \frac{\partial}{\partial t}\left[e^{iq\mathbf{A}\cdot\mathbf{r}/\hbar}\psi^{\beta}\right]$$

$$= e^{iq\mathbf{A}\cdot\mathbf{r}/\hbar}\left[i\hbar \frac{\partial \psi^{\beta}}{\partial t} - q\left(\frac{\partial \mathbf{A}}{\partial t}\cdot\mathbf{r}\right)\psi^{\beta}\right].$$

This gives the following time derivative:

$$i\hbar \frac{\partial \psi^{\alpha}}{\partial t} = \mathscr{B}\left[i\hbar \frac{\partial \psi^{\beta}}{\partial t} + q\mathbf{E}^{\text{rad}}\cdot\mathbf{r}\psi^{\beta}\right].$$

In the last line the vector potential relation (8.4.6b) was used. Assembling the transformed pieces of the α equation yields a new Schrödinger equation in the β picture:

$$i\hbar \frac{\partial \psi^{\beta}}{\partial t} = \left[-\hbar^2\nabla^2/2\mu + V(r) - q\mathbf{E}^{\text{rad}}\cdot\mathbf{r}\right]\psi^{\beta}. \qquad (8.4.15)$$

The transformation which gives the new equation is called a change of "picture" rather than just a change of basis. This terminology serves as a reminder that the transformation operator $B = e^{iq\mathbf{A}(t)\cdot\mathbf{r}/\hbar}$ is an explicit function of time through the vector potential. Nevertheless, the usual rules given in Chapter 1 relate representations of operators. For example, the coordinate representation of $\mathbf{p}(\beta)$ in the new β picture is equal to that of $\mathbf{p}(\alpha)$ in the old α picture according to (8.4.12) and (8.4.13):

$$_{\beta}\langle r'|\mathbf{p}(\beta)|r\rangle_{\beta} = {}_{\alpha}\langle r'|B^{\dagger}\mathbf{p}(\beta)B|r\rangle_{\alpha} = {}_{\alpha}\langle r'|\mathbf{p}(\alpha)|r\rangle_{\alpha}. \qquad (8.4.16)$$

In other words, if $\mathbf{p}(\alpha)$ is represented by $(\hbar/i)\nabla$ in the old picture then the same $(\hbar/i)\nabla$ will represent $\mathbf{p}(\beta)$ in the new picture. Now let us see how a change of picture affects the interaction part of the Hamiltonian.

It is a common practice to write Hamiltonians in the two Schrödinger equations (8.4.10) and (8.4.15) as a sum of a zeroth-order part H_0 and an interaction H_I:

$$H(\mu) = H_0(\mu) + H_I(\mu) \qquad (\mu = \alpha \text{ or } \beta). \qquad (8.4.17)$$

The interaction term for the α picture obviously has a different form than that of the β picture:

$$H_I(\alpha) = m(q/\mu)\mathbf{A} \cdot \mathbf{p}(\alpha) + (q^2/2\mu)\mathbf{A} \cdot \mathbf{A}, \qquad (8.4.18a)$$

$$H_I(\beta) = -q\mathbf{E}^{\text{rad}} \cdot \mathbf{r}, \qquad (8.4.18b)$$

but the zeroth-order term has the same form in either picture:

$$H_0(\alpha) = p(\alpha)^2/2\mu + V(r), \qquad (8.4.19a)$$

$$H_0(\beta) = p(\beta)^2/2\mu + V(r). \qquad (8.4.19b)$$

If the (α, β) labeling is deleted (as it almost always is), the two H_0 operators appear to be identical. Indeed, their corresponding representations *are* identical because of (8.4.16). Add to this the fact that the coordinate operators are the same in each picture and you have what may be one of the worst traps in theoretical physics! In extreme cases the unfortunate victims of this trap will fail to distinguish two different pictures and proceed to equate $H_0(\alpha)$ to $H_0(\beta)$ and $H_I(\alpha)$ to $H_I(\beta)$.

The β picture seems to be the most nearly foolproof picture because it allows canonical momentum and particle momentum to be one and the same thing $(\mathbf{p} = \mathbf{p}(\beta) \rightarrow (h/i)\nabla)$. Therefore, eigenstates $|n\rangle_\beta$ and eigenfunctions $\phi_n^\beta(r) = {}_\beta\langle r|n\rangle_\beta$ of $H_0(\beta)$ behave "normally" when perturbed by $H_I(\beta)$. (We shall consider examples shortly.) A stationary state such as the ground state $|0\rangle_\beta$ of an oscillator potential has zero expectation value for the *particle* momentum $({}_\beta\langle 0|\mathbf{p}(\beta)|0\rangle_\beta = 0)$.

In the α picture, on the other hand, the corresponding oscillator ground eigenstate $|0\rangle_\alpha$ of $H_0(\alpha)$ would have zero *canonical* momentum $({}_\alpha\langle 0|\mathbf{p}(\alpha)|0\rangle_\alpha = 0)$. This means that the particle momentum expectation would be ${}_\alpha\langle 0|\mathbf{p}(\beta)|0\rangle_\alpha = -q\mathbf{A}$ according to (8.4.11a). This is consistent with the basis transformation definition in (8.4.13) which takes the following form:

$$|0\rangle_\alpha = B^\dagger|0\rangle_\beta = e^{-iq\mathbf{A}\cdot\mathbf{r}/\hbar}|0\rangle_\beta. \qquad (8.4.20)$$

Hence, the state $|0\rangle_\alpha$ is a coherent state with momentum $-q\mathbf{A}$ relative to the $|0\rangle_\beta$ state according to the definitions in Section 8.2.

(b) An Attempt to Visualize and Compare A · p and E · r Pictures

The β picture has a lot to recommend it. It seems that the interaction Hamiltonian $(-q\mathbf{E} \cdot \mathbf{r})$ is simpler than the expression $[-(q/\mu)\mathbf{A} \cdot \mathbf{p} + (q^2/2\mu)\mathbf{A} \cdot \mathbf{A}]$ needed in the α picture. Also the particle momentum is the canonical $\mathbf{p}$ in the β picture. One wonders if one should not abandon the α picture altogether.

However, it should be remembered that the β picture is only valid under the conditions of the dipole approximation, and that it was derived, after all,

from the α picture. If one ever intends to accurately describe quantum optics involving higher multipole transitions, then the α picture will have to be the starting point. Furthermore, one can show that particle momentum can be canonical only in the dipole approximation.

Hence, it may be useful to understand the α and β pictures better, perhaps to even have a picture of the two pictures. Such a picture is attempted in Figures 8.4.1(a) and 8.4.1(b). We emphasize that this graphical portrayal is more of a caricature or mnemonic than a real picture. It should be used with caution. It is based upon a literal interpretation of the B transformation [(8.4.13) and (8.4.14)] as a boost which may be objectionable to some.

The β picture which is shown in Figure 8.4.1(b) is just a simple sketch of a slowly oscillating **E** field perturbing a particle in a fixed oscillator potential $V(r)$. The α picture depicted in Figure 8.4.1(a) shows an atomic potential well $V(r)$ attached to reference frame boosted to velocity $q\mathbf{A}/\mu$ so that the particle fixed in this frame would have momentum $q\mathbf{A}$.

The idea is that $\mathbf{p}(\beta) = \mathbf{p}(\alpha) - q\mathbf{A}$ is always equal to the particle momentum relative to the frame in which the potential $V(r)$ is fixed and $\mathbf{p}(\alpha)$ is the momentum in the α-picture frame literally. The α picture has no manifest electric force; the effect of $\mathbf{E}^{\text{rad}}$ is accomplished by the inertial force associated with an accelerated frame. The β picture is analogous to a martini olive being stirred; in the α picture the same excitation is accomplished by shaking the glass.

Visualizing base states $|r\rangle_\beta = B|r\rangle_\alpha$ or $|n\rangle_\beta = B|n\rangle_\alpha$ in these pictures may also be instructive. States $|r\rangle_\beta$ or $|n\rangle_\beta$ are represented by a delta function or wave packet, respectively, fixed relative to the potential $V(r)$, while $|r\rangle_\alpha = B^\dagger|r\rangle_\beta$ or $|n\rangle_\alpha = B^\dagger|n\rangle_\beta$ are always boosted oppositely to the motion of the $V(r)$ frame so that it remains fixed in the α picture. It appears that the $|n\rangle_\beta$ states will be more convenient for describing perturbations between levels in the potential $V(r)$ since it will not be necessary to "unboost" the initial and final eigenstates.

It is important to note that a boost in momentum does not immediately imply a translation in particle coordinate, since the two variables are independent. In fact the coordinate expectations are the same in either picture, since B and r commute:

$$_\alpha\langle n|\mathbf{r}|n\rangle_\alpha = {}_\beta\langle n|\mathbf{r}|n\rangle_\beta. \qquad (8.4.21)$$

This shows that the classical coordinate excursions indicated in Figure 8.4.1(a) are misleading; somehow one needs to picture boost without translation! However, this fact does not invalidate this visual aid for most laser-atom excitations because the actual translations would be so very tiny. The classical translation of the E frame relative to the A frame would be

$$\mathbf{R}(t) = \int (q/\mu)\mathbf{A}\, dt = (q/\mu)\left(E_0/\omega^2\right)\cos(\phi - \omega t)\mathbf{e}_A. \qquad (8.4.22)$$

(b) Force Field Picture for E·r Hamiltonian

$$H^B = p^2/2\mu + V(r) - qE \cdot r$$

Fixed Atomic
Potential V(r)

Electric Force

Field $E = -\dfrac{dA}{dt}$

Time

(a) Velocity Boost Picture for A·p Hamiltonian

$$H^A = [p - q \quad A]^2/2\mu + V(r)$$

Effective Boost
Velocity v = qA/μ

Boosted Atomic
Potential V(r)
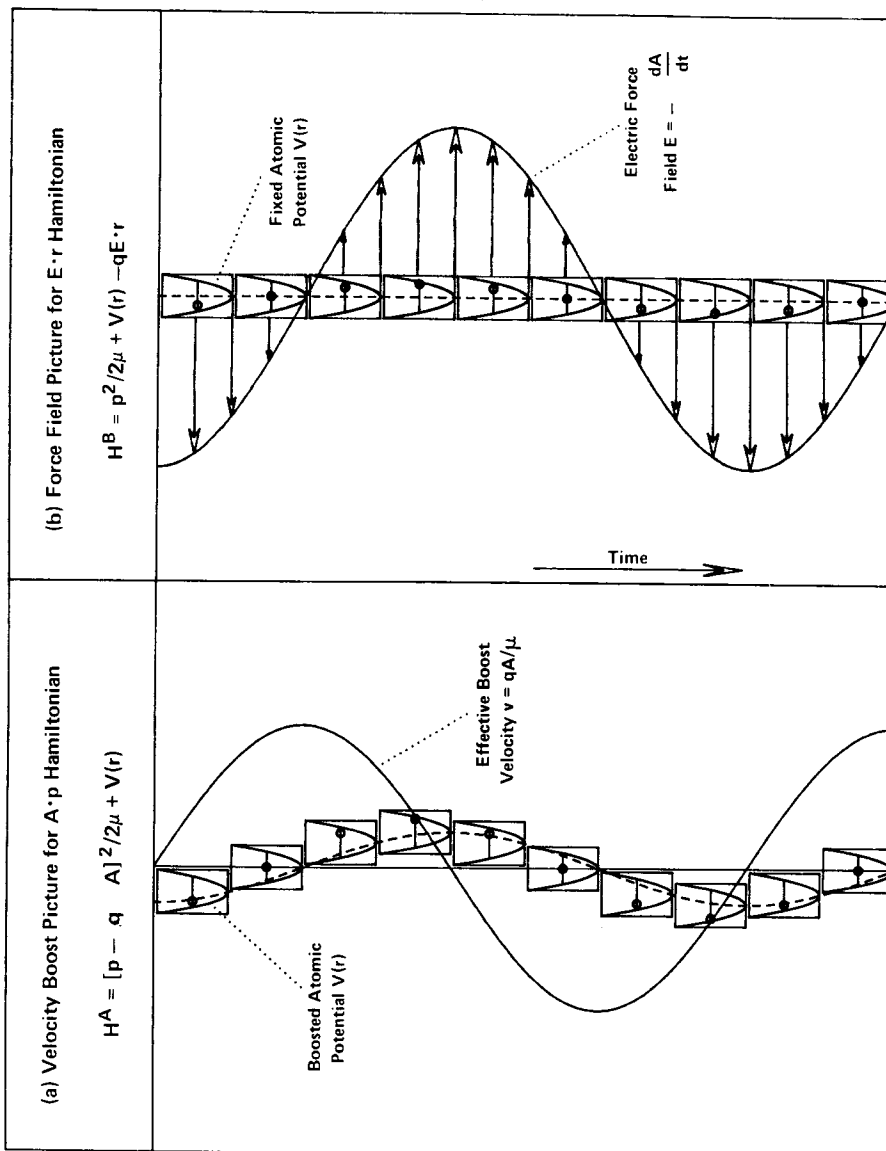
Figure 8.4.1 (a) Velocity boost picture for $A \cdot p$. (b) Force field picture for $E \cdot r$ Hamiltonian.

This is less than one nuclear radius (i.e., about 2×10^{-15} m) for atomic electronic transitions ($q = 1.6 \times 10^{19}$ C, $\mu = 9.1 \times 10^{-31}$ kg, $\omega \cong 10^{16}$) in a laser field of one million volts per meter.

B. Semiclassical Radiation Perturbation Theory

Perturbation theory gives solutions to the Schrödinger equation:

$$ i\hbar \frac{\partial}{\partial t} |\psi(t)\rangle = (H_0 + H_I)|\psi(t)\rangle, \qquad (8.4.23) $$

in terms of a basis of eigensolutions $|N\rangle$ of the Hamiltonian H_0 when the coupling perturbation H_I is zero. The desired solution for nonzero coupling is given by

$$ |\psi(t)\rangle = \sum_N c_N(t)e^{-i\omega_N t}|N\rangle, \qquad (8.4.24) $$

where the $|N\rangle$ and $\hbar\omega_N$ are (supposedly) known eigenvectors and eigenvalues of uncoupled or zeroth-order Hamiltonian H_0:

$$ H_0|N\rangle = \hbar\omega_N|N\rangle. \qquad (8.4.25) $$

The desired coefficients $c_N(t)$ are constants unless the perturbation H_I is nonzero. If H_I is comparatively small, as it must be for standard perturbation theory to work, then the rate of change of $c_N(t)$ will be small compared to frequencies ω_N associated with the excited states. The coefficient of $|N\rangle$ is written $c_N(t)e^{-i\omega_N t}$ so that the unknowns $c_N(t)$ serve as amplitude *modulation* functions rather than whole amplitudes. The $c_N(t)$ modulation will change due to interaction H_I and not due to H_0 alone.

(a) Perturbation Expansion   To derive the $c_N(t)$ time dependence we take the time derivative of (8.4.24):

$$ i\hbar \frac{\partial}{\partial t} |\psi(t)\rangle = \sum_N \left(\hbar\omega_N c_N e^{-i\omega_N t}|N\rangle + i\hbar \frac{\partial c_N}{\partial t} e^{-i\omega_N t}|N\rangle \right). \qquad (8.4.26) $$

The factor $i\hbar$ was included so it is easy to compare this with the Schrödinger time equation (8.4.23) using the eigenequation (8.4.25):

$$ i\hbar \frac{\partial}{\partial t} |\psi(t)\rangle = (H_0 + H_I) \sum_M c_M e^{-i\omega_M t}|M\rangle $$

$$ = \sum_M \left(\hbar\omega_M c_M e^{-i\omega_M t}|M\rangle + c_M e^{-i\omega_M t}H_I|M\rangle \right). \qquad (8.4.27) $$

A comparison shows that the right-hand summation terms for (8.4.26) and (8.4.27) are equal:

$$\sum_N i\hbar \frac{\partial c_N}{\partial t} e^{-i\omega_N t} |N\rangle = \sum_M c_M e^{-i\omega_M t} H_I |M\rangle. \qquad (8.4.28)$$

Using orthogonality ($\langle N|N'\rangle = \delta_{NN'}$) we see how the time derivative of the amplitude modulation function depends on H_I as follows:

$$i\hbar \frac{\partial c_N}{\partial t} = \sum_M c_M e^{i(\omega_N - \omega_M)t} \langle N|H_I|M\rangle$$

$$= \sum_M c_M V_{NM}. \qquad (8.4.29)$$

Here it is convenient to define

$$V_{NM} = e^{i\omega_{NM}t} \langle N|H_I|M\rangle, \qquad (8.4.30a)$$

where

$$\omega_{NM} \equiv \omega_N - \omega_M. \qquad (8.4.30b)$$

If two or more coefficients c_M and c_N are nonzero the state $|\psi(t)\rangle$ in (8.4.24) will be nonstationary; that is, it will change rapidly even if H_I is zero and the c_N's are constant. The change depends on relative phases, i.e., differences like $\omega_{NM} = \omega_N - \omega_M$ which are the "beat" frequencies of the nonstationary state. In order to most easily see the effect of the perturbation H_I we shall choose the initial state to be a single stationary eigenstate $|\psi(0)\rangle = |B\rangle$. This means that the modulation coefficients at $t = 0$ are given by the following "zeroth approximation":

$$c_N^{(0)} = \delta_{NB}. \qquad (8.4.31)$$

To calculate the first approximation this is substituted into the equation (8.4.29) of motion as follows:

$$i\hbar \frac{\partial c_N}{\partial t} = \sum_M \delta_{MB} V_{NM} = V_{NB}.$$

Then the first approximation to the solution to this equation will be

$$c_N^{(1)}(t) = \delta_{NB} + \frac{1}{i\hbar} \int_0^t dt_1 \, V_{NB}(t_1). \qquad (8.4.32)$$

By repeating the substitution into (8.4.29) we obtain the second approximation, the third, and so forth.

$$c_N^{(2)}(t) = \delta_{NB} + \frac{1}{i\hbar} \int_0^t dt_1 V_{NB}(t_1) + \frac{1}{(i\hbar)^2} \sum_M \int_0^t dt_2 V_{NM}(t_2) \int_0^{t_2} dt_1 V_{MB}(t_1),$$

$$c_N^{(3)}(t) = c_N^{(2)}(t) + \frac{1}{(i\hbar)^3} \sum_M \sum_{M'} \int_0^t dt_3 V_{NM}(t_3) \int_0^{t_3} dt_2 V_{MM'}(t_2) \int_0^{t_2} dt_1 V_{M'B}(t_1).$$

$$(8.4.33)$$

The first approximation (8.4.32) becomes

$$c_N^{(1)}(t) = \delta_{NB} + \frac{1}{i\hbar} \int_0^t dt_1 \, e^{i\omega_{NB} t_1} \langle N|H_I|B \rangle. \qquad (8.4.34)$$

Here we will use the β picture and the $\mathbf{E} \cdot \mathbf{r}$ interaction (8.4.18b) for a monochromatic plane wave (8.4.6) of angular frequency ω:

$$\langle N|H_I|B \rangle = -q\mathbf{E} \cdot \langle N|\mathbf{r}|B \rangle = -qE_0 \cos(\omega t - \phi) r_{NB}$$

$$= -q(i\omega a e^{-i\omega t} - i\omega a^* e^{i\omega t}) r_{NB}. \qquad (8.4.35a)$$

The amplitude and phase of the electric field are given by the following definitions

$$E_0 = 2|a|\omega, \qquad (8.4.35b)$$

$$a = -i|a|e^{i\phi}. \qquad (8.4.35c)$$

The dipole expectation value depends on the matrix element of the position operator projected onto the electric polarization vector $\hat{\mathbf{e}}$:

$$r_{NB} = \hat{\mathbf{e}} \cdot \langle N|\mathbf{r}|B \rangle. \qquad (8.4.35d)$$

Inserting these values into (8.4.34) yields the following amplitudes:

$$c_N^{(1)}(t) = \delta_{NB} + q\frac{r_{NB}}{\hbar} \int_0^t dt_1 (-\omega a e^{i(\omega_{NB}-\omega)t_1} + \omega a^* e^{i(\omega_{NB}+\omega)t_1}),$$

$$c_N^{(1)}(t) = \delta_{NB} + q\frac{r_{NB}}{\hbar} \left[i\omega a \frac{(e^{i(\omega_{NB}-\omega)t} - 1)}{\omega_{NB} - \omega} - i\omega a^* \frac{(e^{i(\omega_{NB}+\omega)t} - 1)}{\omega_{NB} + \omega} \right],$$

$$c_N^{(1)}(t) = \delta_{NB} + \frac{qr_{NB}|a|\omega}{\hbar} \left[e^{i\phi} \frac{(e^{i(\omega_{NB}-\omega)t} - 1)}{\omega_{NB} - \omega} + e^{-i\phi} \frac{(e^{i(\omega_{NB}+\omega)t} - 1)}{\omega_{NB} + \omega} \right].$$

$$(8.4.36)$$

(b) Spectral Function   The amplitude (8.4.36) is rewritten as follows

$$c_N^{(1)}(t) = \delta_{NB} + \frac{qr_{NB}E_0}{2\hbar}\left[e^{i\phi}S(\Delta^-,t) + e^{-i\phi}S(\Delta^+,t)\right] \quad (8.4.37)$$

in terms of the *spectral amplitude function*

$$S(\Delta,\tau) = \int_0^\tau dt\, e^{i\Delta t} = (2/\Delta)e^{i\tau\Delta/2}\sin(\tau\Delta/2) \qquad (8.4.38a)$$

and angular frequency *detuning parameters*

$$\Delta^- = \omega_{NB} - \omega, \qquad\qquad (8.4.38b)$$

$$\Delta^+ = \omega_{NB} + \omega. \qquad\qquad (8.4.38c)$$

It is important to visualize the spectral function since it appears repeatedly in spectroscopy and optics. $S(\Delta,\tau)$ is the DC ($\omega = 0$) component of a running Fourier transform of $e^{i\Delta t}$ from $t = 0$ to $t = \tau$.

The probability or spectral intensity function $|S|^2$ is given by

$$|S(\Delta,\tau)|^2 = (4/\Delta^2)\sin^2(\tau\Delta/2). \qquad (8.4.39)$$

This is plotted in Figure 8.4.2 as a function of the detuning (Δ) and time interval (τ). The spectral intensity becomes more and more strongly peaked around the detuning origin ($\Delta = 0$) as time (τ) increases. The frequency integral of the spectral intensity function grows linearly with time:

$$\int_{-\infty}^{\infty} d\Delta\,|S(\Delta,\tau)|^2 = 4\int_{-\infty}^{\infty} d\Delta\,\sin^2(\tau\Delta/2)/\Delta^2 = 2\pi\tau. \quad (8.4.40)$$

This is the basis for the so-called "golden rule" of constant transition rates which is discussed later. Meanwhile, the central peak height grows quadratically with time.

$$|S(0,\tau)|^2 = \tau^2. \qquad\qquad (8.4.41)$$

The sidebands or fringe peaks on either side grow in a similar fashion but are much smaller. The largest sidebands are located at approximately $\Delta = \pm 3\pi/\tau$ on either side of the central peak. Their height is about $0.045\tau^2$ or less than 5% of the central peak. Concentric hyperbolas in the (Δ,τ) plane are the loci of alternating zeros and sideband peaks. The zeros nearest the central peak fall on the hyperbola

$$\Delta = \pm 2\pi/\tau$$
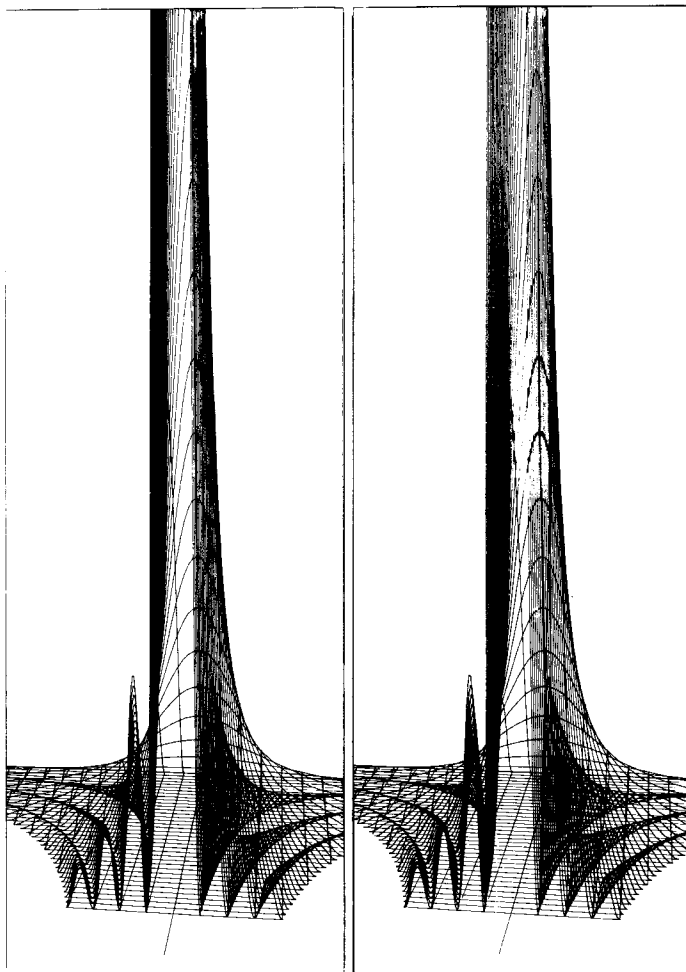
Figure 8.4.2 (Stereoptic pair) Spectral intensity function $|S(\Delta, \tau)|^2$ plotted versus the detuning parameter Δ ($\Delta < 0$ is left and $\Delta > 0$ is right) and elapsed time τ (τ increases coming toward the observer).

or

$$(\hbar\Delta)(\tau) = \pm 2\pi\hbar = \pm h. \tag{8.4.42}$$

This can be viewed as a restatement of Heisenberg's uncertainty relation between the energy detuning range ($\hbar\Delta$) and the time interval (τ) allowed for a given transition. One finds most of the probability within the bounds defined by the first hyperbola.

The interpretation of the semiclassical transition amplitude is complicated by the fact that it contains *two* spectral functions. The first function peaks

when $\Delta^- = 0$ or

$$\omega = \omega_{NB} = \omega_N - \omega_B. \tag{8.4.43}$$

This peak would correspond to an absorption process in which the electron was stimulated at a precise angular frequency ω to jump from beginning state $|B\rangle$ to a higher state $|N\rangle$. The probability for this jump varies with time τ and frequency ω according to $|c_N^{(1)}(t)|^2$. A good approximation to $c^{(1)}(t)$ for $\omega - \omega_{NB}$ involves just the first spectral function in (8.4.37):

$$\left|c_N^{(1)}(t)\right|^2 \cong \frac{q^2 |r_{NB}|^2 E_0^2}{4\hbar^2} |S(\omega_{NB} - \omega, t)|^2_{(\text{Absorption: } \omega \cong \omega_{NB})}. \tag{8.4.44a}$$

On the other hand, if the final state $|N\rangle$ lies below the beginning state $|B\rangle$, then the second term would be the main contribution to an emission probability which would then have the same approximate form:

$$\left|c_N^{(1)}(t)\right|^2 \cong \frac{q^2 |r_{NB}|^2 E_0^2}{4\hbar^2} |S(\omega_{NB} + \omega, t)|^2_{(\text{Emission: } \omega \cong -\omega_{NB})}. \tag{8.4.44b}$$

A prominent feature of the probability function in Figure 8.4.2 are the wiggles or "beats" which occur at the difference frequency $\Delta = \omega_{NB} - \omega$ or $(\Delta = \omega + \omega_{BN})$ for fixed nonzero detuning Δ. This may remind you of the response of an undamped classical oscillator of frequency $\omega_0 = |\omega_{NB}|$ driven at frequency $\omega_s = \omega$. The classical equations derived in Section 6.5 [see Eqs. (6.5.5)–(6.6.8)] give the complex position function $x(t)$ for an undamped ($\Gamma = 0$) initially stationary ($x_0 = 0 = v_0$) oscillator of frequency ω_0 which experiences a stimulating force $E_0 q \cos(\omega_s t - \phi)$. For $\phi = 0$, the square of the position is approximately proportional to the square of the spectral function.

$$\begin{aligned}
|x(t)|^2 &= \left|(q/\mu)E_0(e^{-i\omega_s t} - e^{-i\omega_0 t})/(\omega_0^2 - \omega_s^2)\right|^2 \\
&= \left|4(q/\mu)E_0\right|^2 \sin^2[t(\omega_0 - \omega_s)/2]/(\omega_0^2 - \omega_s^2)^2 \\
&\cong |qE_0/2\mu\omega_0|^2 |S(\omega_0 - \omega_s, t)|^2.
\end{aligned}$$

In the last step the near-resonance approximation ($\omega_0 \cong \omega_s$) is used. The exact classical result for all frequencies and for arbitrary E-field phase (ϕ) follows from (6.5.5)–(6.5.8):

$$\operatorname{Re} x(t) = (qE_0/\mu)$$
$$\times \left[\frac{\cos\phi(\cos\omega_s t - \cos\omega_0 t) + \sin\phi(\sin\omega_s t - (\omega_s/\omega_0)\sin\omega_0 t)}{\omega_0^2 - \omega_s^2} \right]. \tag{8.4.45}$$

(c) Oscillator Strength and Quantum Response An excellent test of semiclassical perturbation theory is a rederivation of the classical response (8.4.45) using a quantum oscillator basis. It can also be used to check $\mathbf{E} \cdot \mathbf{r}$ and $\mathbf{A} \cdot \mathbf{p}$ perturbation schemes. In order to rederive the classical behavior exactly it will be necessary to include both the resonant and nonresonant spectral function terms in the expression (8.4.37) for the amplitudes $c_F(t)$ of the stimulated state. From (8.4.24) and (8.4.31) this state is

$$|\psi(t)\rangle = e^{-i\omega t}\left(|B\rangle + \sum_{F \neq B} e^{-i\omega_{NB}t}c_F(t)|F\rangle\right),$$

and the expectation value of position is

$$\langle\psi|x|\psi\rangle = \sum_{F \neq B} e^{-i\omega_{FB}t}c_F^* x_{FB} + \sum_{F' \neq B} e^{-i\omega_{F'B}t}c_{F'} x_{BF'}.$$

Here we assume zero ground-state position expectation ($x_{BB} \equiv \langle B|x|B\rangle = 0$), and we neglect second-order excited state contributions ($c_F^* c_{F'}\langle F|x|F'\rangle \cong 0$). For the harmonic oscillator states these contributions are exactly zero. From (8.4.36) the expectation value becomes

$$\langle\psi|x|\psi\rangle = 2\,\mathrm{Re}\sum_{F \neq B} e^{-i\omega_{FB}t}c_F x_{BF}$$

$$= (2q|a|\omega/\hbar)\mathrm{Re}\sum_{F \neq B} r_{FB} x_{BF}$$

$$\times \frac{\left[e^{i\phi}(e^{-i\omega t} - e^{-i\omega_{FB}t})(\omega_{FB} + \omega) + e^{-i\phi}(e^{i\omega t} - e^{-i\omega_{FB}t})(\omega_{FB} - \omega)\right]}{\omega_{FB}^2 - \omega^2}.$$

$$(8.4.46)$$

If the position is measured along the E field so $r_{FB} = x_{BF}^*$ then (8.4.35) gives

$$\langle\psi|x|\psi\rangle = \sum_{F \neq B}\left(qE_0|x_{BF}|^2/\hbar\left[2\omega_{FB}\cos\phi(\cos\omega t - \cos\omega_{FB}t)\right.\right.$$

$$\left.\left.+ \sin\phi(2\omega_{FB}\sin\omega t - 2\omega\sin\omega_{FB}t)\right]/(\omega_{FB}^2 - \omega^2)\right.$$

This may be rearranged to correspond to the form of the classical position response (8.4.45) with $\omega_0 = \omega_{FB}$ and $\omega_s = \omega$:

$$\langle\psi|x|\psi\rangle = \sum_{F \neq B}\left\{\frac{2\omega_{FB}|x_{BF}|^2\mu}{\hbar}\right\}\frac{qF_0}{\mu}$$

$$\times \frac{\cos\phi(\cos\omega t - \cos\omega_{FB}t) + \sin\phi(\sin\omega t - (\omega/\omega_{FB})\sin\omega_{FB}t)}{\omega_{FB}^2 - \omega^2}$$

$$= \sum_{F \neq B} f_{FB} x_{\text{classical}}. \qquad (8.4.47a)$$

The leftover factors are called the transition *oscillator strengths*

$$f_{FB} = 2\omega_{FB}|x_{FB}|^2\mu/\hbar. \tag{8.4.47b}$$

For the harmonic oscillator states $\{|B\rangle = |0\rangle,\ |F\rangle = |1\rangle,\ |F'\rangle = |2\rangle, \ldots\}$ only the first oscillator-strength term is nonzero.

$$x_{FB} = \langle F|x|B\rangle = \langle n|a^\dagger + a|0\rangle[\hbar/2\mu\omega_0]^{1/2} = \delta_{n,1}[\hbar/2\mu\omega_{FB}]^{1/2}.$$

For this case the expectation value is precisely the classical one given in (8.4.45) since only the first oscillator strength is unity:

$$f_{n0} = \delta_{n,1}. \tag{8.4.48}$$

It should be noted that a naive replacement of the $(q\mathbf{E} \cdot \mathbf{r})$ perturbation (8.4.18b) with the equivalent $(q\mathbf{A} \cdot \mathbf{p}/\mu)$ perturbation (8.4.18a) would not give the correct oscillator response. The momentum operator is related to position as follows:

$$[H_0, x] = [p^2, x]/2\mu = \hbar p/\mu i, \tag{8.4.49}$$

and the p-matrix elements are then derived as follows:

$$p_{NB} = \langle N|p|B\rangle = \mu i\langle F|[H_0, x]|B\rangle/\hbar = \mu i\omega_{NB}x_{NB}. \tag{8.4.50}$$

The matrix element which would replace (8.4.35a) would be

$$\langle N|H_I|B\rangle = -q\mathbf{A} \cdot \langle N|\mathbf{p}|B\rangle/\mu = -q(2|a|\mu)\sin(\mathbf{k} \cdot \mathbf{r} - \omega t - \phi)p_{NB}$$

$$= -q(ae^{-i\omega t} + a^*e^{i\omega t})p_{NB}/\mu$$

$$= -q(i\omega_{NB}ae^{-i\omega t} + i\omega_{NB}a^*e^{i\omega t})x_{NB}. \tag{8.4.51}$$

The relative phase of these terms differs from (8.4.35a) and when $\omega_{NB} \neq \omega$ they differ in amplitude, as well. Naive replacement will not work; the entire picture needs to be transformed, as discussed in Section 8.3. However, the squares of each item in (8.4.51) are equal to corresponding squares for (8.4.35a) at the point $\omega = \omega_{NB}$. This fact alone is sometimes used to "demonstrate" simple equality of $\mathbf{A} \cdot \mathbf{p}$ and $\mathbf{E} \cdot \mathbf{r}$ perturbations. This sets a trap into which many students fall.

An important spectroscopic principle involves the distribution of oscillator strengths among the quantum transitions. The harmonic oscillator transitions are peculiar in that the strength f_{10} of the $(1 \leftarrow 0)$ transition is unity while f_{n0} is zero for $n \neq 1$. In other atomic potentials the strengths f_{FB} could all

be nonzero but their sum is unity as shown in the following:

$$\sum_F f_{FB} = \sum_F 2\omega_{FB}\langle B|x|F\rangle\langle F|x|B\rangle\mu\hbar$$

$$= \sum_F 2\langle B|x|F\rangle\langle F|p|B\rangle/\hbar i$$

$$= 2\langle B|xp|B\rangle/\hbar i = -2\langle B|px|B\rangle/\hbar i = 1.$$

The commutation $[x, p] = \hbar i$ and momentum matrix element (8.4.50) were used here. This is the Thomas-Reiche-Kuhn relation for atomic oscillator strengths associated with the motion of a single electron.

The foregoing discussion provides a quantum mechanical foundation for the classical Lorentz model for atomic oscillator response. However, it is based upon first-order perturbation approximations (8.4.36) and (8.4.37). It was noted that the spectral function increases quadratically with time at resonance [recall Eq. (8.4.41)]. Eventually such an approximation yields a probability $|c_F|^2$ greater than one. We now derive an improved theory for an atomic oscillator that is strongly driven by an electric field whose frequency ω is close to the resonant frequency ω_{NB} of the atomic oscillator. This is the two-level atom approximation which is discussed next.

8.5 TWO-LEVEL SYSTEM APPROXIMATION

The Hamiltonian for a two-level model of ammonia (NH_3) inversion was introduced in Section 2.12. A representation (2.12.34) of this Hamiltonian was given using base states $\{|up\rangle, |dn\rangle\}$. There $|up\rangle$ corresponded the N atom being "up" along the direction of a positive z-axial E field, and $|dn\rangle$ corresponded to the N atom localized against the field. Symmetry-defined eigenvectors of the zero-field Hamiltonian were denoted by $\{|+\rangle, |-\rangle\}$ and given in terms of $|up\rangle$ and $|dn\rangle$ by (2.12.32), which is repeated in the following using a modified notation:

$$|1\rangle = |+\rangle = (|up\rangle + |dn\rangle)/\sqrt{2}, \qquad (8.5.1a)$$

$$|2\rangle = |-\rangle = (|up\rangle - |dn\rangle)/\sqrt{2}. \qquad (8.5.1b)$$

Let us compare the representation of the Hamiltonian in each of these two bases:

$$\begin{pmatrix} \langle+|H|+\rangle & \langle+|H|-\rangle \\ \langle-|H|+\rangle & \langle-|H|-\rangle \end{pmatrix} = \begin{pmatrix} H-S & -pE \\ -pE & H+S \end{pmatrix}, \qquad (8.5.2a)$$

$$\begin{pmatrix} \langle up|H|up\rangle & \langle up|H|dn\rangle \\ \langle dn|H|up\rangle & \langle dn|H|dn\rangle \end{pmatrix} = \begin{pmatrix} H-pE & -S \\ -S & H+pE \end{pmatrix}. \qquad (8.5.2b)$$

The change of basis from $\{|up\rangle, |dn\rangle\}$ to $\{|+\rangle, |-\rangle\}$ causes the tunneling parameter (S) or zero-field energy splitting $(2S)$ to change places with the electric field potential energy parameter (pE) in the matrix. The states $|+\rangle$ and $|-\rangle$ are approximate eigenvectors when the electric field energy (pE) is small compared to tunneling (S) since the latter is on the diagonal of the $\{|+\rangle, |-\rangle\}$ representation. For large fields the $\{|up\rangle, |dn\rangle\}$ bases are preferred since it is pE which resides on the diagonal in this representation. The effects of strong versus weak constant electric fields are diagrammed in Figure 2.12.8 and these effects are known as the elementary DC-Stark effects.

This section is devoted to so-called AC-Stark effects, which are due to resonant oscillatory electric fields. The methods of analysis were first applied to nuclear magnetic resonance (NMR) experiments by Rabi, Ramsey, and Schwinger. The analogy between spin resonance and resonance of an arbitrary two-level system was pointed out shortly afterwards by Feynman, Vernon, and Hellwarth. These references were mentioned at the end of Chapter 7. The ammonia inversion maser was one of the first examples of coherent stimulated transitions and a forerunner to modern laser technology. The first part of the following describes the analogy and its geometrical interpretation.

A. Two-State Schrödinger Equations

The Schrödinger equation in the $\{|1\rangle, |2\rangle\}$ basis uses the Hamiltonian (8.5.2) as follows:

$$i\frac{\partial}{\partial t}\begin{pmatrix}\psi_1\\\psi_2\end{pmatrix} = \begin{pmatrix}H-S & -pE\\-pE & H+S\end{pmatrix}\begin{pmatrix}\psi_1\\\psi_2\end{pmatrix}. \tag{8.5.3a}$$

The long-wavelength (dipole) approximation for an oscillating electric field interaction energy is given by $(-q\mathbf{E}\cdot\mathbf{r})$, where $\mathbf{r}$ is the displacement of effective charge q. If the $\mathbf{E}$ and $\mathbf{r}$ are only in the z direction then the parameter pE is given in terms of the following matrix element:

$$-pE/\hbar = -\langle 2|qE_z z|1\rangle/\hbar = r\cos(\Omega t)$$
$$= (r/2)(e^{-i\Omega t} + e^{i\Omega t}). \tag{8.5.3b}$$

Here the constant r is proportional to the interaction strength

$$r = -pE_z(0)/\hbar, \tag{8.5.3c}$$

where the constant

$$p = q\langle 2|z|1\rangle \tag{8.5.3d}$$

is the transition dipole moment measured along the C_3 symmetry axis (z) of

NH$_3$ which connects the two equilibrium positions for the N atom. The parameters are all expressed in units of $\hbar$ in order to simplify the notation for the Schrödinger equation as much as possible:

$$i\frac{\partial}{\partial t}\begin{pmatrix} \psi_1 \\ \psi_2 \end{pmatrix} = \begin{pmatrix} \dfrac{\varepsilon}{2} & \dfrac{r}{2}(e^{-i\Omega t} + e^{i\Omega t}) \\ \dfrac{r}{2}(e^{i\Omega t} + e^{-i\Omega t}) & \dfrac{-\varepsilon}{2} \end{pmatrix}\begin{pmatrix} \psi_1 \\ \psi_2 \end{pmatrix} \qquad (8.5.4\text{a})$$

It is also convenient to reset the energy zero ($H = 0$) and let

$$\varepsilon = -2S/\hbar \qquad (8.5.4\text{b})$$

be the difference between zero-field atomic or molecular levels 1 and 2 in angular frequency units. (Note that level 1 is below level 2 if $S > 0$ or $\varepsilon < 0$.)

For many applications one may drop either the positive or else the negative frequency component of the interaction $\langle 2|\mathbf{E}\cdot\mathbf{r}|1\rangle$ to obtain the following:

$$i\frac{\partial}{\partial t}\begin{pmatrix} \psi_1 \\ \psi_2 \end{pmatrix} = \begin{pmatrix} \dfrac{\varepsilon}{2} & \dfrac{r}{2}e^{-i\Omega t} \\ \dfrac{r}{2}e^{i\Omega t} & -\dfrac{\varepsilon}{2} \end{pmatrix}\begin{pmatrix} \psi_1 \\ \psi_2 \end{pmatrix}. \qquad (8.5.5)$$

This is the equation we will discuss first. It contains a complex interaction term $(r/2)e^{i\Omega t}$ which exactly models a certain type of rotating NMR excitation field as explained in the following. For the analogous NH$_3$ excitation it is only an approximation, albeit a very good one.

B. Spin and Crank Vector Visualization of Two-State Hamiltonian

Either equation (8.5.4) or (8.5.5) can be visualized more easily by appealing to the three-dimensional ($R(3)$) picture of the two-state (SU(2)) system. To do this one may calculate the position of the Hamiltonian crank vector ω indicated in Figure 7.5.3. [See also Eq. (7.5.5).] The result is a crank which flops around at laser angular frequency Ω in addition to its usual cranking at angular frequency ω. The Cartesian crank components are as follows for the Hamiltonian in (8.5.5):

$$\begin{aligned} \omega_x &= 2\,\mathrm{Re}\,H_{21} & \omega_y &= 2\,\mathrm{Im}\,H_{21} & \omega_z &= H_{11} - H_{22} \\ &= r\cos\Omega t & &= r\sin\Omega t & &= \varepsilon. \end{aligned} \qquad (8.5.6)$$

If the real Hamiltonian in (8.5.4) is used, then the following crank components result:

$$\omega_x = 2r \cos \Omega t, \qquad \omega_y = 0, \qquad \omega_z = \varepsilon. \qquad (8.5.7)$$

In the latter case only the ω_x component oscillates, but with twice the amplitude. In the former case given by (8.5.6) the ω vector traces out an inverted cone of altitude ε and radius r. One may imagine the tail of the ω vector fixed at origin and its tip rotating at angular velocity Ω counterclockwise around a horizontal circle of radius r. The base circle of the cone is centered at a point on the ω_z axis at ε units above origin.

The well-known interaction between a magnetic moment $\mathbf{m} = g\mathbf{S}$ and field $\mathbf{B}$ is given by the elementary nuclear magnetic resonance Hamiltonian which describes precession of the moment or spin vector. The coefficient g is the gyromagnetic ratio between the spin and moment of a particle:

$$H_{\text{NMR}} = \mathbf{m} \cdot \mathbf{B} = g\mathbf{S} \cdot \mathbf{B}. \qquad (8.5.8)$$

We have seen that any Hamiltonian of the form $\boldsymbol{\omega} \cdot \mathbf{S}$ causes $\mathbf{S}$ to precess at angular velocity $|\boldsymbol{\omega}|$ around vector $\boldsymbol{\omega}$. So for NMR theory the crank or $\boldsymbol{\omega}$ vector is in the direction of the $\mathbf{B}$ field:

$$\boldsymbol{\omega} = g\mathbf{B}. \qquad (8.5.9)$$

In principle, the $\mathbf{B}$ field can be aimed in any direction in space and made to follow an arbitrary curve. For example, it could follow the circle prescribed by (8.5.6). If vectors $\boldsymbol{\omega}$ and $\mathbf{B}$ are stationary or moving very slowly ($\Omega \sim 0$) the spin vector $\mathbf{S}$ precesses around $\boldsymbol{\omega}$ as shown in Figure 7.5.3b. For greater Ω values (particularly for $\Omega \sim \varepsilon$) the spin vector $\mathbf{S}$ may not be able to keep up. Then there is more complicated spin resonance motion which we will describe shortly. For much higher values ($\Omega \gg \varepsilon$) the $\mathbf{S}$ vector will simply process around the average value of $\boldsymbol{\omega}$.

In the NH_3 two-level model the direction of the analogous $\boldsymbol{\omega}$ vector depends on the relative amounts of the real and imaginary parts of the interaction matrix element $H_{21} = \langle 2|q\mathbf{E} \cdot \mathbf{r}|1 \rangle$. Normally, the matrix element H_{21} is real and then only x and z components of $\boldsymbol{\omega}$ are nonzero. We need to remember that the three-dimensional quasispin space shown in Figure 7.5.1(b3) is a fiction. Its components should be labeled $\{A, B, C\}$ instead of $\{x, y, z\}$ as they were in Figure 7.5.1(b2) to avoid confusion with ordinary 3-space. The electric-dipole moment or position expectation vector $\langle p_z \rangle = q\langle z \rangle$ is assumed to lie along the electric field direction which is along the molecular z axis, and so this motion is constrained to one spatial dimension. *So, how does one interpret the three dimensions of the spin vectors* $\mathbf{S}$?

The spin vector A or x component $S_x = \langle J_x \rangle$ turns out to be proportional to the position or dipole moment expectation value:

$$\langle z \rangle = \langle \psi | z | \psi \rangle = \left(\psi_1^* \langle 1 | + \psi_2^* \langle 2 | \right) z \left(|1\rangle \psi_1 + |2\rangle \psi_2 \right)$$

$$= \psi_1^* \psi_2 \langle 1 | z | 2 \rangle + \psi_2^* \psi_1 \langle 2 | z | 1 \rangle$$

$$= \langle 1 | z | 2 \rangle 2 \, \mathrm{Re} \, \psi_1^* \psi_2.$$

From Figure 7.5.2 it follows that

$$\langle z \rangle = 2 \langle 1 | z | 2 \rangle S_x.$$

For zero field the C_2 symmetry of the NH_3 model demands that the position matrix element $\langle 1 | z | 2 \rangle$ is real and that diagonal elements are zero $\langle 1 | z | 1 \rangle = 0 = \langle 2 | z | 2 \rangle$.

Furthermore, in the absence of electric field perturbation, the time derivative of position turns out to be proportional to $S_y = \langle J_y \rangle$. Using (8.5.5) we have the following:

$$\frac{d}{dt} \langle z \rangle = \langle 1 | z | 2 \rangle \left(\dot{\psi}_1^* \psi_2 + \dot{\psi}_2^* \psi_1 + \psi_1^* \dot{\psi}_2 + \psi_2^* \dot{\psi}_1 \right)$$

$$= \langle 1 | z | 2 \rangle i \frac{\varepsilon}{2} \left(\psi_1^* \psi_2 - \psi_2^* \psi_1 + \psi_1^* \psi_2 - \psi_2^* \psi_1 \right)$$

$$= -\langle 1 | z | 2 \rangle \varepsilon 2 \, \mathrm{Im} \, \psi_1^* \psi_2.$$

Then from Figure 7.5.2, we deduce

$$\langle \dot{z} \rangle = -2\varepsilon \langle 1 | z | 2 \rangle S_y.$$

The components S_x and S_y of the **S** vector form a "shadow" on the horizontal plane, as indicated in Figure 7.4.2. We have just shown that this shadow vector can be visualized as phasor components $(z, dz/dt)$ for the atomic oscillator. (The minus sign on $\langle z \rangle$ indicates the natural phasor direction is *clockwise* in the S_x and S_y plane for $\varepsilon > 0$.)

We recall from Section 8.4B(c) that a classical phasor picture of an atomic oscillator is valid if the perturbing field is weak and Ω is far enough from resonance to keep the responding phasor oscillations small. Then the **S** vector oscillates very near to the S_z axis and S_z does not change much. Now we see what happens to this picture as Ω approaches a resonant value. Near resonance there will be a change of the *third* component (S_z) of the spin vector as the first two "phasor" components grow larger with the resonance.

C. Rotating-Wave Solutions

The time-dependent Schrödinger equation (8.5.5) is characterized by a crank vector $\boldsymbol{\omega}$ in (8.5.6) whose direction rotates counterclockwise with angular frequency Ω around the S_z axis (or J_z axis; here we shall use S and J interchangeably to denote spin coordinates). A rotational transformation in the opposite direction is defined as follows:

$$|\psi^R\rangle \equiv R^\dagger(0.0.-\Omega t)|\psi\rangle = e^{i\Omega t J_z}|\psi\rangle. \qquad (8.5.10)$$

It can be applied to the Hamiltonian in (8.5.5) to stop this rotation in its tracks. The result is the following Hamiltonian:

$$H^R = R^\dagger(0,0,\Omega t)HR(0,0,\Omega t),$$

whose representation is calculated as follows:

$$\langle H^R\rangle = \begin{pmatrix} e^{i\Omega t/2} & 0 \\ 0 & e^{-i\Omega t/2} \end{pmatrix}\frac{1}{2}\begin{pmatrix} \varepsilon & re^{-i\Omega t} \\ re^{i\Omega t} & -\varepsilon \end{pmatrix}\begin{pmatrix} e^{-i\Omega t/2} & 0 \\ 0 & e^{i\Omega t/2} \end{pmatrix},$$

$$\langle H^R\rangle = \frac{1}{2}\begin{pmatrix} \varepsilon & r \\ r & -\varepsilon \end{pmatrix}. \qquad (8.5.11)$$

Note that the resulting H^R is the same except for the off-diagonal components which now are constant. The rotation of the crank has been stopped. If we use the rotating R basis the Hamiltonian will be a constant matrix.

However, there is a small price to pay for using this constant Hamiltonian. The time dependence of the transformation adds a $-\Omega J_z$ term to the new Schrödinger equation as calculated in the following. Recall that a "change of picture" usually comes with an extra term. In this case, at least, the term is constant:

$$i\frac{\partial}{\partial t}|\psi^R\rangle = \left(i\frac{\partial}{\partial t}e^{i\Omega t J_z}\right)|\psi\rangle + e^{i\Omega t J_z}\left(i\frac{\partial}{\partial t}|\psi\rangle\right)$$

$$= -\Omega J_z R^\dagger|\psi\rangle + R^\dagger H|\psi\rangle$$

$$= \left(-\Omega J_z + R^\dagger HR\right)|\psi^R\rangle$$

or $\quad i\dfrac{\partial}{\partial t}|\psi^R\rangle = H^{R'}|\psi^R\rangle, \quad$ where $H^{R'} \equiv \left(-\Omega J_z + R^\dagger HR\right).$ (8.5.12)

So finally, the resulting equation for amplitudes

$$\psi_j^R = \langle j|R^\dagger|\psi\rangle \qquad (j = 1,2)$$

in the new rotating picture with basis $\{R|1\rangle, R|2\rangle\}$ is the following:

$$
i\frac{\partial}{\partial t}\begin{pmatrix} \psi_1^R \\ \psi_2^R \end{pmatrix} = \begin{pmatrix} \dfrac{\varepsilon - \Omega}{2} & \dfrac{r}{2} \\ \dfrac{r}{2} & \dfrac{\Omega - \varepsilon}{2} \end{pmatrix}\begin{pmatrix} \psi_1^R \\ \psi_2^R \end{pmatrix}. \qquad (8.5.13a)
$$

In the rotating picture the crank vector $\boldsymbol{\omega}$ is motionless:

$$
\omega_x = 2\,\mathrm{Re}\,H_{21}^{R'} \qquad \omega_y = 2\,\mathrm{Im}\,H_{21}^{R'} \qquad \omega_z = H_{11}^{R'} - H_{22}^{R'}
$$

$$
= r \qquad\qquad\qquad = 0 \qquad\qquad\qquad = \varepsilon - \Omega = \Delta. \quad (8.5.13b)
$$

However, the direction and length of $\boldsymbol{\omega}$ depends on the angular frequency *detuning* parameter which is the difference $\Delta = \varepsilon - \Omega$ between the two-level splitting (ε) and the angular frequency (Ω) of the stimulating laser.

According to (8.5.13b) the $\boldsymbol{\omega}$ vector is nearly aligned to the positive z axis for high positive detuning $(\Delta \gg r)$. This case is shown in Figure 8.5.1(a). Then as the driving frequency Ω approaches the resonant frequency ε, the $\boldsymbol{\omega}$ vector becomes shorter and approaches the x axis as shown in Figures 8.5.1(b) and 8.5.1(c). The precessional motion of a spin vector **S** which started
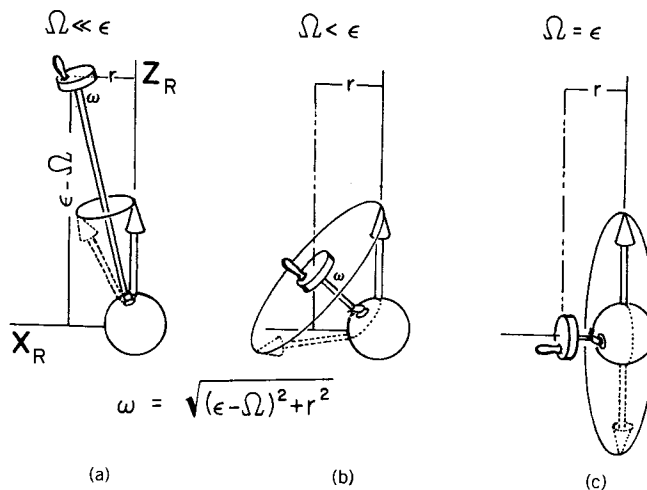
Figure 8.5.1 Motion in rotating frame of quasi-spin vector **S** around Hamiltonian $\boldsymbol{\omega}$ vector. (a) Off-resonance. Rotations or "beats" are rapid and of small amplitude. Angular beat frequency $\omega = \sqrt{\Delta^2 + r^2}$ is nearly equal to the detuning $(\omega \approx \Delta = \Omega - \varepsilon)$. (b) Approaching resonance. Rotations or beats slow down and increase their amplitude. Angular beat frequency approaches Rabi frequency $\omega \to r$. (c) Resonance. Beats have maximum amplitude and minimum frequency $\omega = r$.

out "up" along the z axis takes place on a greater and greater circle as the detuning decreases. Since ω grows shorter as Δ decreases, the precessional frequency $|\omega|$ decreases. It reaches a minimum value of r (rad/s) at the resonance point ($\Delta = 0$) as shown in Figure 8.5.1(c). [Recall that r is the interaction strength in angular units given by (8.5.3c).] This minimum angular frequency (r) of the resonant motion is known as the RABI frequency, and it is the frequency with which the spin "up" is carried into spin "down" and back again in the resonant case depicted by Figure 8.5.1(c). Note that the Rabi frequency is proportional to the field-dipole interaction energy according to (8.5.3d). It is a remarkable property of the atomic oscillator that its beat frequency on resonance is proportional to the driving field. (Recall that the beat frequency of a classical oscillator simply equals the detuning $\Delta = \varepsilon - \Omega$ which depends on the stimulus frequency Ω and not on its amplitude. Also, the classical beat frequency goes to zero at resonance.)

The precessional frequency $\omega = |\omega|$ due to an off-resonant driving field approaches the detuning value Δ as Δ increases. The magnitude of ω from (8.5.13) is

$$\omega = \sqrt{\Delta^2 + r^2}.\tag{8.5.14}$$

For large detuning ($\Delta \gg r$) this approaches the usual harmonic oscillator beat frequency ($\Delta = \varepsilon - \Omega$) and is independent of the field strength. The spin vector expectation value executes small and rapid circles in the rotating frame as shown in Figure 8.5.1(a). This corresponds to a beating motion in the lab frame of the oscillator variable $\langle x \rangle$. Remember that the rotating frame is revolving around the lab z axis at rate Ω. The beat amplitude is approximately proportional to r (and hence to the field strength) for high Δ, and again this corresponds to the classical driven oscillator.

The precessional motion indicated in Figures 8.5.1(a) and 8.5.1(b) is studied in detail in the series of photos shown in Figure 5.3.5. While the rotational axis vector ω is constant, the Euler phase angles α or γ excite a galloping motion that becomes more pronounced as Δ decreases and the crank axis becomes horizontal. At exactly resonance values ($\Delta = 0$) the Euler phase angles freeze while the population angle β turns at the Rabi frequency. The Euler angles can be derived by applying the axis-angle representation (5.5.1) for an axis vector $\omega = (r, 0, \Delta)$ which has zero azimuthal angle ($\phi = 0$) and polar angle $\theta = \tan^{-1}(r/\Delta)$. The precession of the spin-up state $|1\rangle$ is then given in the rotating picture as follows:

$$\begin{pmatrix} \psi_1^R(t) \\ \psi_2^R(t) \end{pmatrix} = \begin{pmatrix} \cos(\omega t/2) - i\cos\theta \sin(\omega t/2) \\ -i\sin\theta \sin(\omega t/2) \end{pmatrix}$$

$$= \begin{pmatrix} \cos(\omega t/2) - i(\Delta/\omega)\sin(\omega t/2) \\ -i(r/\omega)\sin(\omega t/2) \end{pmatrix}.\tag{8.5.15a}$$

Here the polar angle θ is given in terms of the angular frequencies r and ω:

$$\sin \theta = r/\omega, \tag{8.5.15b}$$

$$\cos \theta = \Delta/\omega. \tag{8.5.15c}$$

Now let us undo the rotational transformation (8.5.10) or (8.5.11) which we used to get to the rotating frame. The amplitudes in the original lab picture have different phases but the same magnitudes:

$$\psi_1(t) = e^{-i\Omega t/2}\psi_1^R(t),$$

$$\psi_2(t) = e^{i\Omega t/2}\psi_2^R(t). \tag{8.5.16}$$

Hence, the probability for a transition from the initial lab state $|1\rangle$ to a final state $|2\rangle$ is given by the square of the 2-component of (8.5.15a):

$$|c_2(t)|^2 = |\psi_2(t)|^2 = [r^2/\omega^2]\sin^2(\omega t/2)$$

$$= [r^2/(\Delta^2 + r^2)]\sin^2(t\sqrt{\Delta^2 + r^2}/2). \tag{8.5.17}$$

For large detuning ($\Delta \gg r$) this probability agrees with the first-order perturbation result given by (8.4.44):

$$|c_2(t)|^2 \Rightarrow (r^2/\Delta^2)\sin^2(t\Delta/2) = (r^2/4)|S(\Delta,t)|^2 \qquad (\text{for } \Delta \gg r). \tag{8.5.18}$$

Here the Rabi angular frequency is given again by (8.5.3c):

$$|r| = |pE/\hbar| = |qE\langle 1|z|2\rangle|/\hbar.$$

The probability $|c_2|^2$ for the two-level transition is plotted in Figure 8.5.2 using the same format as the plot of the elementary spectral function in Figure 8.4.2.

The main difference between Figures 8.4.2 and 8.5.2 are found near the resonance line ($\Delta = 0$). The elementary spectral probability (8.5.18) is unbounded along $\Delta = 0$ and will eventually exceed the physical limit of unit probability. However, the exact result (8.5.17) is bounded by unity and its value at resonance ($\Delta = 0$) oscillates between unity and zero. It is interesting to note that a perfectly resonant stimulus will actually yield *zero* transition probability at the end of each Rabi period ($\tau_{RABI} = 2\pi/r$). The spectrum at the end of the first period is indicated by the nearest set of peaks drawn in Figure 8.5.2. The huge peak in the approximate spectral function (Figure 8.4.2) has been replaced by a spectral valley and the neighboring peaks have been beefed up and pulled in toward $\Delta = 0$.
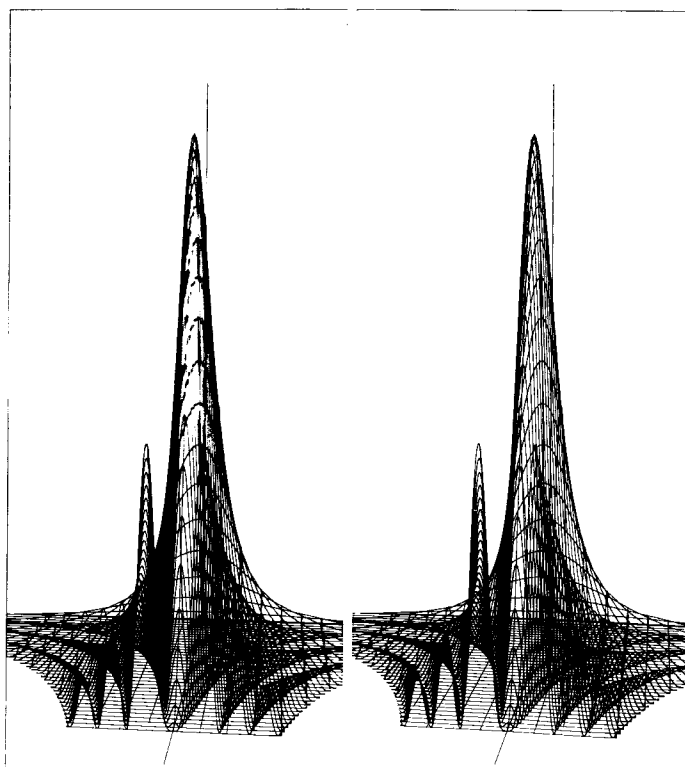
Figure 8.5.2 (Stereoptic pair) Two-level atomic transition probability plotted versus the detuning parameter Δ ($\Delta < 0$ is left and $\Delta > 0$ is right) and elapsed time τ (τ increases coming toward the observer). This is to be compared with approximate probability plotted in Fig. 8.4.2.

In and around the neighborhood between $\Delta = \pm r$ both the approximate quantum theory and the classical phasor picture of the Lorentz model fail. The two-level dipole moment cannot exceed the fixed value of $p = q\langle 2|z|1\rangle$ and therefore cannot grow indefinitely like the classical oscillator without involving more quantum levels. The maximum dipole expectation value is achieved the first time the spin vector is driven to the equator of the spin sphere, that is, when $\beta = \pm \pi/2$ in Eq. (7.4.2) and the states $|1\rangle$ and $|2\rangle$ have equal probabilities. This will happen when the crank polar angle θ in Eq. (8.5.15) exceeds $\pi/4$, and this occurs when $|\Delta|$ is less than the Rabi frequency $|r|$. When the spin vector is horizontal the transition moment is "saturated." Any further excitation or increase in S_z actually causes the $\{S_x S_y\}$ phasor to shrink. Then the system enters the extraordinary regime of "population inversion" in which the excited state $|2\rangle$ has greater probability than the initial state $|1\rangle$. From this discussion one should appreciate how the

infinite phasor plane of the Lorentz model has been replaced by a finite sphere. Atomic phasor space is round!

The spectral envelope of the two-level response curve given by (8.5.17) is the following Lorentzian function:

$$P(\Delta) = r^2/(\Delta^2 + r^2).$$

The half-maximum values of $P(\Delta)$ are $\Delta = \pm r$. This means that the width of the envelope equals the Rabi frequency which is proportional to the amplitude of the driving field and to the induced dipole transition moment. This increase in spectral width due to increased pumping is an elementary example of what is known as laser POWER BROADENING. The extra Fourier sidebands are due to the Rabi oscillation which turns the transition on and off at a rate which depends on the field amplitude and detuning.

D. Bloch-Siegert Corrections

An exact solution for the precessing crank Hamiltonian is given by Eqs. (8.5.5) and (8.5.6). However, this is only an approximate solution to the original Hamiltonian in Eq. (8.5.4b) for which the crank vector oscillates in the x direction only. If we apply the same clockwise rotation operator defined by (8.5.10) the resulting Hamiltonian matrix is not constant. Instead of (8.5.11), we get

$$H^R = R^\dagger(0,0,\Omega t)HR(0,0,\Omega t) = \frac{1}{2}\begin{pmatrix} \varepsilon & r + re^{2i\Omega t} \\ re^{-2i\Omega t} + r & -\varepsilon \end{pmatrix}. \quad (8.5.19)$$

Then the time term $-\Omega J_z$ in (8.5.12) is included and the resulting Schrödinger equation is the following:

$$i\frac{\partial}{\partial t}\begin{pmatrix} \psi_1^R \\ \psi_2^R \end{pmatrix} = \begin{pmatrix} \dfrac{\varepsilon - \Omega}{2} & \dfrac{1}{2}(r + re^{2i\Omega t}) \\ \dfrac{1}{2}(re^{-2i\Omega t} + r) & \dfrac{-\varepsilon + \Omega}{2} \end{pmatrix}\begin{pmatrix} \psi_1^R \\ \psi_2^R \end{pmatrix}. \quad (8.5.20)$$

The off-diagonal terms $((r/2)e^{\pm 2i\Omega t})$ which oscillate at twice the driving frequency are neglected in the so-called *rotating-wave approximation*. Then the resulting equation is the same as (8.5.13a). The crank vector for the exact Hamiltonian consists of the usual static vector $(r, 0, \varepsilon - \Omega)$ [recall Eq. (8.5.13b)] added to another vector of length r which is rotating counterclockwise at angular frequency 2Ω in the xy plane. The total crank vector is given by the following:

$$\omega_x = r + r\cos 2\Omega t, \qquad \omega_y = r\sin 2\Omega t, \qquad \omega_z = \varepsilon - \Omega. \quad (8.5.21)$$

If we had applied the *counter*clockwise rotation operator R instead of $R^\dagger$ we get the same Schrödinger equation as (8.5.20) except everywhere Ω is replaced by $-\Omega$. The resulting Hamiltonian corresponds now to a different static crank vector $(r, 0, \varepsilon + \Omega)$ added to another vector of length r which is rotating *clock*wise in the xy plane at angular frequency 2Ω.

In either case the precessional motion generated by the static part of the crank vector may be perturbed by the rotating r vector. The perturbation will be maximal when the r-vector rotation is synchronized with the precession. The static part of the crank given in (8.5.21) generates a precession angular rate of

$$\omega_{\text{static}} = \pm \sqrt{r^2 + (\varepsilon - \Omega)^2}.$$

Resonance may occur when this is matched by the r-vector rate:

$$-2\Omega = -\left[(\varepsilon - \Omega)^2 + r^2\right]^{1/2}. \qquad (8.5.22)$$

In the counterclockwise frame the same reasoning gives a similar relation:

$$2\Omega = +\left[(\varepsilon + \Omega)^2 + r^2\right]^{1/2}. \qquad (8.5.23)$$

Either of the two preceding equations yield the same magnitudes for the resonant Ω values; only the sign is different. Rearranging the second equation gives

$$3\Omega^2 - 2\varepsilon\Omega - (r^2 + \varepsilon^2) = 0, \qquad (8.5.24)$$

and the possible solutions are

$$\Omega = \left(\varepsilon \pm [4\varepsilon^2 + 3r^2]^{1/2}\right)/3. \qquad (8.5.25)$$

For relatively small Rabi frequency ($r \ll \varepsilon$) the radical may be expanded to give

$$[4\varepsilon^2 + 3r^2]^{1/2} \cong 2\varepsilon + 3r^2/4\varepsilon + \cdots.$$

Then the possible resonances are given approximately as follows:

$$\Omega_1 = \varepsilon\left(1 + (r^2/4\varepsilon^2)\right), \qquad (8.5.26a)$$

$$\Omega_2 = -\varepsilon\left(\tfrac{1}{3} + (r^2/4\varepsilon^2)\right). \qquad (8.5.26b)$$

The first result is only slightly shifted from the RWA value ($\Omega = \varepsilon$ or $\Delta = 0$). The shifting fraction

$$\delta = r^2/4\varepsilon^2 \qquad (8.5.27)$$

is called the Bloch-Siegert shift. For optical laser-induced transitions the Rabi rate is typically $r \equiv 10^{10}$ Hz. This is small compared to the optical frequency which is typically $\varepsilon \equiv 10^{16}$ Hz. This gives a typical shift ratio of $r^2/4\varepsilon^2 \cong 0.25 \times 10^{-12}$, which, until recently, would be considered unobservable. However, if the Rabi rate is significantly increased or if lower-frequency transitions are probed then the RWA predictions must be corrected.

The second solution (8.5.26b) lies at approximately one-third of the primary resonance frequency. This subharmonic resonance is not a strong effect when r is relatively small, but it may lead to interesting effects in other situations.

E. Damping and the Bloch Equations

So far we have considered only the ideal pure states of the pumped two-level system. Now a brief introduction to the real-world effects of decay and noise will be given. This is important for any study of spectroscopy, since rarely, if ever, are these effects totally negligible. In fact, radiative decay and other "damping" mechanisms are so strong that they completely obscured the Rabi two-level optical transition effects until after the laser was invented. Earlier nuclear magnetic spin resonance (NMR) experiments were the first to exhibit two-level oscillation and damping effects, since radiative decay is very small at radio or microwave frequencies. The Bloch theory described below was developed first for NMR phenomenology.

(a) **Time Behavior of the Density Matrix** Statistical treatment of quantum ensembles rely on the density operator ρ introduced in Section 1.3.B. For a pure state $|\Psi\rangle$ the density operator is simply $\rho = |\psi\rangle\langle\psi|$. For an ensemble of systems in various states, ρ will be a weighted sum of such terms.

A representation of a density operator provides a compact way to record the components of the quasispin or Stokes-vector expectation values. For the general pure state vector represented in Figure 7.5.2 the density matrix is the following:

$$\langle \rho \rangle = \begin{pmatrix} \langle 1|\Psi\rangle\langle\Psi|1\rangle & \langle 1|\Psi\rangle\langle\Psi|2\rangle \\ \\ \langle 2|\Psi\rangle\langle\Psi|1\rangle & \langle 2|\Psi\rangle\langle\Psi|2\rangle \end{pmatrix} = \begin{pmatrix} \Psi_1^*\Psi_1 & \Psi_1^*\Psi_2 \\ \\ \Psi_2^*\Psi_1 & \Psi_2^*\Psi_2 \end{pmatrix}$$

$$= \begin{pmatrix} \cos^2 \dfrac{\beta}{2} & e^{-i\alpha} \sin \dfrac{\beta}{2} \cos \dfrac{\beta}{2} \\ \\ e^{i\alpha} \sin \dfrac{\beta}{2} \cos \dfrac{\beta}{2} & \sin^2 \dfrac{\beta}{2} \end{pmatrix}. \qquad (8.5.28)$$

The density matrix may be expanded in terms of the Pauli matrices,

$$\langle \rho \rangle = \frac{1}{2}\begin{pmatrix} 1 & 0 \\ 0 & 1 \end{pmatrix} + \frac{\cos \alpha \sin \beta}{2}\begin{pmatrix} 0 & 1 \\ 1 & 0 \end{pmatrix}$$

$$+ \frac{\sin \alpha \sin \beta}{2}\begin{pmatrix} 0 & -i \\ i & 0 \end{pmatrix} + \frac{\cos \beta}{2}\begin{pmatrix} 1 & 0 \\ 0 & -1 \end{pmatrix}. \qquad (8.5.29)$$

The coefficients of this expansion include the expected spin vector components which were given in terms of Euler angles in Figure 7.5.2 (note that overall phase angle γ disappears):

$$\rho = \tfrac{1}{2}\mathbf{1} + S_x\sigma_x + S_y\sigma_y + S_z\sigma_z,$$

$$\rho = S_0\mathbf{1} + \mathbf{S} \cdot \boldsymbol{\sigma}. \qquad (8.5.30)$$

In general, the quantities $S_i = \text{Trace}(\rho\sigma_i)$ $(i = x, y, z)$ will be the ensemble summed expectation values for the respective components, and S_0 will be the total population of the two levels together throughout the ensemble. Then the summed spin vector magnitude $|\mathbf{S}|$ may be less than S_0. Incoherent or unpolarized ensembles have a zero value for the summed spin vector $(\mathbf{S} = \mathbf{0})$.

The time derivative of a pure state density operator is given using the Schrödinger equation:

$$i\hbar\frac{\partial \rho}{\partial t} = i\hbar\left(\frac{\partial |\psi\rangle}{\partial t}\right)\langle \Psi| + i\hbar|\Psi\rangle\left(\frac{\partial \langle \psi|}{\partial t}\right)$$

$$= H|\Psi\rangle\langle \Psi| - |\Psi\rangle\langle \Psi|H = [H, \rho]. \qquad (8.5.31)$$

The Pauli spinor expansion in Eq. (7.5.4) relates the Hamiltonian to its crank vector $\boldsymbol{\omega}$ and overall phase rate ω_0 (recall, also, Figure 7.5.3):

$$H = \omega_0\mathbf{1} + \boldsymbol{\omega} \cdot \boldsymbol{\sigma}. \qquad (8.5.32)$$

Substituting the Pauli expansions for H and ρ into (8.5.31) yields

$$i\frac{\partial \mathbf{S}}{\partial t} \cdot \boldsymbol{\sigma} = [(\boldsymbol{\omega} \cdot \boldsymbol{\sigma})(\mathbf{S} \cdot \boldsymbol{\sigma}) - (\mathbf{S} \cdot \boldsymbol{\sigma})(\boldsymbol{\omega} \cdot \boldsymbol{\sigma})]/2$$

$$= i[\boldsymbol{\omega} \times \mathbf{S}] \cdot \boldsymbol{\sigma}, \qquad (8.5.33)$$

where the Pauli identity $(\boldsymbol{\sigma} \cdot \mathbf{A})(\boldsymbol{\sigma} \cdot \mathbf{B}) + \mathbf{A} \cdot \mathbf{B} = i\,(\mathbf{A} \times \mathbf{B})$ has been used. The pure state Bloch equation is then given:

$$\frac{\partial \mathbf{S}}{\partial t} = \boldsymbol{\omega} \times \mathbf{S}. \qquad (8.5.34)$$

This is consistent with the picture of the crank vector ω causing the spin vector S to precess as shown in Figure 7.5.3(b).

(b) Bloch Equations

The usual generalization of the Bloch equation to an ensemble involves the addition of phenomenological damping terms as follows. Let us write

$$\frac{\partial S}{\partial t} = \omega \times S - \left[\gamma_2 (S_x - S_x(0)) e_x + \gamma_2 (S_y - S_y(0)) e_y + \gamma_1 (S_z - S_z(0)) e_z \right],$$

$$(8.5.35a)$$

where

$$\gamma_2 = 1/T_2, \qquad \gamma_1 = 1/T_1 \qquad (8.5.35b)$$

relate transverse and longitudinal decay rates γ_1 and γ_2 to transverse and longitudinal lifetimes T_1 and T_2, respectively. The quantities $S_i(0)$ ($i = x, y, z$) are the equilibrium values to which the spin vector components tend to decay. Generally, they are ground state values: $S_x(0) = 0 = S_y(0)$, and $S_z(0) = 1/2$.

The Boltzman population factors for an equilibrated two-level system appear on the diagonal of the density matrix,

$$\langle \rho \rangle = \begin{pmatrix} e^{-\varepsilon_1 \beta} & 0 \\ 0 & e^{-\varepsilon_2 \beta} \end{pmatrix} Z^{-1}. \qquad (8.5.36)$$

Here the Boltzman factor varies inversely with temperature

$$\beta = 1/kT, \qquad (8.5.37)$$

and the partition function

$$Z = e^{-\varepsilon_1 \beta} + e^{-\varepsilon_2 \beta} \qquad (8.5.38)$$

depends on energies ε_1 and ε_2 of the two levels. The average value of the transverse spin components for this system are zero ($S_x(0) = 0 = S_y(0)$) while the longitudinal or z component is the following:

$$\langle S_z(0) \rangle = \frac{1}{2} \text{Trace}(\rho \sigma_z) = \frac{1}{2} \frac{\varepsilon^{-\varepsilon_1 \beta} - \varepsilon^{-\varepsilon_2 \beta}}{\varepsilon^{-\varepsilon_1 \beta} + e^{-\varepsilon_2 \beta}} = \frac{1}{2} \frac{1 - e^{-\varepsilon \beta}}{1 + e^{-\varepsilon \beta}}.$$

Here the two-level energy interval $\varepsilon = \varepsilon_2 - \varepsilon_1$ is assumed positive. For high temperatures ($\varepsilon \beta \to 0$) the z-component approaches zero. For low temperatures ($\varepsilon \beta \gg 1$) the z component approaches its maximum value ($S_z(0) = 1/2$).

E. Dressed Eigenstates

In the rotating frame there are two directions in which the spin vector may be placed and will remain fixed while under the influence of the RWA Hamiltonian. These directions are along and against the ω axis of the crank vector defined by (8.5.13b). The states associated with these spin vectors are called the *dressed eigenstates*. They are simply the eigenstates of the RWA matrix $H^{R'}$ which appears in (8.5.13a). [$H^{R'}$ is simply H^R plus the picture changing term $-\Omega J_z$ as given by Eq. (8.5.12).]

$$H^{R'} = \begin{pmatrix} \dfrac{\Delta}{2} & \dfrac{r}{2} \\ \dfrac{r}{2} & \dfrac{-\Delta}{2} \end{pmatrix}. \tag{8.5.39}$$

The crank axis is tipped by angle $\theta = \tan^{-1}(r/\Delta)$ toward the rotating X_R axis. Hence you can construct dressed eigenstates by simply rotating the spin "up" and "down" states $|1\rangle^R$ and $|2\rangle^R$ by θ around the Y_R axis. The transformation matrix is [from Eqs. (5.4.30) or (7.5.2)]

$$\langle R_D \rangle = \langle e^{-i\theta \mathbf{J}^R} \rangle = \begin{pmatrix} \cos\dfrac{\theta}{2} & -\sin\dfrac{\theta}{2} \\ \sin\dfrac{\theta}{2} & \cos\dfrac{\theta}{2} \end{pmatrix} = \begin{pmatrix} {}^R\langle 1|1\rangle^D & {}^R\langle 1|2\rangle^D \\ {}^R\langle 2|1\rangle^D & {}^R\langle 2|2\rangle^D \end{pmatrix} \tag{8.5.40}$$

It is important to remember that the Y_R axis is rotating around the $Z = Z_R$ axis with angular frequency equal to the laser stimulus frequency Ω. The dressed eigenstates are given in terms of the rotating bases as follows:

$$|1\rangle^D = R_D(0,\theta,0)|1\rangle^R = \cos\frac{\theta}{2}|1\rangle^R + \sin\frac{\theta}{2}|2\rangle^R,$$

$$|2\rangle^D = R_D(0,\theta,0)|2\rangle^R = -\sin\frac{\theta}{2}|1\rangle^R + \cos\frac{\theta}{2}|2\rangle^R. \tag{8.5.41}$$

We check that this transformation diagonalizes matrix $\langle H_{R'} \rangle$.

$$\langle R_D^\dagger H^{R'} R_D \rangle = \begin{pmatrix} \cos\dfrac{\theta}{2} & \sin\dfrac{\theta}{2} \\ -\sin\dfrac{\theta}{2} & \cos\dfrac{\theta}{2} \end{pmatrix} \begin{pmatrix} \dfrac{\Delta}{2} & \dfrac{r}{2} \\ \dfrac{r}{2} & \dfrac{-\Delta}{2} \end{pmatrix} \begin{pmatrix} \cos\dfrac{\theta}{2} & -\sin\dfrac{\theta}{2} \\ \sin\dfrac{\theta}{2} & \cos\dfrac{\theta}{2} \end{pmatrix}$$

$$= \begin{pmatrix} \dfrac{\omega}{2} & 0 \\ 0 & \dfrac{-\omega}{2} \end{pmatrix}. \tag{8.5.42}$$

Here ω is given by (8.5.15) in terms of r, Δ, and θ. This can be rewritten in terms of J_z^D which is the dressed z component.

$$R_D^\dagger H^{R'} R_D = \omega J_z^D. \qquad (8.5.42)$$

The dressed-state amplitudes follow from (8.5.41):

$$\psi_1^D = {}^D\langle 1|\psi\rangle = {}^R\langle 1|R_D^\dagger|\psi\rangle = \cos\frac{\theta}{2}\psi_1^R + \sin\frac{\theta}{2}\psi_2^R,$$

$$\psi_2^D = {}^D\langle 2|\psi\rangle = {}^R\langle 2|R_D^\dagger|\psi\rangle = -\sin\frac{\theta}{2}\psi_1^R + \cos\frac{\theta}{2}\psi_2^R. \qquad (8.5.44)$$

(a) The AC Stark Shifts The two angular frequencies ε and Ω are fundamental to the theory of two-level resonance. The first frequency ε is the frequency of the unperturbed atomic oscillator which is the energy difference of the two unperturbed levels divided by $\hbar$. [Recall Eq. (8.5.4b).] The second frequency Ω is that of the stimulating laser. It is helpful to regard these as the unperturbed frequency levels for the atom and laser, respectively, and the frequency center of gravity is the average value $(\varepsilon + \Omega)/2$. Now we shall see how the dressed eigenlevels are shifted from the unperturbed values ε or Ω if the laser-atom coupling parameter (or Rabi frequency) r is nonzero. The corresponding shifts are called AC-Stark shifts.

If the average value $(\varepsilon + \Omega)/2$ is added to each of the dressed eigenvalues $(\pm\omega/2)$ then one obtains the following:

$$\frac{\varepsilon + \Omega}{2} + \frac{\omega}{2} = \varepsilon + \frac{\omega - \varepsilon + \Omega}{2} = \varepsilon + \frac{\omega - \Delta}{2} \equiv \varepsilon + \frac{\delta}{2}, \qquad (8.5.45a)$$

$$\frac{\varepsilon + \Omega}{2} - \frac{\omega}{2} = \Omega - \frac{\omega - \varepsilon + \Omega}{2} = \Omega - \frac{\omega - \Delta}{2} \equiv \Omega - \frac{\delta}{2}, \qquad (8.5.45b)$$

where $\delta/2$ is defined to be the AC-Stark shift with δ given by the first of the following:

$$\delta = \delta(\Delta) = \omega - \Delta = (\Delta^2 + r^2)^{1/2} - \Delta, \qquad (8.5.45c)$$

$$\delta' = \delta'(\Delta) = \omega + \Delta = (\Delta^2 + r^2)^{1/2} + \Delta. \qquad (8.5.45d)$$

Here, $\Delta = \varepsilon - \Omega$ is the previously defined detuning parameter. When the detuning is negative the "alternate" AC-Stark shift δ' may be more convenient to use. When the stimulus Ω is much greater than resonance frequency ε then $-\Delta \gg r$ and δ' will be a small shift while δ will approach -2Δ.

The shift $\delta/2$ is defined in analogy to the zero-frequency ($\Omega = 0$) shifts or DC-Stark shifts $\delta(\varepsilon)$:

$$\delta(\varepsilon) = \sqrt{\varepsilon^2 + r^2} - \varepsilon. \qquad (8.5.46a)$$

A plot of DC-Stark levels versus the field coupling parameter r was given in Figure 2.12.8 for fixed two-level energy ε. The shift $\delta(\varepsilon)/2$ is the difference between the hyperbola and electric field energy asymptotes. The difference is small when the field energy r is large compared to the unperturbed two-level energy ε.

By analogy, a plot of dressed AC-Stark levels (8.5.45a) is shown in Figure 8.5.3, only now it is made versus the detuning parameter Δ for fixed r and ε. Again, the shift $\delta(\Delta)/2$ represents the spacing between hyperbolic eigen-levels and their respective asymptotes. The DC shifts are indicated above the ($\Omega = 0$) point on the left-hand side of the Figure 8.5.3. These shifts grow into

Atom-Laser
Energy
(Angular frequncy units)

$\varepsilon + \delta(\Delta)/2$

$(\varepsilon + \Omega)/2$

DC
Stark
Shift
$\delta(\varepsilon)/2$

AC
Stark
Shift
$\delta(\Delta)/2$

Rabi
Splitting
2r

$\Omega - \delta(\Delta)/2$

Detuning
$\Delta = \varepsilon - \Omega$

Dressed
Atom
Splitting ω

$\delta(\Delta) = \omega - \Delta$

$\omega(\Delta) = \sqrt{\Delta^2 + r^2}$

$\Delta = \varepsilon - \Omega$

$\varepsilon = 1.0$

$r = 0.5$

Bare
Atom
Splitting
ε

$\delta(\Delta)/2$

$\Delta = \varepsilon$
$\Omega = 0$

$\Delta = 0$
$\Omega = \varepsilon$

Laser Angular
Frequency Ω
or
Detuning Δ

$\delta(\varepsilon)/2$
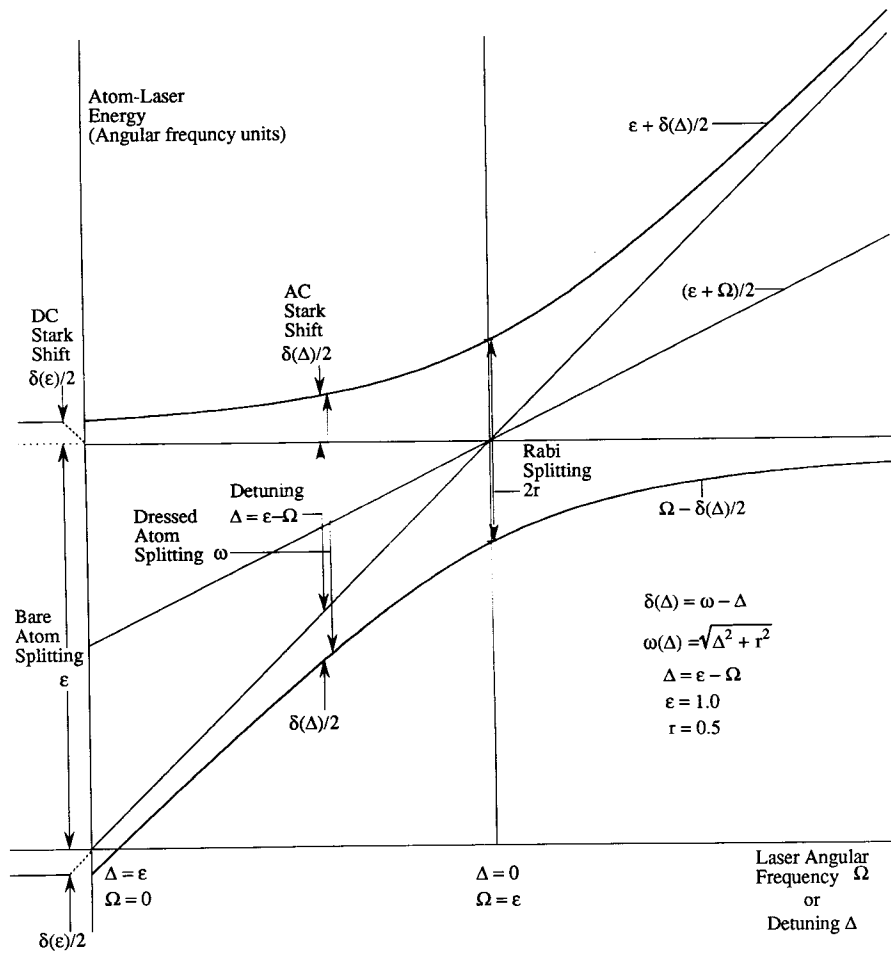
Figure 8.5.3 AC Stark shifts and energy levels for the two-state system. Levels and shifts are plotted as functions of the stimulating laser frequency Ω or detuning parameter $\Delta = \Omega - \varepsilon$ from DC ($\Omega = 0$) to above resonance ($\Omega > \varepsilon$).

larger and larger AC-Stark shifts as the laser frequency increases, and they equal $\delta(0)/2 = r/2$ at resonance. The increasing shift of the excited-state hyperbola above the ε asymptote corresponds to an increasing component of the ground state in the dressed excited state. Similarly, the ground dressed state takes on more of the excited-state character as the lower hyperbola veers away from the Ω asymptote and approaches the horizontal ε asymptote.

To provide a quantitative geometrical interpretation of the mixing let us consider a picture of the quantities Δ, δ, ω, and r in Figure 8.5.4. This is a more detailed representation of the crank diagram in Figure 8.5.1, which shows how to visualize the relevant variables ω and δ as Δ approaches zero. The diagram is based upon the definitions $\delta = \omega - \Delta$, $\omega^2 = \Delta^2 + r^2$, and the relation

$$\delta^2 + r^2 = (\omega - \Delta)^2 + r^2 = 2\Delta^2 + 2r^2 - 2\omega\Delta$$

$$= 2\omega(\omega - \Delta) = 2\omega\delta, \tag{8.5.46b}$$

and the relations (8.5.15b) and (8.5.15c) involving angle θ. We construct three mutually tangent circles of radii δ, Δ, and δ'. The center of the δ and δ' circles lie at the tip of the ω vector, while the Δ circle is centered at the origin and base of ω. (Recall $\delta + \Delta = \omega = \delta' - \Delta$.) This yields a right triangle with altitude δ, base r, hypotenuse $\sqrt{(2\delta\omega)}$, and angle $\theta/2$, as indicated in Figure 8.5.4(a). According to the dressing or diagonalizing transformation (8.5.40) the components of the dressed eigenstates relative to the rotating frame are proportional to the base and altitude, respectively, of this triangle. The state belonging to the lower hyperbola has the following amplitudes in the $\{|1\rangle^R, |2\rangle^R\}$ basis:

$$|1\rangle^D \rightarrow \begin{pmatrix} \cos\dfrac{\theta}{2} \\[2mm] \sin\dfrac{\theta}{2} \end{pmatrix} = \begin{pmatrix} \dfrac{r}{\sqrt{2\delta\omega}} \\[4mm] \dfrac{\delta}{\sqrt{2\delta\omega}} \end{pmatrix}, \tag{8.5.47}$$

while the upper hyperbola belongs to the following orthogonal set of components:

$$|2\rangle^D \rightarrow \begin{pmatrix} -\sin\dfrac{\theta}{2} \\[2mm] \cos\dfrac{\theta}{2} \end{pmatrix} = \begin{pmatrix} \dfrac{-\delta}{\sqrt{2\delta\omega}} \\[4mm] \dfrac{r}{\sqrt{2\delta\omega}} \end{pmatrix}. \tag{8.5.48}$$

On the left-hand side of Figure 8.5.2 the upper hyperbola is shifted by a small amount $((\omega - \Delta)/2 = \delta/2)$ above the ε asymptote and a large amount
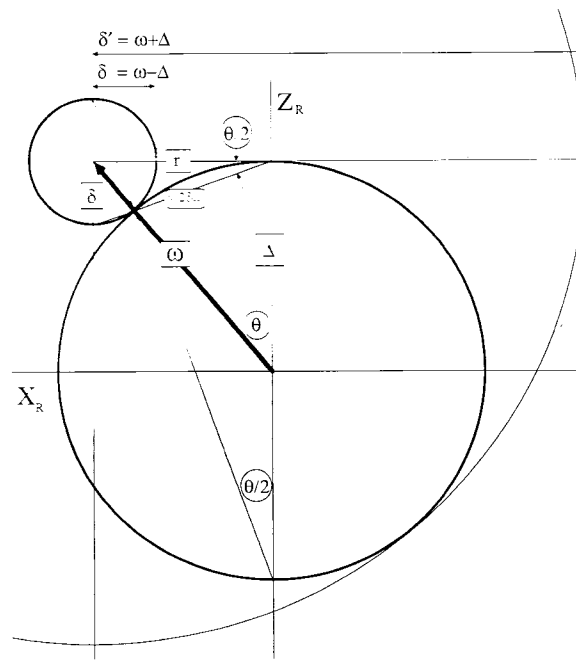
(a) AC-Stark shifts ($\Delta = 1.2$)
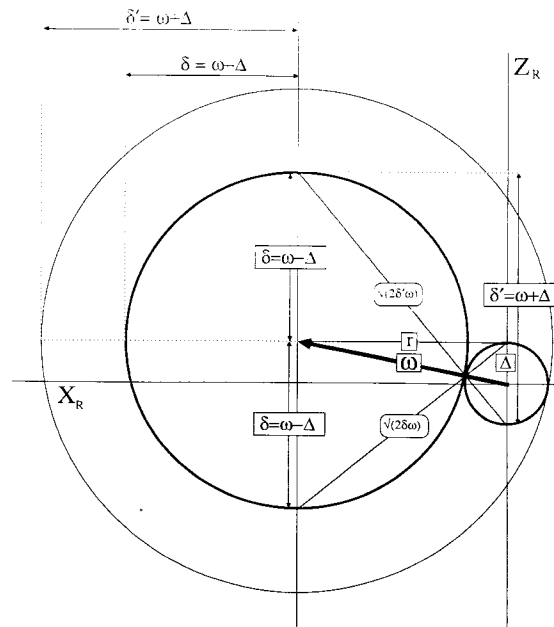
(b) ($\Delta = 0.2$)

Figure 8.5.4 Geometry of ω vector in rotating frame for four values of detuning parameter Δ and fixed Rabi frequency r. This is a detailed version of Figure 8.5.1 which shows the magnitudes of the AC Stark shifts (δ and δ') and the dressed eigenstate amplitudes ($\sqrt{2\delta\omega}$ and $\sqrt{2\delta'\omega}$). (a) Below resonance ($\Delta = 1.2$). (b) Approaching resonance ($\Delta = 0.2$). (c) Just above resonance ($\Delta = 0.2$). (d) Above resonance ($\Delta = -1.2$).

(c) $(\Delta = -0.1)$

(d) $(\Delta = -1.2)$
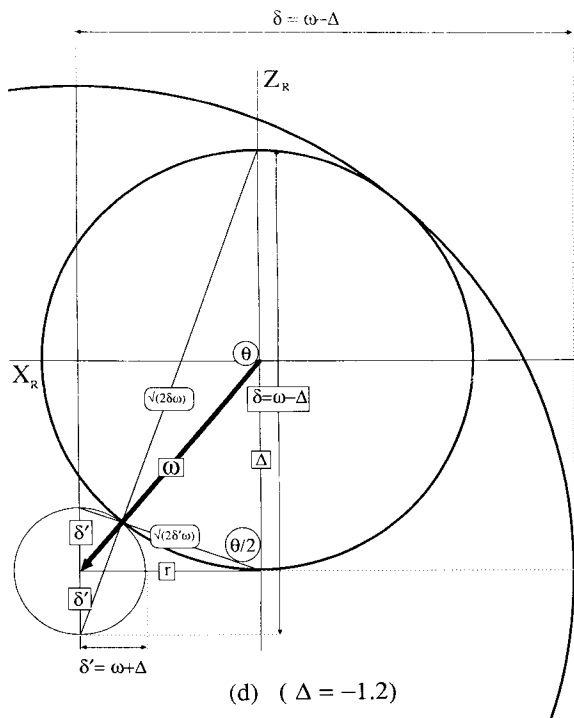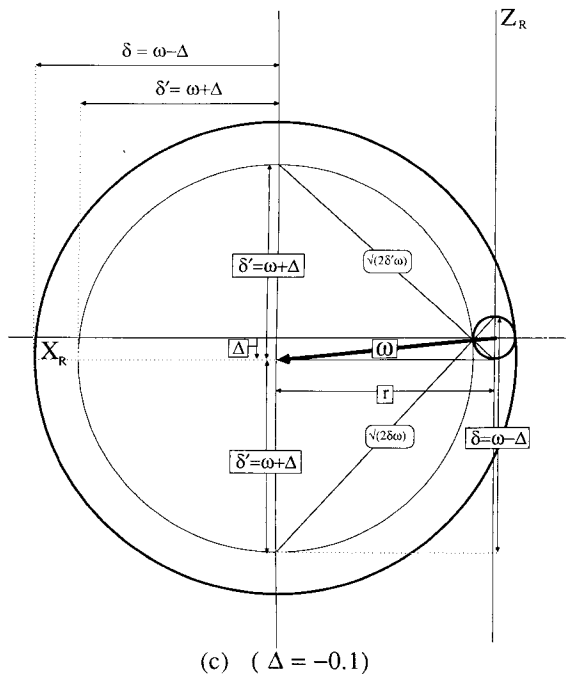
Figure 8.5.4 *(Continued)*.

$((\omega + \Delta)/2 = \delta'/2)$ above the Ω asymptote. The ε asymptote is horizontal while the Ω asymptote has unit slope in the figure. At the resonance point $(\Omega = \varepsilon)$, the detuning parameter Δ changes sign. Then the shift $(\omega - \Delta)/2 = \delta/2$ becomes much larger and approaches Δ while the shift $(\omega + \Delta)/2 = \delta'/2$ becomes smaller as the upper hyperbola moves close to the Ω asymptote.

Meanwhile (for $\Omega > \varepsilon$), the lower hyperbola moves away from the Ω asymptote. The corresponding lower dressed eigenstate represented by (8.5.47) changes from mostly ground state $|1\rangle^R$ $(\delta \ll r)$ to mostly excited state $|2\rangle^R$ $(\delta \gg r)$ as detuning Δ varies from positive to negative values. If Δ is varied slowly enough, and if damping is negligible, then this process can be used to excite two-level systems to nearly 100% inversion. When this happens the systems are said to adiabatically follow the detuning. The angle between the spin vector and the instantaneous crank vector is nearly invariant to slow changes in r or Δ.

The Schrödinger equation for describing the adiabatic following of a dressed state is derived now. First, the derivative of any dressed state is as follows:

$$i\frac{\partial}{\partial t}R_D^\dagger|\psi\rangle^R = i\frac{\partial R_D^\dagger}{\partial t}|\psi\rangle^R + R_D^\dagger i\frac{\partial|\psi\rangle^R}{\partial t}. \qquad (8.5.49)$$

Suppose we let the rate $d\theta/dt$ be a measure of the change of detuning. Then the time derivative of the dressing transformation (8.5.40) is the following:

$$i\frac{\partial R_D^\dagger}{\partial t} = i\frac{\partial e^{i\theta J_y^R}}{\partial t} = -\dot{\theta}J_y^R R_D^\dagger.$$

The derivative of the rotating-wave ket is repeated from Eq. (8.5.12):

$$i\frac{\partial}{\partial t}|\psi\rangle^R = H^{R'}|\psi\rangle^R.$$

Finally, (8.5.43) and the definition (8.5.44) of dressed kets give the following:

$$i\frac{\partial}{\partial t}R_D^\dagger|\psi\rangle^R = -\dot{\theta}J_y^R R_D^\dagger|\psi\rangle^R + R_D^\dagger H^{R'}R_D R_D^\dagger|\psi\rangle^R.$$

This amounts to a contest between a y^R angular velocity of $-d\theta/dt$ and a z^D angular velocity of ω around the crank:

$$i\frac{\partial}{\partial t}|\psi\rangle^D = \left(-\dot{\theta}J_y^R + \omega J_z^D\right)|\psi\rangle^D. \qquad (8.5.50)$$

When the condition $d\theta/dt \ll \omega$ holds it may be possible for the spin vector to follow the crank vector adiabatically. However, this condition is neither necessary nor sufficient for following.

(b) Dressed Bloch Equations The Bloch equations (8.5.35) in the dressed state basis are obtained by applying a y rotation by angle θ to the density operator in the rotating wave basis. This y rotation is represented in the vector basis by a standard Cartesian 3×3 matrix $\langle x_j^D | x_k^R \rangle = \mathbf{e}_j^D \cdot \mathbf{e}_k^R$, where

$$\mathbf{e}_x^D \cdot \mathbf{e}_x^R = \cos\theta, \qquad \mathbf{e}_x^D \cdot \mathbf{e}_y^R = 0, \qquad \mathbf{e}_x^D \cdot \mathbf{e}_z^R = -\sin\theta, \quad \text{etc.}$$

Applying this matrix and its inverse to Γ^R in the rotating wave basis $\{\mathbf{e}_x^R, \mathbf{e}_y^R, \mathbf{e}_z^R\}$ gives the following transformed damping matrix expressed in the dressed basis $\{\mathbf{e}_x^D, \mathbf{e}_y^D, \mathbf{e}_z^D\}$.

$$
\langle \Gamma \rangle^D = \begin{pmatrix} \cos\theta & 0 & -\sin\theta \\ 0 & 1 & 0 \\ \sin\theta & 0 & \cos\theta \end{pmatrix} \begin{pmatrix} \gamma_2 & \cdot & \cdot \\ \cdot & \gamma_2 & \cdot \\ \cdot & \cdot & \gamma_1 \end{pmatrix} \begin{pmatrix} \cos\theta & 0 & \sin\theta \\ 0 & 1 & 0 \\ -\sin\theta & 0 & \cos\theta \end{pmatrix}
$$

$$
= \begin{pmatrix} \gamma_2 \cos^2\theta + \gamma_1 \sin^2\theta & 0 & -(\gamma_1 - \gamma_2)\cos\theta\sin\theta \\ 0 & \gamma_2 & 0 \\ -(\gamma_1 - \gamma_2)\cos\theta\sin\theta & 0 & \gamma_1 \cos^2\theta + \gamma_2 \sin^2\theta \end{pmatrix}
$$

The effective crank vector for constant detuning $\Delta = \varepsilon - \Omega$ has only an $\mathbf{e}_z^D$ component,

$$\boldsymbol{\omega} = \omega \mathbf{e}_z^D,$$

where according to equation (8.5.15c)

$$\omega = \frac{\Delta}{\cos\theta}.$$

If the detuning is changing, the crank vector also has an $\mathbf{e}_y^D$ component according to Eq. (8.5.50),

$$\boldsymbol{\omega} = \omega \mathbf{e}_z^D - \dot\theta \mathbf{e}_y^D.$$

The dressed Bloch equations (8.5.35) then become the following:

$$
\dot{S}_x^D = -\omega S_y^D - \dot\theta S_z^D - \left(\gamma_2 \cos^2\theta + \gamma_1 \sin^2\theta\right)\left(S_x^D - S_x^D(0)\right)
$$
$$
+ (\gamma_1 - \gamma_2)\cos\theta\sin\theta\left(S_z^D - S_z^D(0)\right),
$$
$$
\dot{S}_y^D = \omega S_x^D - \gamma_2\left(S_y^D - S_y^D(0)\right),
$$
$$
\dot{S}_z^D = \dot\theta S_x^D + (\gamma_1 - \gamma_2)\cos\theta\sin\theta\left(S_x^D - S_x^D(0)\right)
$$
$$
- \left(\gamma_2 \sin^2\theta + \gamma_1 \cos^2\theta\right)\left(S_z^D - S_z^D(0)\right).
$$

These are the equations that replace the Lorentz forced damped oscillator model for atomic spectral transitions. Many texts have been written describing the nature of their solutions as it applies to laser dynamics and quantum electronics.

8.6 QUANTUM ELECTROMAGNETIC FIELDS AND TRANSITIONS

The fully quantum-mechanical treatment of electromagnetic spectral transitions will be given now. It begins by converting the classical em field equations to harmonic oscillator equations for which the quantum states are well known.

A linearly polarized plane wave was described by the classical vector potential (8.4.6) as follows:

$$\mathbf{A} = \mathbf{e}_1 2|a|\sin(\mathbf{k} \cdot \mathbf{r} - \omega t + \phi). \tag{8.6.1a}$$

This gives the following em fields (we neglect the nonradiative or static field $\mathbf{E} = -\nabla\Phi$):

$$\mathbf{E} = -\frac{\partial \mathbf{A}}{\partial t} \qquad\qquad \mathbf{B} = \nabla \times \mathbf{A}$$

$$= \mathbf{e}_1 E_0 \cos(\mathbf{k} \cdot \mathbf{r} - \omega t + \phi) \qquad = (\mathbf{k} \times \mathbf{e}_1)B_0 \cos(\mathbf{k} \cdot \mathbf{r} - \omega t + \phi). \tag{8.6.1b}$$

The electric E-polarization vector at zero phase is along unit vector $\mathbf{e}_1$:

$$E_0 \mathbf{e}_1 = 2|a|\omega \mathbf{e}_1. \tag{8.6.1c}$$

At the same time the magnetic B-polarization vector is along a unit vector $\mathbf{b}_1 = \mathbf{e}_2$, which is orthogonal to $\mathbf{e}_1$ and wave vector $\mathbf{k}$:

$$B_0 \mathbf{b}_1 = B_0(\mathbf{k} \times \mathbf{e}_1) = \mathbf{e}_2 2|a|\omega/c \qquad (\text{where } k = \omega/c). \tag{8.6.1d}$$

In preparation for a quantum-mechanical theory we shall rewrite the vector potential $\mathbf{A}$ as follows:

$$\mathbf{A} = a_{k,1}\mathbf{e}_1 e^{i(\mathbf{k}\cdot\mathbf{r} - \omega t)} + a_{k,1}^* \mathbf{e}_1 e^{-i(\mathbf{k}\cdot\mathbf{r} - \omega t)}, \tag{8.6.2a}$$

where the complex phasor amplitude $a = a_{k,1}$ is given by

$$a_{k,1} = -i|a_{k,1}|e^{i\phi_{k,1}}. \tag{8.6.2b}$$

This will be made to give classical canonical phase-space coordinate of the field and, eventually, the quantum field operators.

It is instructive to calculate the magnitude of the phasor for one quantum of em action. In other words, we need the magnitude of the vector potential

for a wave which contains one "photon" in a cavity of volume V. The time averaged em field energy $\langle U \rangle V$ for a plane wave in volume V follows using $\langle \cos^2 \omega t \rangle = \frac{1}{2}$:

$$\langle U \rangle V = \left\langle \frac{\varepsilon_0}{2} \mathbf{E} \cdot \mathbf{E} + \frac{1}{2\mu_0} \mathbf{B} \cdot \mathbf{B} \right\rangle V$$

$$= V \left(\frac{\varepsilon_0}{2} 4|a|^2 \omega^2 + 4 \frac{|a|^2}{2\mu_0} \right) \langle \cos^2 (\mathbf{k} \cdot \mathbf{r} - \omega t + \phi) \rangle$$

$$= 2\varepsilon_0 \omega^2 |a|^2 V = 2(k^2/\mu_0)|a|^2 V. \tag{8.6.3}$$

By equating this to Planck's quantum ($\langle U \rangle V = \hbar\omega$) we derive

$$|a| = \sqrt{\frac{\hbar\omega}{2\varepsilon_0 \omega^2 V}} = \sqrt{\frac{\hbar}{2\varepsilon_0 \omega V}} = A \qquad \text{(for one photon).} \tag{8.6.4}$$

This is the "photon unit" of quantum field $\mathbf{A}$. Note that it is an inverse root function of frequency which in turn is proportional to the magnitude k of wave vector $\mathbf{k}$ through the vacuum dispersion relation $\omega = ck = k/\sqrt{\mu_0\varepsilon_0}$.

A. Electromagnetic Fields and Operators

To completely describe an electromagnetic field in a box or "cavity" we need one phasor term like (8.6.2) for every possible value of $\mathbf{k}$ and for each choice $\mathbf{e}_1$ or $\mathbf{e}_2$ of polarization orthogonal to $\mathbf{k}$. The complete expression for the classical $\mathbf{A}$ is a sum over the possible modes:

$$\mathbf{A} = \sum_{\mathbf{k}} \left[(a_{\mathbf{k}1}\mathbf{e}_1 + a_{\mathbf{k}2}\mathbf{e}_2) e^{i(\mathbf{k} \cdot \mathbf{r} - \omega t)} + \text{c.c.} \right]$$

$$= \sum_{\mathbf{k}} \sum_{\alpha=1}^{2} \left[a_{\mathbf{k}\alpha}\mathbf{e}_\alpha e^{i(\mathbf{k} \cdot \mathbf{r} - \omega t)} + a_{\mathbf{k}\alpha}^* \mathbf{e}_\alpha e^{-i(\mathbf{k} \cdot \mathbf{r} - \omega t)} \right]. \tag{8.6.5a}$$

Here the $\mathbf{k}$ vector satisfies box boundary conditions

$$k_\beta = n_\beta \frac{2\pi}{L} \qquad (n_\beta = 1, 2, \ldots, j, \quad \beta = x, y, z), \tag{8.6.5b}$$

where L is the length of any side of the box. The classical electric field is

$$\mathbf{E} = \sum_{\mathbf{k}} \sum_{\alpha} \left[i a_{\mathbf{k}\alpha} \omega \mathbf{e}_\alpha e^{i(\mathbf{k} \cdot \mathbf{r} - \omega t)} - i a_{\mathbf{k}\alpha}^* \omega \mathbf{e}_\alpha e^{-i(\mathbf{k} \cdot \mathbf{r} - \omega t)} \right]. \tag{8.6.5c}$$

The magnetic field is

$$\mathbf{B} = \sum_{\mathbf{k}} \sum_{\alpha} \left[i a_{\mathbf{k}\alpha} k \mathbf{b}_{\alpha} e^{i(\mathbf{k}\cdot\mathbf{r}-\omega t)} - i a_{\mathbf{k}\alpha} k \mathbf{b}_{\alpha} e^{-i(\mathbf{k}\cdot\mathbf{r}-\omega t)} \right], \quad (8.6.5d)$$

where unit vector $\mathbf{b}_{\alpha} = \mathbf{k} \times \mathbf{e}_{\alpha}/k$ is orthogonal to $\mathbf{k}$ and $\mathbf{e}_{\alpha}$.

(a) Classical Phasor Energy Relations The classical Hamiltonian follows from an integral over volume V of the energy density in (8.6.3). The electric contribution is

$$U_E V = \frac{\varepsilon_0}{2} \int d^3 \mathbf{r} \, \mathbf{E} \cdot \mathbf{E}, \quad (8.6.6a)$$

where

$$\mathbf{E} \cdot \mathbf{E} = \sum_{\mathbf{k}'\alpha'} \sum_{\mathbf{k}\alpha} \left(i a_{\mathbf{k}'\alpha'} \omega' \mathbf{e}_{\alpha'} e^{i(\mathbf{k}'\cdot\mathbf{r}-\omega' t)} + \text{c.c.} \right) \cdot \left(i a_{\mathbf{k}\alpha} \omega \mathbf{e}_{\alpha} e^{i(\mathbf{k}\cdot\mathbf{r}-\omega t)} + \text{c.c.} \right)$$

$$= \sum_{\mathbf{k}'\alpha'} \sum_{\mathbf{k}\alpha} \Big[-a_{\mathbf{k}'\alpha'} a_{\mathbf{k}\alpha} \omega' \omega \mathbf{e}_{\alpha'} \cdot \mathbf{e}_{\alpha} e^{i(\mathbf{k}'+\mathbf{k})\cdot\mathbf{r}-i(\omega'+\omega)t}$$

$$-a_{\mathbf{k}'\alpha'}^* a_{\mathbf{k}\alpha}^* \omega' \omega \mathbf{e}_{\alpha'} \cdot \mathbf{e}_{\alpha} e^{-i(\mathbf{k}'+\mathbf{k})\cdot\mathbf{r}+i(\omega'+\omega)t}$$

$$+a_{\mathbf{k}'\alpha'}^* a_{\mathbf{k}\alpha} \omega' \omega \mathbf{e}_{\alpha'} \cdot \mathbf{e}_{\alpha} e^{i(\mathbf{k}'-\mathbf{k})\cdot\mathbf{r}-i(\omega'-\omega)t}$$

$$+a_{\mathbf{k}'\alpha'} a_{\mathbf{k}\alpha}^* \omega' \omega \mathbf{e}_{\alpha'} \cdot \mathbf{e}_{\alpha} e^{-i(\mathbf{k}'-\mathbf{k})\cdot\mathbf{r}+i(\omega'-\omega)t} \Big]. \quad (8.6.6b)$$

This simplifies if we use wave and polarization normalization conditions:

$$\int d^3 \mathbf{r} \, e^{i(\mathbf{k}'+\mathbf{k})\cdot\mathbf{r}} = \delta_{\mathbf{k}',-\mathbf{k}} V \quad \text{and} \quad \mathbf{e}_{\alpha'} \cdot \mathbf{e}_{\alpha} = \delta_{\alpha'\alpha}.$$

The result is

$$U_E V = \sum_{\mathbf{k}\alpha} \frac{\varepsilon_0 V}{2} \left[2|a_{\mathbf{k}\alpha}|^2 \omega^2 - a_{-\mathbf{k}\alpha}^* a_{\mathbf{k}\alpha}^* \omega^2 e^{2i\omega t} - a_{-\mathbf{k}\alpha} a_{\mathbf{k}\alpha} \omega^2 e^{-2i\omega t} \right]. \quad (8.6.7)$$

The magnetic energy $U_B V = \int d^3 r \, \mathbf{B} \cdot \mathbf{B}/2u_0$ has the same form as (8.6.6) if we do the following substitutions

$$\mathbf{E} \to \mathbf{B}, \ \frac{\varepsilon_0}{2} \to \frac{1}{2\mu_0}, \ \omega \mathbf{e}_{\alpha} \to k \mathbf{b}_{\alpha} \equiv \mathbf{k} \times \mathbf{e}_{\alpha}, \ \omega' \mathbf{e}_{\alpha'} \to k' \mathbf{b}_{\alpha'} \equiv \mathbf{k}' \times \mathbf{e}_{\alpha'}.$$

After integration the cross terms have the opposite sign as they did in (8.6.6b). We get $\delta_{\mathbf{k}',-\mathbf{k}} kk' = -k^2$ in the $\mathbf{B} \cdot \mathbf{B}$ integral instead of $\delta_{\mathbf{k}',-\mathbf{k}} \omega \omega' =$

ω^2 which arose in the $\mathbf{E} \cdot \mathbf{E}$ integral. The magnetic energy is

$$U_B V = \sum_{\mathbf{k}\alpha} \frac{V}{2\mu_0} \left[2|a_{\mathbf{k}\alpha}|^2 k^2 + a^*_{-\mathbf{k}\alpha} a^*_{\mathbf{k}\alpha} k^2 e^{2i\omega t} + a_{-\mathbf{k}\alpha} a_{\mathbf{k}\alpha} k^2 e^{-2i\omega t} \right]$$

$$= \sum_{\mathbf{k}\alpha} \frac{\varepsilon_0 V}{2} \left[2|a_{\mathbf{k}\alpha}|^2 \omega^2 + a^*_{-\mathbf{k}\alpha} a^*_{\mathbf{k}\alpha} \omega^2 e^{2i\omega t} + a_{-\mathbf{k}\alpha} a_{\mathbf{k}\alpha} \omega^2 e^{-2i\omega t} \right]. \quad (8.6.8)$$

In the second line of the foregoing we use the dispersion relation for light:

$$\omega^2 = c^2 k^2 = k^2 / (\mu_0 \varepsilon_0). \quad (8.6.9)$$

The change of sign makes the electric cross-terms cancel the magnetic ones. The sum of electric and magnetic energies [(8.6.7) and (8.6.8)] is then just a sum of elementary mode energy density values (8.6.3). That simple formula is all we need!

$$UV = (U_E + U_B)V = \sum_{\mathbf{k}\alpha} 2\varepsilon_0 \omega^2 |a_{\mathbf{k}\alpha}|^2 V. \quad (8.6.10)$$

Each mode labeled $\mathbf{k}$ and polarization α is described by a classical complex phasor variable $a_{\mathbf{k}\alpha}$. The real and imaginary parts of this variable can be treated as classical position Q and momentum P of an oscillator as described in Chapter 7. [Recall (7.5.9) and (7.5.10).]

(b)   Classical Field Oscillator Variables   Let us factor the phasor expression for field energy as follows:

$$UV = \sum_{\mathbf{k}\alpha} 2\varepsilon_0 V \omega^2 a^*_{\mathbf{k}\alpha} a_{\mathbf{k}\alpha} = \sum_{\mathbf{k}\alpha} \tfrac{1}{2} \left[2\omega\sqrt{\varepsilon_0 V}\left(a^{\mathrm{Re}}_{\mathbf{k}\alpha} - i a^{\mathrm{Im}}_{\mathbf{k}\alpha}\right) \right] \left[2\omega\sqrt{\varepsilon_0 V}\left(a^{\mathrm{Re}}_{\mathbf{k}\alpha} + i a^{\mathrm{Im}}_{\mathbf{k}\alpha}\right) \right]$$

$$= \sum_{\mathbf{k}\alpha} \tfrac{1}{2}\left[\omega Q_{\mathbf{k}\alpha} - i P_{\mathbf{k}\alpha}\right]\left[\omega Q_{\mathbf{k}\alpha} + i P_{\mathbf{k}\alpha}\right]$$

$$= \sum_{\mathbf{k}\alpha} \tfrac{1}{2}\left(P^2_{\mathbf{k}\alpha} + \omega^2 Q^2_{\mathbf{k}\alpha}\right). \quad (8.6.11)$$

Note that frequency $\omega = \omega(k)$ is a function of k. The canonical phase space variables are

$$Q_{\mathbf{k}\alpha} = 2\sqrt{\varepsilon_0 V}\, a^{\mathrm{Re}}_{\mathbf{k}\alpha} = \sqrt{\varepsilon_0 V}\,(a_{\mathbf{k}\alpha} + a^*_{\mathbf{k}\alpha}), \quad (8.6.12\mathrm{a})$$

$$P_{\mathbf{k}\alpha} = 2\omega\sqrt{\varepsilon_0 V}\, a^{\mathrm{Im}}_{\mathbf{k}\alpha} = \omega\sqrt{\varepsilon_0 V}\,(a_{\mathbf{k}\alpha} - a^*_{\mathbf{k}\alpha})/i. \quad (8.6.12\mathrm{b})$$

The inverse of the foregoing gives the original phasor variables and their

conjugates in terms of P's and Q's:

$$a_{\mathbf{k}\alpha} = a_{\mathbf{k}\alpha}^{\mathrm{Re}} + ia_{\mathbf{k}\alpha}^{\mathrm{Im}} = \frac{1}{2\sqrt{\varepsilon_0 V}} (Q_{\mathbf{k}\alpha} + iP_{\mathbf{k}\alpha}/\omega), \qquad (8.6.13a)$$

$$a_{\mathbf{k}\alpha}^* = a_{\mathbf{k}\alpha}^{\mathrm{Re}} - ia_{\mathbf{k}\alpha}^{\mathrm{Im}} = \frac{1}{2\sqrt{\varepsilon_0 V}} (Q_{\mathbf{k}\alpha} - iP_{\mathbf{k}\alpha}/\omega). \qquad (8.6.13b)$$

The cavity energy UV in (8.6.11) shall be the classical electromagnetic field Hamiltonian $H = H(Q, P)$. H describes a set of independent harmonic oscillators. To obtain a quantum field theory we make these into quantum oscillators. The situation is very similar to the molecular vibration problem in which a set of classical normal modes were "quantized" in Chapter 4.

(c) Quantum Field Operators   Oscillator ladder operations $\mathbf{a}$ and $\mathbf{a}^\dagger$ were defined in (4.4.50) in terms of coordinate and momentum operators. For each em mode $(\mathbf{k}, \alpha)$ this definition translates to the following:

$$\mathbf{a}_{\mathbf{k}\alpha} = \sqrt{\frac{\omega}{2\hbar}} (\mathbf{Q}_{\mathbf{k}\alpha} + i\mathbf{P}_{\mathbf{k}\alpha}/\omega), \qquad (8.6.14a)$$

$$\mathbf{a}_{\mathbf{k}\alpha}^\dagger = \sqrt{\frac{\omega}{2\hbar}} (\mathbf{Q}_{\mathbf{k}\alpha} - i\mathbf{P}_{\mathbf{k}\alpha}/\omega), \qquad (8.6.14b)$$

where boldface notation $\mathbf{Q}_{\mathbf{k}\alpha}$ and $\mathbf{P}_{\mathbf{k}\alpha}$ indicates the quantum operators that correspond to the classical phase variables $Q_{\mathbf{k}\alpha}$ and $P_{\mathbf{k}\alpha}$, respectively.

By comparing (8.6.14) with (8.6.13) we note that the ladder operators are proportional to whatever operator would correspond to the classical phasor amplitude. So with correspondences $Q_{\mathbf{k}\alpha} \to \mathbf{Q}_{\mathbf{k}\alpha}$ and $P_{\mathbf{k}\alpha} \to \mathbf{P}_{\mathbf{k}\alpha}$ we have the phasor correspondence relations:

$$a_{\mathbf{k}\alpha} = \frac{1}{2\sqrt{\varepsilon_0 V}}(Q_{\mathbf{k}\alpha} + iP_{\mathbf{k}\alpha}/\omega) \to \frac{1}{2\sqrt{\varepsilon_0 V}}(\mathbf{Q}_{\mathbf{k}\alpha} + i\mathbf{P}_{\mathbf{k}\alpha}/\omega)$$

$$= \frac{1}{2\sqrt{\varepsilon_0 V}} \sqrt{\frac{2\hbar}{\omega}} \mathbf{a}_{\mathbf{k}\alpha} = \sqrt{\frac{\hbar}{2\varepsilon_0 \omega V}} \mathbf{a}_{\mathbf{k}\alpha},$$

$$a_{\mathbf{k}\alpha}^* = \frac{1}{2\sqrt{\varepsilon_0 V}}(Q_{\mathbf{k}\alpha} - iP_{\mathbf{k}\alpha}/\omega) \to \frac{1}{2\sqrt{\varepsilon_0 V}}(\mathbf{Q}_{\mathbf{k}\alpha} - i\mathbf{P}_{\mathbf{k}\alpha}/\omega)$$

$$= \frac{1}{2\sqrt{\varepsilon_0 V}} \sqrt{\frac{2\hbar}{\omega}} \mathbf{a}_{\mathbf{k}\alpha}^\dagger = \sqrt{\frac{\hbar}{2\varepsilon_0 \omega V}} \mathbf{a}_{\mathbf{k}\alpha}^\dagger. \qquad (8.6.15)$$

The proportionality or scale factor (8.6.15) turns out to be the quantum

amplitude derived in (8.6.4). Note that coordinate and momentum operators are observables and are self-conjugate ($\mathbf{Q} = \mathbf{Q}^\dagger$ and $\mathbf{P} = \mathbf{P}^\dagger$). The phasor operator $\mathbf{a}$ is a complex combination of observables and therefore is not self-conjugate.

The oscillator Hamiltonian operator for the quantum field is the same form as (4.4.52), namely,

$$\mathbf{H} = \sum_{\mathbf{k}\alpha} \hbar\omega\left(\mathbf{a}_{\mathbf{k}\alpha}^\dagger \mathbf{a}_{\mathbf{k}\alpha} + \tfrac{1}{2}\right). \tag{8.6.16}$$

This is the same for the classical energy (8.5.10) or (8.6.11) except for the extra $\hbar\omega/2$ terms which are each mode's quantum zero-point energy. The eigenvalues of the number operator $\mathbf{a}_{\mathbf{k}\alpha}^\dagger \mathbf{a}_{\mathbf{k}\alpha}$ are the number $n_{\mathbf{k}\alpha}$ of photons in mode $(\mathbf{k}, \alpha)$. The creation or destruction operators $\mathbf{a}_{\mathbf{k}\alpha}^\dagger$ and $\mathbf{a}_{\mathbf{k}\alpha}$ raise or lower the photon number:

$$\mathbf{a}_{\mathbf{k}\alpha}^\dagger | \cdots n_{\mathbf{k}\alpha} \cdots n_{\mathbf{k}'\alpha'} \cdots \rangle = \sqrt{n_{\mathbf{k}\alpha} + 1} | \cdots n_{\mathbf{k}\alpha} + 1 \cdots n_{\mathbf{k}'\alpha'} \cdots \rangle,$$

$$\mathbf{a}_{\mathbf{k}\alpha} | \cdots n_{\mathbf{k}\alpha} \cdots n_{\mathbf{k}'\alpha'} \cdots \rangle = \sqrt{n_{\mathbf{k}\alpha}} | \cdots n_{\mathbf{k}\alpha} - 1 \cdots n_{\mathbf{k}'\alpha'} \cdots \rangle,$$

$$\mathbf{a}_{\mathbf{k}'\alpha'}^\dagger | \cdots n_{\mathbf{k}\alpha} \cdots n_{\mathbf{k}'\alpha'} \cdots \rangle = \sqrt{n_{\mathbf{k}'\alpha'} + 1} | \cdots n_{\mathbf{k}\alpha} \cdots n_{\mathbf{k}'\alpha'} + 1 \cdots \rangle,$$

$$\mathbf{a}_{\mathbf{k}'\alpha'} | \cdots n_{\mathbf{k}\alpha} \cdots n_{\mathbf{k}'\alpha'} \cdots \rangle = \sqrt{n_{\mathbf{k}'\alpha'}} | \cdots n_{\mathbf{k}\alpha} \cdots n_{\mathbf{k}'\alpha'} - 1 \cdots \rangle.$$

$$\tag{8.6.17}$$

Again, these relations are the same as before. [See (4.4.62).] Here each additional quanta contributes an increase in $\mathbf{A}$ amplitude equal to the scale factor $\sqrt{\hbar/2\varepsilon_0\omega V}$ in the correspondence relation (8.6.15).

The quantum $\mathbf{A}$-field operator corresponding to the classical field (8.6.5a) is found by replacing $a_{\mathbf{k}\alpha}$ and $a_{\mathbf{k}\alpha}^*$ according to (8.6.15):

$$\mathbf{A} = \sum_{\mathbf{k}\alpha} \sqrt{\frac{\hbar}{2\varepsilon_0\omega V}} \left[\mathbf{a}_{\mathbf{k}\alpha} \mathbf{e}_\alpha e^{i(\mathbf{k}\cdot\mathbf{r} - \omega t)} + \mathbf{a}_{\mathbf{k}\alpha}^\dagger \mathbf{e}_\alpha e^{-i(\mathbf{k}\cdot\mathbf{r} - \omega t)} \right]. \tag{8.6.18}$$

The time dependence of the ladder operators is determined by the operator equations: $i\hbar\dot{\mathbf{O}} = [\mathbf{H}, \mathbf{O}]$ [recall (8.5.31)]:

$$i\hbar\dot{\mathbf{a}}_{\mathbf{k}\alpha} = [\mathbf{H}, \mathbf{a}_{\mathbf{k}\alpha}] \qquad i\hbar\dot{\mathbf{a}}_{\mathbf{k}\alpha}^\dagger = \left[\mathbf{H}, \mathbf{a}_{\mathbf{k}\alpha}^\dagger\right]$$

$$= -\hbar\omega\mathbf{a}_{\mathbf{k}\alpha} \qquad\qquad = \hbar\omega\mathbf{a}_{\mathbf{k}\alpha}^\dagger.$$

Here we use the $\mathbf{a}^\dagger\mathbf{a}$ form (8.6.16) of the field Hamiltonian and the standard commutation relation (4.4.51) which is repeated in the following

[recall also (4.4.53)]:

$$\left[\mathbf{a}_{\mathbf{k}\alpha}, \mathbf{a}_{\mathbf{k}'\alpha'}^{\dagger}\right] = \delta_{\mathbf{k},\mathbf{k}'}\delta_{\alpha,\alpha'}\mathbf{1}. \qquad (8.6.19)$$

According to the foregoing à equations the ladder operators have the following time-dependent phases:

$$\mathbf{a}_{\mathbf{k}\alpha} = \mathbf{a}_{\mathbf{k}\alpha}(0)e^{i\omega t}. \qquad \mathbf{a}_{\mathbf{k}\alpha} = \mathbf{a}_{\mathbf{k}\alpha}^{\dagger}(0)e^{-i\omega t}.$$

The phases cancel time factors in (8.6.18) to give a time-independent field operators

$$\mathbf{A} = \sum_{\mathbf{k}\alpha} \sqrt{\frac{\hbar}{2\varepsilon_0\omega V}} \left[\mathbf{a}_{\mathbf{k}\alpha}(0)e^{i\mathbf{k}\cdot\mathbf{r}} + \mathbf{a}_{\mathbf{k}\alpha}^{\dagger}(0)e^{-i\mathbf{k}\cdot\mathbf{r}}\right]\mathbf{e}_{\alpha}. \qquad (8.6.20\text{a})$$

The electric and magnetic quantum field operators follow:

$$\mathbf{E} = \sum_{\mathbf{k}\alpha} \sqrt{\frac{\hbar}{2\varepsilon_0\omega V}} \left[-i\omega\mathbf{a}_{\mathbf{k}\alpha}(0)e^{i\mathbf{k}\cdot\mathbf{r}} + i\omega\mathbf{a}_{\mathbf{k}\alpha}^{\dagger}(0)e^{-i\mathbf{k}\cdot\mathbf{r}}\right]\mathbf{e}_{\alpha}, \qquad (8.6.20\text{b})$$

$$\mathbf{B} = \sum_{\mathbf{k}\alpha} \sqrt{\frac{\hbar}{2\varepsilon_0\omega V}} \left[ik\mathbf{a}_{\mathbf{k}\alpha}(0)e^{i\mathbf{k}\cdot\mathbf{r}} - ik\mathbf{a}_{\mathbf{k}\alpha}^{\dagger}(0)e^{-i\mathbf{k}\cdot\mathbf{r}}\right]\mathbf{b}_{\alpha}. \qquad (8.6.20\text{c})$$

When atoms are much smaller than the wavelength ($\lambda = 2\pi/k$) of the radiation, the fields can be simplified by the dipole approximation $e^{i\mathbf{k}\cdot\mathbf{r}} \cong 1$.

$$\mathbf{A} \cong \sum_{\mathbf{k}\alpha} \sqrt{\frac{\hbar}{2\varepsilon_0\omega V}} \left[\mathbf{a}_{\mathbf{k}\alpha} + i\omega\mathbf{a}_{\mathbf{k}\alpha}^{\dagger}\right]\mathbf{e}_{\alpha} = \sum_{\mathbf{k}\alpha} \sqrt{\frac{1}{\varepsilon_0 V}}\, \mathbf{Q}_{\mathbf{k}\alpha}\mathbf{e}_{\alpha}, \qquad (8.6.20\text{d})$$

$$\mathbf{E} \cong \sum_{\mathbf{k}\alpha} \sqrt{\frac{\hbar}{2\varepsilon_0\omega V}}\, i\omega\left[\mathbf{a}_{\mathbf{k}\alpha}^{\dagger} - \mathbf{a}_{\mathbf{k}\alpha}\right]\mathbf{e}_{\alpha} = \sum_{\mathbf{k}\alpha} \sqrt{\frac{1}{\varepsilon_0 V}}\, \mathbf{P}_{\mathbf{k}\alpha}\mathbf{e}_{\alpha}, \qquad (8.6.20\text{e})$$

$$\mathbf{B} \cong \sum_{\mathbf{k}\alpha} \sqrt{\frac{\hbar}{2\varepsilon_0\omega V}}\, ik\left[\mathbf{a}_{\mathbf{k}\alpha} - \mathbf{a}_{\mathbf{k}\alpha}^{\dagger}\right]\mathbf{b}_{\alpha}. \qquad (8.6.20\text{f})$$

Note also the simple connection between the approximate **A** and **E** and the canonical field coordinates $\mathbf{Q}_{\mathbf{k}\alpha}$ and momenta $\mathbf{P}_{\mathbf{k}\alpha}$ which follows from (8.6.14).

B. Electromagnetic Quantum States and Transitions

Consider an atom coupled to an electromagnetic cavity. Suppose this system starts in a state in which the atomic state is $|s\rangle$ and all the photon numbers $n_{\mathbf{k}\alpha}^s$ are definitely known. We consider some of the possible final states and their probabilities as a function of time.

The states of the whole system at the start and finish will be labeled $|S\rangle$ and $|F\rangle$, respectively. The starting state $|S\rangle$ is a ket-ket product of atomic $|s\rangle$ and radiation $|\cdots n^s_{k\alpha} \cdots n^s_{k'\alpha'} \cdots\rangle$ states:

$$|S\rangle = |s\rangle|\cdots n^s_{k\alpha} \cdots n^s_{k'\alpha'} \cdots\rangle.$$

The final state is written in a similar way:

$$|F\rangle = |f\rangle|\cdots n^f_{k\alpha} \cdots n^f_{k'\alpha'} \cdots\rangle.$$

One may picture the states by imagining atomic and electromagnetic levels as sketched in Figure 8.6.1. A typical transition which conserves energy (more or less) can be imagined as going from the state on one side of the figure to the other. There we imagine that the atom jumps *up* from level $|s\rangle$ to $|f\rangle$ while simultaneously a mode number jumps *down* one level. This is an atomic *absorption* process. (The atom appears to swallow a photon.) If this is reversed, or if the atom jumps *down* from level $|s\rangle$ to $|f'\rangle$ while a mode number jumps *up* the process is called an *emission*. (The atom appears to spit out a photon.) As we will see these two processes are usually the most likely ones.

The derivation of the probabilities for quantum field atomic transitions of the type shown in Figure 8.6.1 are given now. This derivation uses the first-order perturbation formula, because we only need to create or destroy one photon:

$$c_F^{(1)}(t) = \delta_{FS} + \frac{1}{i\hbar}\int_0^t dt_1\, e^{i\omega_{FS}t_i}\langle F|H_1|S\rangle$$

$$= \delta_{FS} + \frac{1}{i\hbar}S(\omega_{FS}, t)\langle F|H_1|S\rangle. \qquad (8.6.21a)$$

Starting State $|\,S\,\rangle$ Final State $|\,F\,\rangle$
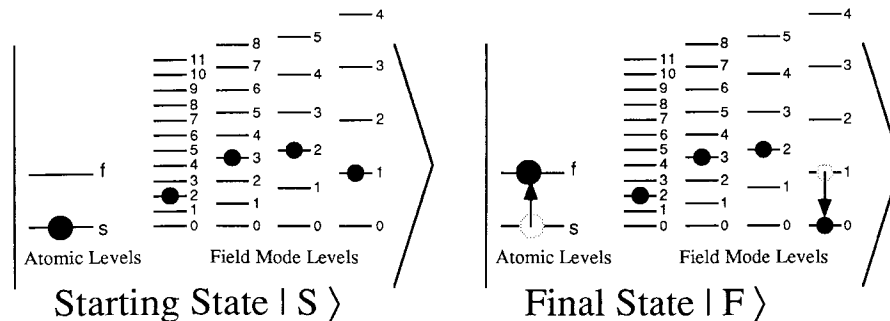
Figure 8.6.1 Atom-field energy levels for initial and final states in an atomic absorption process involving a single photon from a resonant electromagnetic field mode.

Here the spectral function is the following:

$$S(\Delta, t) = 2e^{it\Delta/2} \frac{\sin(t\Delta/2)}{\Delta}. \qquad (8.6.21b)$$

[Recall (8.4.34) and (8.4.38) and discussion of Figure 8.4.2.] The detuning parameter Δ must include the difference of both the atomic and radiation energy:

$$\Delta = \omega_{FS} \equiv \omega_F - \omega_S = \left[\omega_f + \sum_{\mathbf{k}\alpha}\left(n_{\mathbf{k}\alpha}^f + \tfrac{1}{2}\right)\omega_{\mathbf{k}}\right] - \left[\omega_s + \sum_{\mathbf{k}\alpha}\left(n_{\mathbf{k}\alpha}^s + \tfrac{1}{2}\right)\omega_{\mathbf{k}}\right].$$
$$(8.6.22)$$

For the absorption process depicted in Figure 8.6.1 the mode number has gone down one step for the $(\mathbf{k}\alpha)$ mode $(n_{\mathbf{k}\alpha}^f = n_{\mathbf{k}\alpha}^s - 1)$ while the atom went up. All other quanta stayed the same, so the detuning is

$$\Delta = \omega_f - \omega_s - \omega_{\mathbf{k}} = \omega_{fs} - \omega_{\mathbf{k}}.$$

Here zero detuning corresponds to picking a mode whose frequency $\omega_{\mathbf{k}}$ matches the atomic transition frequency ω_{fs}. This is similar to the semiclassical definition of absorption resonance. Compare (8.4.38b) with the foregoing Δ equation.

Now we see some important differences between quantum field theory calculations and semiclassical ones. For one thing, if you really insist on counting every photon, then the absorption and emission processes become clearly separated.

(a) Single-Mode Atomic Dipole Transitions   The first-order S to F transition probability $|c_F|^2$ obtained from (8.6.21) is (assuming $S \neq F$)

$$\underset{F \leftarrow S}{P} = |c_F|^2 = |\langle F|H_I|S\rangle|^2 \frac{\sin^2(t\Delta/2)}{\hbar^2(\Delta/2)^2}. \qquad (8.6.23)$$

We now evaluate the matrix element of the interaction operator (8.4.18b):

$$H_I = q\mathbf{E} \cdot \mathbf{r} \cong -q\sum_{\mathbf{k}\alpha}\sqrt{\frac{\hbar}{2\varepsilon_0\omega V}}\left[i\omega\mathbf{a}_{\mathbf{k}\alpha}^\dagger - i\omega\mathbf{a}_{\mathbf{k}\alpha}\right]\mathbf{e}_\alpha \cdot \mathbf{r}. \qquad (8.6.24)$$

The quantized E field (8.6.20b) is used with the dipole approximation $e^{i\mathbf{k}\cdot\mathbf{r}} \cong 1$. The matrix element consists of a field part followed by the usual

atomic matrix element:

$$\langle F|H_I|S\rangle = q \sum_{\mathbf{k}\alpha} \left[\langle \cdots n^f_{\mathbf{k}\alpha} \cdots |i\mathbf{a}^\dagger_{\mathbf{k}\alpha}| \cdots n^s_{\mathbf{k}\alpha}\rangle - \langle \cdots n^f_{\mathbf{k}\alpha} \cdots |i\mathbf{a}_{\mathbf{k}\alpha}| \cdots n^s_{\mathbf{k}\alpha}\rangle \right]$$

$$\times \sqrt{\frac{\hbar\omega}{2\varepsilon_0 V}}\, \mathbf{e}_\alpha \cdot \langle f|\mathbf{r}|s\rangle.$$

The field part of this matrix element is quite selective. If more than one mode changes its photon number the whole thing is zero. (Recall that $\langle n|n'\rangle = \delta_{nn'}$.) The only possible nonzero elements occur when a single mode goes up or down by exactly one photon. The two possible types of nonzero matrix elements are listed in the following:

$$\langle F|H_I|S\rangle = \left[-i\sqrt{n^s_{\mathbf{k}\alpha}+1} + 0 \right] \sqrt{\frac{\hbar\omega}{2\varepsilon_0 V}}\, q\mathbf{e}_\alpha \cdot \mathbf{r}_{fs},$$

$$\text{if all } n^f = n^s \text{ except } n^f_{\mathbf{k}\alpha} = n^s_{\mathbf{k}\alpha} + 1$$

$$\text{(1 PHOTON EMISSION)}$$

$$= \left[0 + i\sqrt{n^s_{\mathbf{k}\alpha}} \right] \sqrt{\frac{\hbar\omega}{2\varepsilon_0 V}}\, q\mathbf{e}_\alpha \cdot \mathbf{r}_{fs},$$

$$\text{if all } n^f = n^s \text{ except } n^f_{\mathbf{k}\alpha} = n^s_{\mathbf{k}\alpha} - 1$$

$$\text{(1 PHOTON ABSORPTION)}$$

$$= 0, \text{ otherwise.} \quad (8.6.25)$$

The field matrix elements follow from (8.6.17) and the atomic dipole expectation value is denoted by $\mathbf{r}_{fs} = \langle f|\mathbf{r}|s\rangle$.

If matrix element (8.6.25) allows any transition between $|S\rangle$ and $|F\rangle$ it will be an emission or an absorption but not both. If it allows one then the probability for the other is zero. This is very different from the semiclassical transition amplitude (8.4.37) in which both processes would simultaneously have nonvanishing probability. The semiclassical amplitude is a sum of a resonant and a nonresonant spectral function. The quantum amplitude (8.6.21) has only one spectral function in the c_F expression. Strict photon counting prevents absorption from interfering with emission.

(b) Multimode Atomic Dipole Transitions Suppose that we accept (or are forced to accept) any of a set of possible final states going from $|F\rangle = |f\rangle| \cdots n_{\mathbf{k}\alpha} - 1 \cdots n_{\mathbf{k}'\alpha'} \cdots \rangle$ in which mode $(\mathbf{k}, \alpha)$ lost a photon to $|F'\rangle = |f\rangle| \cdots n_{\mathbf{k}\alpha} \cdots n_{\mathbf{k}'\alpha'} - 1 \cdots \rangle$ in which mode $(\mathbf{k}', \alpha')$ lost a photon. In each case the atom jumps up from state $|s\rangle$ to state $|f\rangle$ but now we let it accept a photon from different cavity modes. It is only necessary that the donor modes have nonzero photon number and a frequency ω that is close

enough to the atomic transition frequency $\omega_{fs} = \omega_f - \omega_s$ so the spectral function $|S|^2$ gives a measurable value.

The total probability for the atomic $f \leftarrow s$ transition will be a sum of probabilities $|c_F|^2 + \cdots + |c_{F'}|^2$ as though the contribution of each mode is distinct:

$$
\underset{f \leftarrow s}{P} = |c_F|^2 + \cdots + |c_{F'}|^2 = \sum_{\mathbf{k}\alpha}^{\mathbf{k}'\alpha'} |c_F|^2 = \sum_{\mathbf{k}\alpha}^{\mathbf{k}'\alpha'} \frac{\sin^2(t\Delta/2)}{\hbar^2(\Delta/2)^2} |\langle H_I \rangle|^2. \quad (8.6.26)
$$

Since we are effectively counting the photons from each mode the amplitudes $c_F \ldots c_{F'}$ have random relative phases and interference between them is washed out. Hence the total probability is the sum of their squares $\Sigma |c_F|^2$ instead of the more complicated square of the sum $|\Sigma c_F|^2$. (Recall discussion in Chapter 1, Section 1.1: Axiom 4.)

The sum over mode wave vector $\mathbf{k}$ can be converted to an integral over $k = |\mathbf{k}|$ or over mode frequency $\omega = ck$. According to (8.6.5b) the $\mathbf{k}$ sum is a sum over integer values of photon number $n_\alpha = k_\alpha L/2\pi = 1, 2, \ldots$, or

$$
\sum_{\mathbf{k}} = \sum_{n_x} \sum_{n_y} \sum_{n_z} \Delta n_x \, \Delta n_y \, \Delta n_z \cong \int dk_x \frac{\Delta n_x}{\Delta k_x} \int dk_y \frac{\Delta n_y}{\Delta k_y} \int dk_z \frac{\Delta n_z}{\Delta k_z}
$$

$$
= \left(\frac{L}{2\pi} \right)^3 \int dk_x \int dk_y \int dk_z.
$$

Here the sum is converted to an integral over Cartesian k components using

$$
\Delta n_x = 1 = \frac{L}{2\pi} \Delta k_x, \qquad \Delta n_y = 1 = \frac{L}{2\pi} \Delta k_y, \qquad \Delta n_z = 1 = \frac{L}{2\pi} \Delta k_z.
$$

This sum can then be converted to a polar coordinate integral in k space:

$$
\sum_k = \left(\frac{L}{2\pi} \right)^3 \int d^3\mathbf{k} = \frac{V}{(2\pi)^3} \int d\Omega_\mathbf{k} \int k^2 \, dk = \frac{V}{(2\pi)^3} \int d\phi_\mathbf{k} \int d\theta_\mathbf{k} \sin\theta_\mathbf{k} \int k^2 \, dk,
$$

$$
(8.6.27)
$$

where (ϕ_k, θ_k) are azimuth and polar angles of $\mathbf{k}$, $d\Omega_\mathbf{k}$ is the incremental solid angle in k space, and $V = L^3$ is the cavity volume. This reduces the probability sum (8.6.26) to an integral over solid angle and k or $\omega = ck$:

$$
P_{f \leftarrow s} = \sum_\alpha \frac{V}{(2\pi)^3} \int d\Omega_\mathbf{k} \int_0^\infty k^2 \, dk |c_F|^2 = \sum_\alpha \frac{V}{(2\pi)^3} \int d\Omega_\mathbf{k} \int_0^\infty \frac{\omega^2}{c^3} \, d\omega |c_F|^2
$$

$$
= \sum_\alpha \frac{V}{(2\pi)^3} \int d\Omega_\mathbf{k} \int d\omega \frac{\omega^2}{c^3} \frac{\sin^2(t\Delta/2)}{\hbar^2(\Delta/2)^2} |\langle H_I \rangle|^2. \quad (8.6.28)
$$

Now we approximate the integral of the spectral function $|S(\Delta, t)|^2$ by assuming that time t is large enough that $|S|^2$ becomes very narrow. (Recall Figure 8.4.2.) Then most of the probability comes from the neighborhood around zero detuning ($\Delta = 0$). We may set $\omega = \omega_{fs}$ and put all other functions of frequency outside the integral:

$$P_{f \leftarrow s} \cong \sum_\alpha \frac{V}{(2\pi)^3} \int d\Omega_{\mathbf{k}} \frac{\omega^2}{\hbar^2 c^3} |\langle H_I \rangle|^2 \int_0^\infty d\omega \frac{\sin^2(t\Delta/s)}{\hbar^2 (\Delta/2)^2} .$$

The area under the spectral function is simply the elapsed time multiplied by 2π as was noted before equation (8.4.40).

$$P_{f \leftarrow s} \cong \sum_\alpha \int d\Omega_{\mathbf{k}} \frac{V\omega}{(2\pi)^3 \hbar^2 c^3} |\langle H_I \rangle|^2 2\pi t \qquad (8.6.29)$$

The peak of the spectral function at $\Delta = 0$ goes up quadratically with time, but the area only increases linearly. This is because the width of the peak decreases linearly with time according to the uncertainty relation (8.4.42). As a result the time derivative or rate $R_{f \leftarrow s} = \dot{P}_{f \leftarrow s}$ of the transition probability is a constant in this approximation. This is known as the *Fermi golden rule* of constant transition rates. We write this as

$$R_{f \leftarrow s} = \sum_\alpha \int d\Omega_{\mathbf{k}} \rho(\omega_{fs}) |\langle H_I \rangle|^2 \frac{2\pi}{\hbar^2} , \qquad (8.6.30a)$$

where the spectral density of modes $\rho(\omega)$ is defined here:

$$\rho(\omega) = \frac{V\omega^2}{(2\pi)^3 c^3} . \qquad (8.6.30b)$$

The absorption dipole matrix element (8.6.25) gives the following rate if the photon number in near-resonant modes is $n_{\mathbf{k}\alpha}^s \equiv n$:

$$R_{f \leftarrow s} = n \frac{V\omega^2}{(2\pi)^3 c^3} \frac{2\pi}{\hbar^2} \frac{\hbar\omega}{2\varepsilon_0 V} q^2 \sum_\alpha \int d\Omega_{\mathbf{k}} |\mathbf{e}_\alpha \cdot \mathbf{r}_{fs}|^2$$

$$= n \left(\frac{\omega^3}{\hbar c^3} \right) \left(\frac{q^2}{4\pi\varepsilon_0} \right) \int d\Omega_{\mathbf{k}} \left(|\mathbf{e}_1 \cdot \mathbf{r}_{fs}|^2 + |\mathbf{e}_2 \cdot \mathbf{r}_{fs}|^2 \right) .$$

The polarization sum and integral is simplified by using the vector relation

$$|\mathbf{r}|^2 = |\mathbf{e}_1 \cdot \mathbf{r}|^2 + |\mathbf{e}_2 \cdot \mathbf{r}|^2 + |\hat{\mathbf{k}} \cdot \mathbf{r}|^2 .$$

If we let the induced dipole $\mathbf{r} = \mathbf{r}_{fs}$ be along the polar z axis then $\hat{\mathbf{k}} \cdot \mathbf{r}_{fs} = |\mathbf{r}_{fs}|\cos\theta_{\mathbf{k}}$. The sum and integral is then easily evaluated:

$$\sum_{\alpha} \int d\Omega_{\mathbf{k}} |\mathbf{e}_{\alpha} \cdot \mathbf{r}_{fs}|^2 = \int d\Omega_{\mathbf{k}} \left(|\mathbf{e}_1 \cdot \mathbf{r}_{fs}|^2 + |\mathbf{e}_2 \cdot \mathbf{r}_{fs}|^2 + |\hat{\mathbf{k}} \cdot \mathbf{r}_{fs}|^2 - |\hat{\mathbf{k}} \cdot \mathbf{r}_{fs}|^2 \right)$$

$$= \int d\Omega_{\mathbf{k}} (1 - \cos^2\theta_{\mathbf{k}}) |\mathbf{r}_{fs}|^2 = \int d\phi \int d\theta \sin^3\theta |\mathbf{r}_{fs}|^2 = \frac{8\pi}{3} |\mathbf{r}_{fs}|^2.$$

The resulting absorption rate is

$$R_{f \leftarrow s}(\text{absorption}) \equiv nA = n \frac{4\omega^3}{3\hbar c^3} \frac{q^2}{4\pi\varepsilon_0} |\mathbf{r}_{fs}|^2 = B. \qquad (8.6.31)$$

The corresponding emission rate is the same form except that a factor $(n + 1)$ replaces n in the matrix element (8.6.25):

$$R_{f' \leftarrow s}(\text{emission}) = (n + 1)A = A + B. \qquad (8.6.32a)$$

The first term is the famous Einstein A coefficient, which is the spontaneous decay rate of an excited atom in a vacuum $(n = 0)$:

$$A = \frac{4\omega^3}{3\hbar c^3} \frac{q^2}{4\pi\varepsilon_0} |\mathbf{r}_{fs}|^2. \qquad (8.6.32b)$$

The second term is the Einstein B coefficient which is the decay rate induced by the presence of n resonant photons:

$$B = nA = n \frac{4\omega^3}{3\hbar c^3} \frac{q^2}{4\pi\varepsilon_0} |\mathbf{r}_{fs}|^2 \qquad (8.6.32c)$$

B is the only contribution to the absorption rate (8.6.31) since spontaneous excitation is impossible in this approximation.

(c) "Impotence" of Photon Number States We noted that the first-order transition amplitude $c_F^{(1)}$ in (8.6.21) could only have an absorption term or else an emission term but not both. This is because the quantum field transition matrix element (8.6.25) cannot be nonzero for both processes at once. We also noted that the semiclassical transition amplitude (8.4.36) does have terms from both processes. In fact, the derivation of resonant excitation of the oscillator expectation value $\langle x \rangle$ depends upon the precise interference between these two terms to reproduce the classical result. [Recall comparison of (8.4.45) and (8.4.47).]

The calculation of the atomic position expectation value $\langle \Psi | x | \Psi \rangle$ using quantum field number states is quite different and so are the results. The

perturbed atom-field state is

$$|\Psi\rangle = |S\rangle + \sum_{F \neq S} e^{-i\omega_{FS}t} c_F |F\rangle,$$

where the first-order approximation to the amplitude is

$$c_F^{(1)} = \delta_{FS} + \frac{1}{i\hbar} \int_0^t dt_1\, e^{i\omega_{FS}t_1} \langle F|H_I|S\rangle,$$

according to the basic time-dependent perturbation formulas (8.4.34). The matrix element is given by matrix elements (8.6.25) between the initial state $|S\rangle = |s\rangle_{\text{atom}} |n_{\mathbf{k}\alpha}^s \cdots n_{\mathbf{k'}\alpha'}^s\rangle_{\text{field}}$ and final state $|F\rangle = |f\rangle_{\text{atom}} |n_{\mathbf{k}\alpha}^f \cdots n_{\mathbf{k'}\alpha'}^f\rangle_{\text{field}}$. The atom part only requires that the induced dipole moment $q\mathbf{r}_{fs} \equiv \langle f|\mathbf{r}|s\rangle q$ be nonzero. The field part is more restrictive; it requires that exactly one mode gain or lose a single photon. The result is a perturbed state of the form

$$
\begin{aligned}
|\Psi\rangle = |S\rangle = |s\rangle |n_{\mathbf{k}\alpha}^s \cdots n_{\mathbf{k'}\alpha'}^s\rangle &+ d_{\mathbf{k}\alpha}^a(f)|f\rangle |n_{\mathbf{k}\alpha}^s - 1 \cdots n_{\mathbf{k'}\alpha'}^s\rangle + \cdots \\
&+ d_{\mathbf{k'}\alpha'}^a(f)|f\rangle |n_{\mathbf{k}\alpha}^s \cdots n_{\mathbf{k'}\alpha'}^s - 1\rangle + \cdots \\
&+ d_{\mathbf{k}\alpha}^e(f')|f'\rangle |n_{\mathbf{k}\alpha}^s + 1 \cdots n_{\mathbf{k'}\alpha'}^s\rangle + \cdots \\
&+ d_{\mathbf{k'}\alpha'}^e(f')|f'\rangle |n_{\mathbf{k}\alpha}^s \cdots n_{\mathbf{k'}\alpha'}^s + 1\rangle + \cdots,
\end{aligned}
$$

where the transition amplitude to a higher state $|f\rangle$ due to absorption from mode $(\mathbf{k}, \alpha)$ is

$$d_{\mathbf{k}\alpha}^a(f) = \frac{e^{-i\omega_F t}}{\hbar} \int_0^t dt_1\, e^{it_1\Delta} w_{\mathbf{k}} \sqrt{n_{\mathbf{k}\alpha}}\, \mathbf{e}_\alpha \cdot \mathbf{r}_{f's} \qquad (\Delta = \omega_{fs} - \omega_{\mathbf{k}}),$$

and the transition amplitude to a lower state $|f'\rangle$ due to emission from mode $(\mathbf{k}, \alpha)$ is

$$d_{\mathbf{k}\alpha}^e(f') = \frac{e^{-i\omega_F t}}{\hbar} \int_0^t dt_1\, e^{it_1\Delta} w_{\mathbf{k}} \sqrt{n_{\mathbf{k}\alpha} + 1}\, \mathbf{e}_\alpha \cdot \mathbf{r}_{f's} \qquad (\Delta = \omega_{f's} + \omega_{\mathbf{k}}),$$

and $w_{\mathbf{k}}$ is the scale factor (8.6.4) times frequency ω and charge q.

$$w_{\mathbf{k}\alpha} = \omega_{\mathbf{k}} q \sqrt{\frac{\hbar}{2\varepsilon_0 \omega_{\mathbf{k}} V}}$$

If $|s\rangle$ is the atomic ground state the emission terms with d^e amplitudes are nonexistent. However, there may be several atomic states $|f\rangle, |f'\rangle, \ldots$ which

can be reached by near-resonant absorption. The same goes for state reached by emission if $|s\rangle$ is an excited state.

Now the expectation value $\langle \Psi|x|\Psi \rangle$ can be evaluated. We write the bra and ket on the left and top, respectively, of the box in the following, and we collect the scalar products inside:

$$\langle \Psi|x|\Psi \rangle =$$

$$
\begin{array}{c}
 |s\rangle|n_{\mathbf{k}\alpha}^s \cdots \rangle + d_{\mathbf{k}\alpha}^a|f\rangle|n_{\mathbf{k}\alpha}^s - 1 \cdots \rangle + \cdots \\
\langle n_{\mathbf{k}\alpha}^a \cdots |\langle s|x \; \Big\lvert \; \overline{\langle s|x|s\rangle\langle 1\rangle + d_{\mathbf{k}\alpha}^a\langle s|x|f\rangle\langle 0\rangle + \cdots} \\
+d_{\mathbf{k}\alpha}^{a*}\langle n_{\mathbf{k}\alpha}^s - 1 \cdots |\langle f|x \; \Big\lvert \; +d_{\mathbf{k}\alpha}^{a*}\langle f|x|s\rangle\langle 0\rangle + |d_{\mathbf{k}\alpha}^a|^2\langle f|x|f\rangle\langle 1\rangle + \cdots .
\end{array}
$$

The sum includes only one field mode and one higher atomic state $|f\rangle$. This is enough to see that all the results must be zero if the atomic states have definite parity ($\langle s|x|s\rangle = 0 = \langle f|x|f\rangle$). The orthogonality ($\langle n_{\mathbf{k}}|n_{\mathbf{k}} - 1\rangle = 0$) of the photon states kills the possibility of any contribution from the induced moment matrix elements $\langle s|x|f\rangle$ or $\langle f|x|s\rangle$, however large they may be.

So photon number states are "impotent"; they cannot create a coherent excitation of an atom. This is consistent with the idea that classical phase is completely uncertain or random for a field oscillator eigenstate which has probability distributed more or less evenly over its phase space. To have a well-defined phase we need a nonstationary coherent oscillator state $|\alpha_{\mathbf{k}\beta}\rangle$ for a mode $(\mathbf{k}, \beta)$ instead of a stationary eigenstate $|n_{\mathbf{k}\beta}\rangle$. This will give a wave packet in $(Q_{\mathbf{k}\beta}, P_{\mathbf{k}\beta})$ phase space or $(\mathbf{A}, \mathbf{E})$ space which may have well-defined phase as shown in the next section.

Photon number states may be "impotent" but they are not powerless. They can create large fluctuations in expectation $\langle \Psi|x^2|\Psi \rangle$ even though $\langle \Psi|x|\Psi \rangle$ is identically zero. From the foregoing calculation we get the following:

$$\langle \Psi|x^2|\Psi \rangle = \langle s|x^2|s\rangle + \left|d_{\mathbf{k}\alpha}^a\right|^2 \langle f|x^2|f\rangle + \cdots . \qquad (8.6.33)$$

The expectation of x^2 is proportional to the photon intensity $n_{\mathbf{k}\alpha}$, the square $|\mathbf{r}_{fs}|^2$ of the atomic induced moment, and the mean square x for the final state $|f\rangle$.

(d) ***Coherent Radiation States***   A much better description of a laser-cavity mode includes the nonstationary coherent or wave packet states $|\alpha_{\mathbf{k}\beta}\rangle$. According to (8.2.17) these may be defined as follows in terms of photon number states $|n_{\mathbf{k}\beta}\rangle$ for a single-cavity mode $(\mathbf{k}, \beta)$:

$$|\alpha_{\mathbf{k}\beta}\rangle = e^{-|\alpha_{\mathbf{k}\beta}|^2/2} \sum_{n_{\mathbf{k}\beta}} (\alpha_{\mathbf{k}\beta})^{n_{\mathbf{k}\beta}} |n_{\mathbf{k}\beta}00 \cdots \rangle / \sqrt{n_{\mathbf{k}\beta}!} . \qquad (8.6.34)$$

The complex parameter $\alpha_{k\beta}$ is the field phasor expectation value and the quasieigenvalues of the ladder operators:

$$\mathbf{a}_{k\beta}|\alpha_{k\beta}\rangle = \alpha_{k\beta}|\alpha_{k\beta}\rangle, \qquad \langle\alpha_{k\beta}|\mathbf{a}^{\dagger}_{k\beta} = \langle\alpha_{k\beta}|\alpha^{*}_{k\beta}. \qquad (8.6.35)$$

Recall (8.2.23) and (8.2.24). We assume here that only the $(\mathbf{k}, \beta)$ mode is excited and all others are in their ground or vacuum states.

The A-field expectation value should equal the classical expression (8.6.2a) which began this section:

$$\langle\alpha_{k\beta}|\mathbf{A}|\alpha_{k\beta}\rangle = \sqrt{\frac{\hbar}{2\varepsilon_0\omega V}}\left[\langle\alpha_{k\beta}|\mathbf{a}_{k\beta}|\alpha_{k\beta}\rangle + \langle\alpha_{k\beta}|\mathbf{a}^{\dagger}_{k\beta}|\alpha_{k\beta}\rangle\right]\mathbf{e}_\beta$$

$$= \sqrt{\frac{\hbar}{2\varepsilon_0\omega V}}\left[\alpha_{k\beta} + \alpha^{*}_{k\beta}\right]\mathbf{e}_\beta$$

$$= \left[a_{k\beta}e^{-i\omega t} + a^{*}_{k\beta}e^{i\omega t}\right]\mathbf{e}_\beta.$$

In the last line is the classical value. Note that the dipole approximation $e^{i\mathbf{k}\cdot\mathbf{r}} \cong 1$ is used here. The α has the necessary $e^{-i\omega t}$ time dependence noted in (8.2.20c). This gives the nonstationary phase packet motion described by (8.2.22). The relation between α and the classical amplitude a involves the phasor and the quantum scale (8.6.4):

$$\alpha_{k\beta} = a_{k\beta}e^{-i\omega_k t}\sqrt{\frac{2\varepsilon_0\omega V}{\hbar}}.$$

The α_k expectation value of the $-q\mathbf{E}\cdot\mathbf{r}$ interaction in a coherent state then becomes equal to the classical value quoted in (8.4.35a):

$$\langle\alpha_{k\beta}|H_I|\alpha_{k\beta}\rangle = -i\omega_k q\mathbf{e}_\beta\cdot\mathbf{r}\left(a_{k\beta}e^{-i\omega t} - a^{*}e^{i\omega t}\right).$$

It has the positive and negative frequency parts needed to coherently excite an atom.

This might lead you to believe that a coherent quantum field can reproduce the effect on an atom of a classical wave. Indeed, for very high α_k and short enough time the effect of the two are nearly the same. However, eventually the coherent wave produces dephasing and rephasing effects which are quite remarkable. These coherent decays and "revivals" are discussed in works listed at the end of this chapter and are the subject of much ongoing research.

8.7 SPECTRA OF ATOM IN LASER CAVITY

When the atom interacts strongly or resonantly with an electromagnetic field the distinction between the field and the atom is blurred. Observer and the observed become a single entity that is more than just a sum of its parts. It is as though the atom had become part of a molecule in which the excited levels involve excitation of all the constituent parts.

An atom interacting strongly with a single mode of a simple cavity is described by what is called the Jaynes-Cummings model. Here we will give a brief qualitative sketch of states and levels of this model. This is an important model for beginning to understand spectroscopic effects of strong laser fields. It is also a simple solvable example of an atom interacting with something that has a multitude of states. This is the kind of problem one encounters when atomic motions go together to make a molecular rotation or vibration spectrum.

A. Jaynes-Cummings Hamiltonian

In a static electric field the two-level atomic system Hamiltonian has the following representation (8.5.2b) in the basis of atomic eigenstates:

$$H_{\text{atom}} = H\begin{pmatrix} 1 & 0 \\ 0 & 1 \end{pmatrix} + S\begin{pmatrix} 1 & 0 \\ 0 & -1 \end{pmatrix} - pE\begin{pmatrix} 0 & 1 \\ 1 & 0 \end{pmatrix} = H\mathbf{1} + S\sigma_z - pE\sigma_x.$$

$$(8.7.1a)$$

Generally the electric field-dipole factor pE is folded into the Rabi coefficient

$$r = -pE_z/\hbar. \qquad (8.7.1b)$$

In an oscillating electric field the Hamiltonian is transformed into rotating-wave form (8.5.13), which is now rewritten:

$$H_{\text{RW}} = \frac{\Delta}{2}\begin{pmatrix} 1 & 0 \\ 0 & -1 \end{pmatrix} + \frac{r}{2}\begin{pmatrix} 0 & 1 \\ 1 & 0 \end{pmatrix} = \frac{\Delta}{2}\sigma_z + \frac{r}{2}\sigma_x. \qquad (8.7.2a)$$

Here the detuning factor

$$\Delta = \varepsilon - \Omega \qquad (8.7.2b)$$

is the difference between the atomic transition angular frequency ε and the angular frequency Ω of the stimulating laser.

In preparation for using a quantum field we need to separate the atomic and radiative contributions to the Hamiltonian. In the following the terms

which involve the laser frequency Ω have been collected into one term which is labeled H_{field}:

$$H_{\text{RW}} = \Omega \begin{pmatrix} 0 & 0 \\ 0 & 1 \end{pmatrix} - \frac{\varepsilon + \Omega}{2} \begin{pmatrix} 1 & 0 \\ 0 & 1 \end{pmatrix} + \varepsilon \begin{pmatrix} 1 & 0 \\ 0 & 0 \end{pmatrix} + \frac{r}{2} \begin{pmatrix} 0 & 1 \\ 1 & 0 \end{pmatrix}$$

$$= H_{\text{field}} + \frac{\varepsilon}{2}(\sigma_z + 1) + \frac{r}{2}\sigma_x$$

$$= H_{\text{field}} + H_{\text{atom}} + H_{\text{interaction}}.$$

In the Jaynes-Cummings model the classical electric field is replaced by an expression using its quantized form. However, only one mode of the field is considered and only the dipole terms (8.6.20e) are used. We shall drop the unit matrix term. The resulting Hamiltonian is as follows:

$$H_{\text{JC}} = H_{\text{field}} + H_{\text{atom}} + H_{\text{interaction}},$$

$$H_{\text{JC}} = \Omega a^\dagger a + \frac{\varepsilon}{2}(\sigma_z + 1) + i\frac{g}{2}(a^\dagger - a)\sigma_x, \qquad (8.7.3a)$$

where the coefficient

$$g = \sqrt{\frac{\hbar\Omega}{2\varepsilon_0 V}} \frac{q\langle 2|z|1\rangle}{\hbar} \qquad (8.7.3b)$$

is the Rabi factor that would correspond to a one-photon laser field. [Recall (8.6.4).] The field amplitude for an N-photon field is proportional to $\sqrt{N}$, so we have the following relation between the semiclassical and quantum interaction constant:

$$r = g\sqrt{N}. \qquad (8.7.3c)$$

We let $a_{\mathbf{k}\alpha} = a$ since only one laser cavity mode $\mathbf{k}\alpha$ of frequency $\Omega = \omega$ is being considered. By expressing σ_x in terms of spinor raising and lowering operators, $\sigma_x = (\sigma_+ + \sigma_-)$, this becomes

$$H_{\text{JC}} = \Omega a^\dagger a + \frac{\varepsilon}{2}(\sigma_z + 1) + i\frac{g}{2}(a^\dagger - a)(\sigma_+ + \sigma_-). \qquad (8.7.4)$$

A final approximation to the model keeps only the interaction term $a^\dagger\sigma_-$ in which a photon is created while the atom drops from the upper ($\uparrow$) level 2 to the lower ($\downarrow$) level 1 and the term $a\sigma_+$ in which the reverse process occurs:

$$H_{\text{JCM}} = \Omega a^\dagger a + \frac{\varepsilon}{2}(\sigma_z + 1) + i\frac{g}{2}\left(a^\dagger\sigma_- - a\sigma_+\right). \qquad (8.7.5)$$

Let us apply the Hamiltonian (8.7.5) in turn to the radiation-atom product states with $N = 0, 1, 2, \ldots$ photons which we label $\{|0\rangle|\downarrow\rangle,$ $|0\rangle|\uparrow\rangle, |1\rangle|\uparrow\rangle, |2\rangle|\downarrow\rangle, |2\rangle|\uparrow\rangle, \ldots\}$. The following sequence of state transformation equations results:

$$H_{\text{JCM}}|0\rangle|\downarrow\rangle = (0 \cdot \Omega + 0)|0\rangle|\downarrow\rangle + i\frac{g}{2}(0 - 0),$$

$$H_{\text{JCM}}|0\rangle|\uparrow\rangle = (0 \cdot \Omega + \varepsilon)|0\rangle|\uparrow\rangle + i\frac{g}{2}(\sqrt{1}|1\rangle|\downarrow\rangle - 0),$$

$$H_{\text{JCM}}|1\rangle|\downarrow\rangle = (1 \cdot \Omega + 0)|1\rangle|\downarrow\rangle + i\frac{g}{2}(0 - \sqrt{1}|0\rangle|\uparrow\rangle),$$

$$H_{\text{JCM}}|1\rangle|\uparrow\rangle = (1 \cdot \Omega + \varepsilon)|1\rangle|\uparrow\rangle + i\frac{g}{2}(\sqrt{2}|2\rangle|\downarrow\rangle - 0),$$

$$H_{\text{JCM}}|2\rangle|\downarrow\rangle = (2 \cdot \Omega + 0)|2\rangle|\downarrow\rangle + i\frac{g}{2}(0 - \sqrt{2}|1\rangle|\uparrow\rangle),$$

$$H_{\text{JCM}}|2\rangle|\uparrow\rangle = (2 \cdot \Omega + \varepsilon)|2\rangle|\uparrow\rangle + i\frac{g}{2}(\sqrt{3}|3\rangle|\downarrow\rangle - 0), \quad (8.7.6)$$

It is easy to see that an infinite series of two-by-two matrices results in this representation of H_{JCM}:

	$0\rangle|\downarrow\rangle$	$|0\rangle|\uparrow\rangle$	$|1\rangle|\downarrow\rangle$	$|1\rangle|\uparrow\rangle$	$|2\rangle|\downarrow\rangle \cdots$
$\langle 0 \quad$	$0 \cdot \Omega + 0$	$\cdot$	$\cdot$	$\cdot$	$\cdot$
$\langle 0|\langle\uparrow$	$\cdot$	$0 \cdot \Omega + \varepsilon$	$\dfrac{-ig\sqrt{1}}{2}$	$\cdot$	$\cdot$
$\langle 1|\langle\downarrow|$	$\cdot$	$\dfrac{ig\sqrt{1}}{2}$	$1 \cdot \Omega + 0$	$\cdot$	$\cdot$
$\langle 1|\langle\uparrow|$	$\cdot$	$\cdot$	$\cdot$	$1 \cdot \Omega + \varepsilon$	$\dfrac{-ig\sqrt{2}}{2} \cdot$
$\langle 2|\langle\downarrow|$	$\cdot$	$\cdot$	$\cdot$	$\dfrac{ig\sqrt{2}}{2}$	$2 \cdot \Omega + 0$

$$(8.7.7)$$

The general form of each two-by-two matrix is the following:

		$|N - 1\rangle|\downarrow\rangle$	$|N\rangle|\uparrow\rangle$
$\langle h_{\text{JCM}}\rangle =$	$\langle N - 1|\langle\downarrow|$	$(N - 1)\Omega + \varepsilon$	$\dfrac{-ig\sqrt{N}}{2}$
	$\langle N|\langle\uparrow|$	$\dfrac{ig\sqrt{N}}{2}$	$N\Omega + 0$

$$(8.7.8)$$

In the classical limit of large N the two-by-two matrix begins to look something like the semiclassical matrix (8.7.2a). We can write the two-by-two part of the Hamiltonian as follows:

$$\langle h_{\text{JCM}} \rangle = (N-1)\Omega \begin{pmatrix} 1 & 0 \\ 0 & 1 \end{pmatrix} + \Omega \begin{pmatrix} 0 & 0 \\ 0 & 1 \end{pmatrix} + \varepsilon \begin{pmatrix} 1 & 0 \\ 0 & 0 \end{pmatrix} + \frac{g\sqrt{N}}{2} \begin{pmatrix} 0 & -i \\ i & 0 \end{pmatrix}$$

$$= \left((N-1)\Omega + \frac{\varepsilon + \Omega}{2} \right) \begin{pmatrix} 1 & 0 \\ 0 & 1 \end{pmatrix} + \frac{\varepsilon - \Omega}{2} \begin{pmatrix} 1 & 0 \\ 0 & -1 \end{pmatrix} + \frac{g\sqrt{N}}{2} \begin{pmatrix} 0 & -i \\ i & 0 \end{pmatrix}$$

$$= \left((N-1)\Omega + \frac{\varepsilon + \Omega}{2} \right) \begin{pmatrix} 1 & 0 \\ 0 & 1 \end{pmatrix} + \frac{\Delta}{2} \begin{pmatrix} 1 & 0 \\ 0 & -1 \end{pmatrix} + \frac{r}{2} \begin{pmatrix} 0 & -i \\ i & 0 \end{pmatrix}.$$

$$(8.7.9)$$

The Rabi factor $r = g\sqrt{N}$ for N photons is recovered. The factor of (i) is due to our choice of phase for the field operators.

No essential physics is changed if we use the following modified Hamiltonian in which this phase is absorbed:

$$H'_{\text{JCM}} = \Omega a^\dagger a + \frac{\varepsilon}{2}(\sigma_z + 1) + \frac{g}{2}(a^\dagger \sigma_- + a\sigma_+).$$

Then we can apply the semiclassical dressed eigensolutions (8.5.41)–(8.5.46) to the following real two-by-two matrices:

$$\langle h'_{\text{JCM}} \rangle = \begin{array}{c|cc} & |N-1\rangle|\downarrow\rangle & |N\rangle|\uparrow\rangle \\ \hline \langle N-1|\langle\downarrow| & (N-1)\Omega + \varepsilon & \dfrac{g\sqrt{N}}{2} \\ \langle N|\langle\uparrow| & \dfrac{g\sqrt{N}}{2} & N\Omega \end{array} = N\Omega \mathbf{1} + \begin{pmatrix} \Delta & \dfrac{r}{2} \\ \dfrac{r}{2} & 0 \end{pmatrix}$$

$$= \left((N-1)\Omega + \frac{\varepsilon + \Omega}{2} \right) \mathbf{1} + \begin{pmatrix} \dfrac{\Delta}{2} & \dfrac{r}{2} \\ \dfrac{r}{2} & -\dfrac{\Delta}{2} \end{pmatrix}. \qquad (8.7.10)$$

These matrices have the same eigenvectors as the semiclassical matrices. The only difference is that the Rabi factor r depends upon photon number N and there is a pair of levels for all N greater than zero. The eigenvalues are the

same. too. except for the unit matrix term which yields a ladder of doublet eigenvalues. We examine this ladder of levels now.

B. Jaynes-Cummings Eigensolutions

An attempt to picture the dressed eigenlevels is made in Figure 8.7.1. A column containing stacks of energy levels is shown for each of three cases of detuning: (a) laser tuned below atomic transition ($\Delta > 0$); (b) at resonance ($\Delta = 0$), and (c) laser tuned higher ($\Delta < 0$). Recall that the detuning parameter is $\Delta = \varepsilon - \Omega$.

Two stacks of horizontal lines on each side of the (a), (b), and (c) columns in Figure 8.7.1 indicate what the levels would be without any interaction between atom and field ($r = g\sqrt{N} = 0$). An N-photon level in which the atom is in the first $|1\rangle = |\uparrow\rangle$ or second $|2\rangle = |\downarrow\rangle$ state is labeled $|1, N\rangle$ or $|2, N\rangle$, respectively. Each of these levels for $N > 0$ is connected to a pair of lines in the center of the column that are shifted up and down by $\pm\delta/2$. The quantity δ is the AC-Stark shift discussed in Section 8.5 (recall Eq. (8.5.45c)). The shifted lines are the "dressed" eigenlevels with the interaction turned on ($r = g\sqrt{N} > 0$). The lines that connect the shorter lines to the zero-field levels indicate the relative the greater of the two amplitudes ($\sin \theta/2$ or $\cos \theta/2$) of the zero-field states in each the dressed eigenstates corresponding to that level. Recall Eqs. (8.5.47) and (8.5.48).

Below resonance ($\Delta > 0$) the Hamiltonian rotation vector ω makes an acute angle ($\theta < \pi/2$) with the z-axis. The lower dressed eigenstate $|1^D N + 1, N\rangle$ indicated at the top left-hand side of Figure 8.7.1 is mostly composed of the atom-field product state $|1, N + 1\rangle$ while the higher dressed state $|2^D N + 1, N\rangle$ is mostly composed of $|2, N\rangle$.

As the detuning approaches resonance ($\Delta = 0$) the zero-field levels get lined up, the AC-shifts reach their maximum, and the rotation angle θ approaches $\pi/2$. One may use the diagrams from Section 8.5.E to quantify the variation. However, caution should be used since the Rabi parameter $r = g\sqrt{N}$ is here a function of N. In other words, the Rabi parameter which was a constant in the semiclassical theory is now dependent upon what level you are on. It increases with the laser mode electric field amplitude, which is proportional to the root $\sqrt{N}$ of the photon number.

At resonance ($\Delta = 0$) the rotation angle is $\theta = \pi/2$. Then the Hamiltonian rotation vector ω makes an angle of $\pi/2$ with the z-axis and has its minimum magnitude of $|\omega| = r$, which is the Rabi frequency. This was shown in Figure 8.5.1c. The resonance values for the dressed eigenstate amplitudes are $\sin \theta/2 = 1/\sqrt{2}$ and $\cos \theta/2 = 1/\sqrt{2}$. This corresponds to 50-50 mixtures of the atom-field product states $|1, N + 1\rangle$ and $|2, N\rangle$ in the dressed eigenstates $|1^D N + 1, N\rangle$ and $|2^D N + 1, N\rangle$.

Above resonance ($\Delta < 0$) the Hamiltonian rotation vector ω makes an obtuse angle ($\theta > \pi/2$) with the z-axis. Now the lower dressed eigenstate $|1^D N + 1, N\rangle$ is mostly composed of $|2, N\rangle$ while the upper dressed state

Dressed
Levels:

$$|2^D, N+1, N\rangle = -\sin\frac{\theta}{2}|1, N+1\rangle + \cos\frac{\theta}{2}|2, N\rangle$$

$$|1^D, N+1, N\rangle = \cos\frac{\theta}{2}|1, N+1\rangle + \sin\frac{\theta}{2}|2, N\rangle$$

$|1, N+1\rangle$ $|2, N\rangle$

$|2, N\rangle$

$|1, N+1\rangle$ Ω_L

$|1, N\rangle$ $|2, N\rangle$

$N\Omega_L + \Delta$

$|2, N-1\rangle$ $|1, N\rangle$ $|2, N-1\rangle$

$|2, N-1\rangle$

$N\Omega_L$

$|1, N\rangle$ Ω_F

Ω_3

Ω_F

$|1, N-1\rangle$ $|2, N-1\rangle$ $|2, N-2\rangle$

$|2, N-2\rangle$ Ω_3

$|1, N-1\rangle$ $|1, N-1\rangle$ $|2, N-2\rangle$

3-Photon CSRS $\Omega_3 = \Omega_L - \sqrt{\Delta^2 + r^2} \approx \Omega_L - \Delta = 2\Omega_L - \varepsilon$

Rayleigh Scattering Ω_L

Fluorescence $\Omega_F = \Omega_L + \sqrt{\Delta^2 + r^2} \approx \Omega_L + \Delta = \varepsilon$

$3\Omega_L$ $3\Omega_L + \Delta$
   $N=2$
$\overline{N=3}$

$2\Omega_L + \Delta$
$2\Omega_L$ $N=1$
$\overline{N=2}$

$\omega = \Delta + \delta = \sqrt{\Delta^2 + r^2}$

$\Omega_L + \Delta = \varepsilon$
Ω_L $N=0$
$\overline{N=1}$

(a) Detuning $\Delta > 0$ Ω_L Below ε	(b) Detuning $\Delta = 0$ $\Omega_L = \varepsilon$ (Resonance)	(c) Detuning $\Delta < 0$ Ω_L Above ε

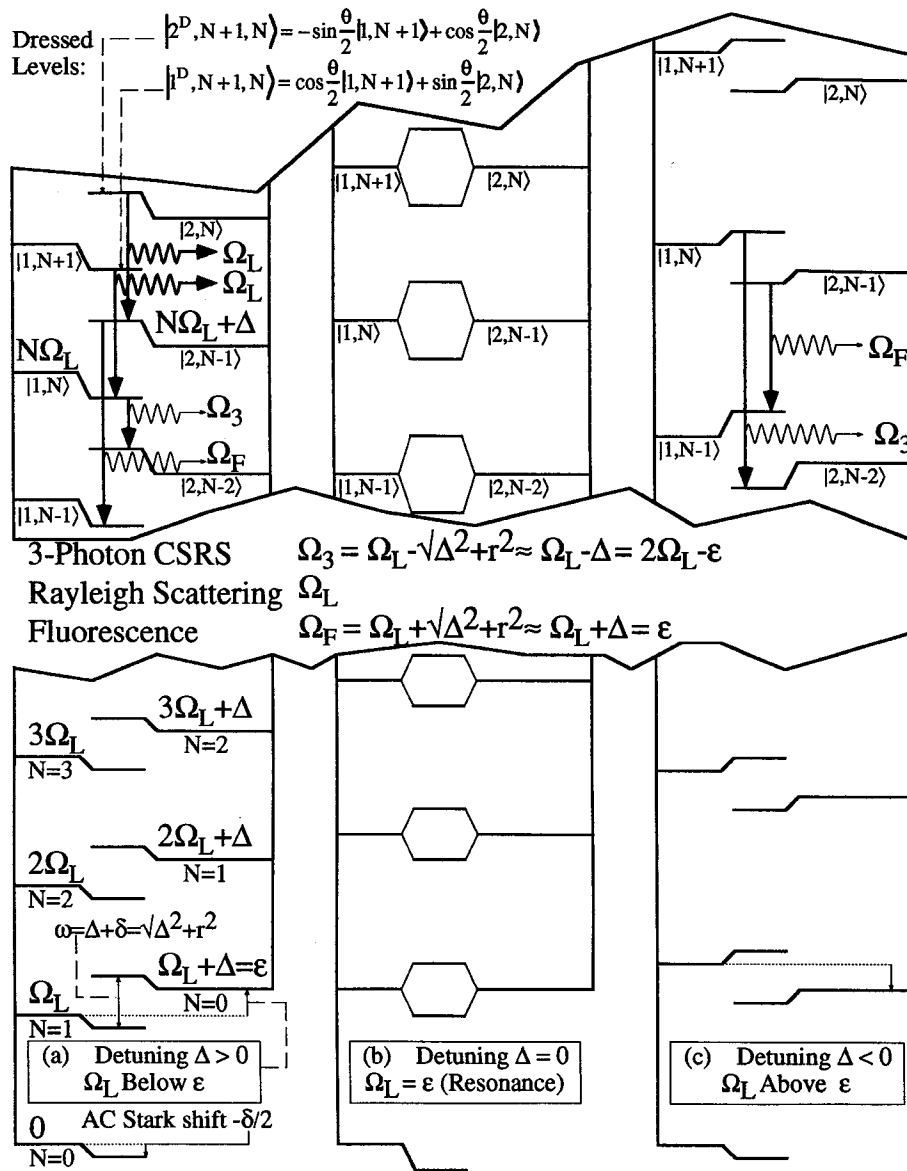0   AC Stark shift $-\delta/2$
$\overline{N=0}$

Figure 8.7.1   Level structure of 2-level atom and 1-mode cavity showing elementary transition processes of fluorescence, Rayleigh scattering, and three-photon coherent Stokes-Raman scattering (CSRS). Transitions are between levels belonging to dressed eigenstates.

$|2^D N - 1, N\rangle$ is mostly composed of $|1, N + 1\rangle$, as shown in the upper right-hand side of the figure.

C. Transitions in the Jaynes-Cummings Model

The diagram of levels in Figure 8.7.1 involves just one $\Omega_L = \Omega$ mode interacting with the two-level atom. We have ignored all the other field mode levels such as were sketched in Figure 8.6.1. We have just concentrated on loading photons into one laser cavity mode whose frequency $\Omega_L = \Omega$ is being tuned close to the value $\varepsilon = \omega_f - \omega_s$ of the atomic transition.

However, if these other modes are off-resonance by enough or only have one or two photons, one can treat them using perturbation theory as was discussed in Section 8.6.B. Transition rates between the dressed states of a laser driven atom can be derived using the Fermi golden rule (8.6.30).

Some of the commonly observed transitions are indicated by vertical arrows in the Figure 8.7.1. The strongest transitions involved the so-called RAYLEIGH SCATTERING processes such as $|1, N + 1\rangle \rightarrow |1, N\rangle$ for $N = 0, 1, 2, \ldots$ or $|2, N\rangle \rightarrow |2, N - 1\rangle$ for $N = 1, 2, \ldots$, where only the photon number changes and the system emits one of its laser-mode photons into an external mode of the same frequency Ω_L. These transitions yield light with the frequency of the laser just like classical Rayleigh scattered light discussed in Section 6.5.B.

The other transitions are more complicated. One called FLUORES-CENCE is a transition between dressed states which involve fundamental transitions such as $|2, N\rangle \rightarrow |1, N\rangle$ or $|2, N - 1\rangle \rightarrow |1, N - 1\rangle$. The latter is the major part of the transition indicated by an Ω_F arrow in the upper left-hand side of the figure since the initial (upper) dressed state $|2^D N, N - 1\rangle$ is mostly composed of $|2, N - 1\rangle$ and $|1^D N, N - 1\rangle$ is mostly composed of $|1, N - 1\rangle$ in the final (lower) dressed state.

The fluorescence transition angular frequency is the difference between the initial and final dressed eigenlevels connected by the Ω_F arrow. The initial and final eigenvalues are

$$\varepsilon^D(2, N, N - 1) = N\Omega_L + \Delta + \delta/2,$$

$$\varepsilon^D(1, N - 1, N - 2) = (N - 1)\Omega_L - \delta/2.$$

The difference is the fluorescence transition frequency,

$$\Omega_F = \Omega_L + \Delta + \delta = \Omega_L + \sqrt{\Delta^2 + r^2}. \tag{8.7.11}$$

For small values of the Rabi factor ($r \ll \Delta$) or large detuning ($\Delta \gg r$) this

becomes

$$\Omega_F \to \Omega_L + \Delta = \varepsilon, \qquad r \ll \Delta, \tag{8.7.12}$$

which is the atomic transition frequency. This transition drops the atom from its upper state $|2\rangle$ to its lower state $|1\rangle$ but takes no photons out of the cavity mode since N stays constant. It emits one photon into an external mode of frequency Ω_F.

Another transition called the three-photon process or COHERENT STOKES RAMAN SCATTERING (CSRS) is a transition between dressed states which mostly involves transitions of the type $|1, N\rangle \to |2, N - 2\rangle$. The latter is the major part of the transition indicated by an Ω_3 arrow in the upper left-hand side of the figure since the initial (upper) dressed state $|1^D N, N - 1\rangle$ is mostly composed of $|1, N\rangle$, and $|2^D N - 1, N - 2\rangle$ is mostly composed of $|2, N - 2\rangle$ in the final (lower) dressed state.

The CSRS transition angular frequency is the difference between the initial and final dressed eigenlevels connected by the Ω_3 arrow. The initial and final eigenvalues are

$$\varepsilon^D(1, N, N - 1) = N\Omega_L - \delta/2,$$

$$\varepsilon^D(2, N - 1, N - 2) = (N - 1)\Omega_L + \Delta - \delta/2.$$

The difference is the CSRS transition frequency.

$$\Omega_3 = \Omega_{\mathrm{CSRS}} = \Omega_L - \Delta - \delta = \Omega_L - \sqrt{\Delta^2 + r^2} \tag{8.7.13}$$
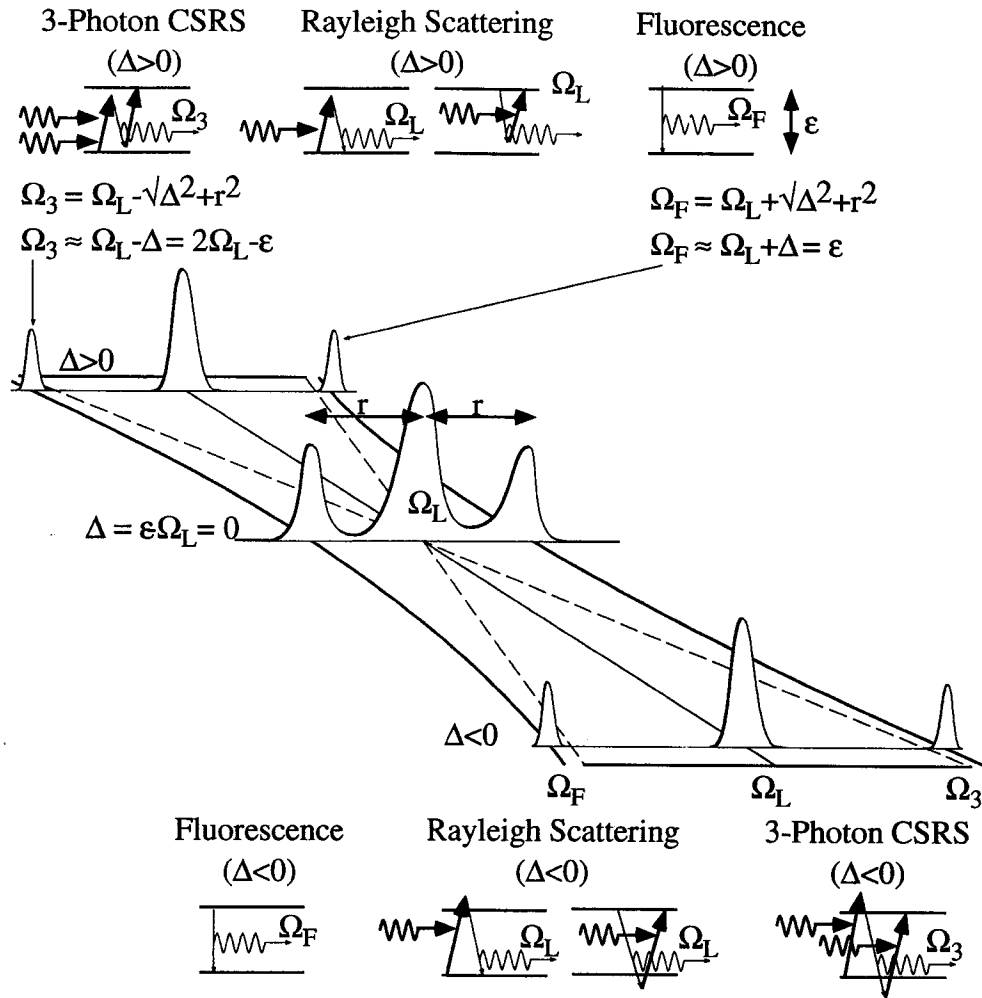
For small values of the Rabi factor ($r \ll \Delta$) or large detuning ($r \ll \Delta$) this becomes

$$\Omega_3 = \Omega_{\mathrm{CSRS}} \to \Omega_L - \Delta = 2\Omega_L - \varepsilon, \qquad r \ll \Delta, \tag{8.7.14}$$

which is the difference between two laser photons and the atomic transition frequency. This transition raises the atom from its lower state $|1\rangle$ to its upper state $|2\rangle$. It also takes two photons out of the cavity mode since N decreases by two. It emits one photon into an external mode of frequency Ω_3 which is approximately the difference between 2Ω and the atomic transition frequency ε.

A direct transition of frequency $\omega = \sqrt{\Delta^2 + r^2} \approx \Delta$ between $|1^D N, N - 1\rangle$ and $|2^D N - 1, N - 2\rangle$ is forbidden by C_2 parity. However, in a system that does not have C_2 symmetry it would be possible to have such a transition as is indicated by the small vertical arrow near the bottom of Figure 8.7.1(a).

The three allowed transitions account for three main spectral components that may be observed coming out of the sides of a laser atom cavity. It consists of a strong Rayleigh line at $\Omega_L = \Omega$ and two sidebands Ω_F and Ω_3 as shown in Figure 8.7.2. The triple-pronged spectral line is called the

3-Photon CSRS   Rayleigh Scattering   Fluorescence
($\Delta > 0$)   ($\Delta > 0$)   ($\Delta > 0$)

$\Omega_3 = \Omega_L - \sqrt{\Delta^2 + r^2}$

$\Omega_3 \approx \Omega_L - \Delta = 2\Omega_L - \varepsilon$

$\Omega_F = \Omega_L + \sqrt{\Delta^2 + r^2}$

$\Omega_F \approx \Omega_L + \Delta = \varepsilon$

$\Delta > 0$

$\Delta = \varepsilon \Omega_L = 0$

$\Delta < 0$

Ω_F Ω_L Ω_3

Fluorescence   Rayleigh Scattering   3-Photon CSRS
($\Delta < 0$)   ($\Delta < 0$)   ($\Delta < 0$)

Figure 8.7.2 Structure of the Mollow spectrum and its elementary processes of fluorescence, Rayleigh scattering, and three-photon coherent Stokes-Raman scattering (CSRS).

MOLLOW LINE SHAPE. One sideband is centered at $\Omega_F = \Omega + \omega$ which is approximately $\Omega + \Delta$ far from resonance, and the other is at $\Omega_3 = \Omega - \omega$, which is approximately $\Omega - \Delta$.

Near resonance at $\Delta = 0$ the sidebands will follow AC Stark shift hyperbolic paths given by (8.7.11) and (8.7.13) rather than simply collapsing upon Ω at $\Delta = 0$. The hyperbolic curves in the semiclassical level diagram in Figure 8.5.3 are approximate traces of the spectral sidebands for variable detuning Δ around resonance. At resonance ($\Delta = 0$) there will still be two sidebands but now they will be located at $\Omega \pm r$, where r is the

Rabi parameter. In general, the sidebands are located at $\Omega \pm \omega$, where $\omega = \sqrt{\Delta^2 + r^2} \approx \Delta$ is the frequency of the Rabi precession or crank rotation shown in Section 8.5.

The sidebands correspond roughly to fluorescence and CSRS processes, respectively. With positive detuning ($\varepsilon - \Omega = \Delta > 0$) the upper sideband ($\Omega_F = \Omega + \omega \approx \Omega + \Delta$) is due (mostly) to fluorescence while the lower sideband ($\Omega_3 = \Omega - \omega \approx \Omega - \Delta$) is due (mostly) to the three-photon CSRS process. Above resonance the detuning parameter reverses sign ($\varepsilon - \Omega = \Delta < 0$) and the order is reversed. At resonance ($\Delta = 0$) it is not possible to distinguish the two processes since the initial states $|1, N\rangle$ and $|2, N - 1\rangle$ are mixed 50-50 and so are the final states $|1, N - 1\rangle$ and $|2, N - 2\rangle$.

Below resonance ($\Delta > 0$) the Ω_3 photon from the CSRS process has lower frequency than the Ω_F photon from fluorescence. It also must come earlier in time. The CSRS process pumps the atom from its lower state-1 into its excited state-2. Only then can it emit a fluorescence photon which puts it back into its ground state. Above resonance ($\Delta < 0$) the Ω_3 photon from the CSRS process has higher frequency than the Ω_F photon from fluorescence. Then it is the higher frequency sideband that comes earlier. These time correlations have been observed.

This concludes our introduction to the recent fundamental developments in laser spectroscopy. Many details have been left out of this discussion and many new effects will soon be discovered as this new set of tools becomes more widely used. Perhaps the most important development so far lies in the way we are coming to think about the observed object (atom or molecule) and the observer's tool (radiation). In modern laser spectroscopy the distinction between the observer and the observed has practically disappeared, and the atom-radiation-cavity becomes a single quantum object.

ADDITIONAL READING

Derivation and application of semiclassical quantization and wave-packet propagation techniques are described in the following papers:

E. J. Heller, *J. Chem. Phys.*, **62**, 1544 (1975); *J. Chem. Phys.*, **68**, 3891 (1978).

M. J. Davis and E. J. Heller, *J. Chem. Phys.*, **71**, 3383 (1979).

S. Y. Lep and E. J. Heller, *J. Chem. Phys.*, **71**, 4777 (1979); *J. Chem. Phys.*, **76**, 3035 (1982).

D. J. Tannor and E. J. Heller, *J. Chem. Phys.*, **77**, 202 (1982).

N. DeLeon and E. J. Heller, *J. Chem. Phys.*, **78**, 4005 (1983); *J. Chem. Phys.*, **81**, 5957 (1984).

M. B. Blanco and E. J. Heller, *J. Chem. Phys.*, **83**, 1143 (1985).

J. R. Reimers and E. J. Heller, *J. Chem. Phys.*, **83**, 516 (1985).

N. DeLeon, *J. Chem. Phys.*, **87**, 4722 (1987); *Comp. Phys. Rep.*, **8**, 321 (1988).

An early paper on action quantization which uses color graphics to approximate quantum wave fronts is

M. J. Davis and E. J. Heller, *J. Chem. Phys.*, **75**, 3916 (1981).

The computer program *Color U(2)* mentioned at the end of Chapter 7 uses color quantization and color animation to show the dynamics of quantum wave fronts.
The idea of wave-packet coherent states can be traced back to Schrödinger.

E. Schrödinger, *Naturwissenschaften*, **14**, 664 (1926).

Their introduction in quantum optics is probably due to Glauber.

R. J. Glauber, *Phys. Rev.*, **131**, 2766 (1963).

Other approaches to semiclassical quantization are found in the following papers (this is by no means an exhaustive list of this large and growing field):

I. C. Percival, *Adv. Chem. Phys.*, **36**, 1 (1977).

D. W. Noid, M. L. Kosykowski, and R. A. Marcus, *Ann. Rev. Phys. Chem.*, **32**, 267 (1981).

S. A. Rice, *Adv. Chem. Phys.*, **47I**, 117 (1981).

W. Eastes and R. A. Marcus. *J. Chem. Phys.*, **61**, 4301 (1974).

D. W. Noid and R. A. Marcus. *J. Chem. Phys.*. **62**. 2119 (1975).

I. C. Percival and N. Pomphrey. *Mol. Phys.*. **31**. 97 (1976).

S. Chapman, B. C. Garrett, and W. H. Miller. *J. Chem. Phys.*, **64**, 502 (1976).

K. S. Sorbie and N. C. Handy, *Mol. Phys.*. **33**. 1319 (1977).

C. Jaffe and W. P. Reinhardt, *J. Chem. Phys.*. **71**, 1862 (1979).

R. T. Swim and J. B. Delos, *J. Chem. Phys.*, **71**, 1706 (1979).

R. B. Shirts and W. P. Reinhardt, *J. Chem. Phys.*, **77**, 5204 (1982).

C. C. Martens and G. S. Ezra, *J. Chem. Phys.*, **86**, 279 (19875).

C. W. Eaker and G. C. Shatz, *J. Chem. Phys.*, **81**, 2394 (1984).

W. H. Miller, *J. Chem. Phys.*, **81**, 3573 (1984).

References to the original EBK quantization are as follows:

A. Einstein, *Dent. Ges. Berlin Verh.*, **19**, 9/10 (1917).

M. L. Brillouin, *J. Phys. Paris (Ser. 6)*, **7**, 353 (1926).

J. B. Keller, *Ann. Phys. (N.Y.)*, **4**, 180 (1958).

F. Reiche, *The Quantum Theory*, (Methuen, London, 1922).

A good modern reference to classical, semiclassical, and quantum theory of radiation for spectroscopy is the following:

C. Cohen-Tannoudji, J. Dupont-Roc, and G. Grynberg, *Photons and Atoms* (Wiley Interscience, New York, 1989).

This discusses the $A \cdot P$ versus $E \cdot r$ perturbations and the Power-Zienau-Wolley transformation. A simplified discussion and other references are in the following paper:

E. A. Power and T. Thirunamachandran, *Ann. J. Phys.*, **46**, 370 (19⁻6).

An early paper which gave a classical transformation between $E \cdot r$ and $A \cdot p$ Hamiltonians is by Marie Goeppert-Mayer:

M. Goeppert-Mayer, *Ann. Physik (Lpzg.)*, **9**, 273 (1931).

The first paper to give a quantum mechanical transformation of $E \cdot r$ to $A \cdot p$ is by Richards. H. S. Synder is credited in the paper.

P. I. Richards, *Phys. Rev.*, **73**, 254 (1948).

A restricted version of this transformation for the case of a magnetic field constant in space and time appears in the following paper:

W. E. Lamb, *Phys. Rev.* **85**, 259 (1952).

It was used again in the same restricted context by the following authors:

B. R. Johnson, J. O. Hirschfelder, and K. H. Yang, *Rev. Mod. Phys.*, **55**, 109 (1983).

Another discussion of the problem is in the following paper:

J. R. Ackerhalt and P. W. Milonni, *J. Opt. Soc. Am.*, **B11**, 116 (1984).

For an example of some of the confusion surrounding the $A \cdot p$ interaction see the following paper:

D. H. Kobe, *Phys. Rev. Lett.*, **40**, 538 (1978).

Some modern treatments of laser-atom lineshape and two-level atom models are listed below. The first papers are seminal ones by B. R. Mollow:

B. R. Mollow, *Phys. Rev.*, **188**, 1969 (1969); *Phys. Rev. A*, **2**, 76 (1969); *Phys. Rev. A*, **12**, 1919 (1969); *Phys. Rev. A*, **13**, 758 (1969).

A discussion which uses the two-level quasi-spin is by Courtens and Szöke:

E. Courtens and A. Szöke, *Phys. Rev. A*, **15**, 1588 (1977).

The two-level atom is presented as a generalization to classical resonance in the following text:

L. Allen and J. H. Eberly, *Optical Resonance and Two-Level Atoms* (Wiley Interscience, New York, 1975).

Applications of radiation theory to laser dynamics is the subject of the following book, which also relates the classical Lorentz model to modern theory:

P. W. Milonni and J. H. Eberly, *Lasers* (Wiley Interscience, New York, 1988).

Recent developments of the problem of an isolated atom-cavity system are based upon the Jaynes-Cummings model.

E. T. Jaynes and F. W. Cummings, *Proc. IEEE*, **51**, 89 (1963).

The phenomenon of "collapse" and "revival" of Jaynes-Cummings solutions is discussed in the following:

J. H. Eberly, N. B. Narozhny. and J. J. Sanchez-Mondragon, *Phys. Rev. Lett.*, **44**, 1323 (1980).

H. J. Yoo, J. J. Sanchez-Mondragon. and J. H. Eberly, *Phys. Rep.*, **118**, 259 (1985).

Recent discoveries have been made about the behavior of the Bloch vector during collapse and revival.

J. Gea-Banacloche, *Phys. Rev. Lett.*, **65**. 3385 (1990); *Phys. Rev. A*, **44**, 5913 (1991); Optical. Commun. **88**, 531 (1992).

Much of the future work on atoms or molecules in cavities will use so-called driven Jaynes-Cummings models. Some discussions of these have just been published.

P. Alsing and H. J. Carmichael, *Quantum Optics.* **3**. 13 (1991).

P. Alsing, D. S. Guo and H. J. Carmichael, *Phys. Rev. A*. **45**, 5135 (1992).

Time correlations between parts of the resonance spectrum are described in the following paper.

A. Aspect, G. Roger, S. Reynaud, J. Dalibard, and C. Cohen-Tannoudji, *Phys. Rev. Letters*, **45**, 617 (1980).